AD NUMBER

AD418092

LIMITATION CHANGES

TO:

Approved for public release; distribution is unlimited.

FROM:

**Distribution authorized to U.S. Gov't. agencies and their contractors;
Administrative/Operational Use; 30 JUN 1963.
Other requests shall be referred to Army Electronics Research and Development Laboratory, Fort Monmouth, NJ.**

AUTHORITY

AERDL ltr dtd 4 Mar 1964

DISCLAIMER NOTICE

THIS DOCUMENT IS THE BEST QUALITY AVAILABLE.

COPY FURNISHED CONTAINED A SIGNIFICANT NUMBER OF PAGES WHICH DO NOT REPRODUCE LEGIBLY.

SOLUBLE CARBONACEOUS FUEL-AIR FUEL CELL

Report No. 3

Contract No. DA 36-039 AMC-00134 (E)

ARPA Order No. 247

Task No. OST 761100338

First Semi-Annual Report, 1 Jan. 1963 - 30 June 1963

U.S. Army Electronics Research and Development Laboratory

Fort Monmouth, New Jersey

ESSO RESEARCH AND ENGINEERING COMPANY
PROCESS RESEARCH DIVISION
LINDEN, NEW JERSEY

PcRD-2M-63

(5) 306 600

(6) SOLUBLE CARBONACEOUS FUEL-AIR FUEL CELL.

(14) REPORT NO. 3; PCRD-2M-63

(15) CONTRACT [redacted] DA 36-039 AMC-00134(E)
(16) ARPA ORDER [redacted] 247
(17) TASK [redacted] OST 761100338

(9) Semiannual rept. no. 1, 1 Jan - 30 Jun 63,

FIRST SEMI-ANNUAL REPORT, 1 JAN. 1963-30 JUNE 1963

OBJECT: CONDUCT INVESTIGATIONS LEADING TO THE DEVELOPMENT OF A SOLUBLE CARBONACEOUS FUEL-AIR FUEL CELL

(10) Authored by:

Barry L. Tarmy,
I-Ming Feng
Eugene L. Holt,
Duane G. Levine and
Kenneth Lewis.
~~Andreas N. Moerikofer~~
~~Eugene H. Okrent~~
~~Joseph A. Shropshire~~
James A. Wilson
~~Charles H. Wolstram~~

(11) 30 Jun 63,

Approved by:

Carl E. Heath

The work performed under this contract was made possible by the support of the Advanced Research Projects Agency under Order No. 247, through the U.S. Army Electronics Research and Development Laboratory.

Esso Research and Engineering Company
Process Research Division
Linden, New Jersey

CONTENTS

Appendix (Cont'd)

ILLUSTRATIONS

TABLES

APPENDIX ILLUSTRATIONS

APPENDIX TABLES

SECTION 1

PURPOSE

The purpose of these investigations is to perform research on the basic components of an electrolyte-soluble carbonaceous fuel - air fuel cell. The major emphasis of the program is on the simultaneous development of all components in order to optimize the performance of the entire cell and to take into account interactions between components.

The program is a continuation of the work carried out under contract DA-36-039 SC-89156. The work is aimed toward the development of a practical fuel cell using a partially oxidized hydrocarbon as the fuel and air as the oxidant. The fuel must be capable of reacting completely to CO_2, be reasonably available, and pose no unusual corrosion, toxicity, or handling problems. In addition the cell must use a CO_2 rejecting electrolyte and operate at temperatures and pressures below 152°C and 5 atm. Other objectives include high electrical output per unit weight and volume, high efficiency, long life, high reliability, reasonable cost, and ruggedness.

The program is divided into three parts. These are referred to as Tasks A, B, and C in this report. Tasks A and B are, respectively, the development of improved fuel electrodes, and the development of practical air electrodes. Task C includes work carried out on establishing the basic cell design, especially with regard to the operation of all components in a single cell and in multi-cell systems.

SECTION 2

ABSTRACT

Research on the soluble carbonaceous fuel-air cell has continued to concentrate on improving the performance of individual cell components and on translating these results into compatible electrode—electrolyte systems. These efforts encompass work carried out in three areas; namely, the development of the fuel electrode, the development of the air electrode, and their combination into a total cell.

2.1 Task A, Fuel Electrode

A number of new catalysts were prepared by the $NaBH_4$ reduction of mixed salt solutions. The compensating effect of the kinetic parameters, Tafel slope and exchange current, upon each other generally acted to restrict the activity of these catalysts to a narrow range. However, several exceptions in the form of more active catalysts were found. In addition, one of these was less expensive than Pt, due to the incorporation of a large amount of gold. As yet, though, none of these new systems are as active as the P-type catalyst. Variations in their methods of preparation did not improve their performances.

The P-type catalyst continued to show superior performance. Further improvements were not made by alterations in composition or preparation methods. The initial activity was dependent on the storage conditions of the catalyst, but life tests of up to 1000 hours showed very stable long term performance. Studies of performance variables showed that there is an activation energy of about 10 kcal/mole for this system and that a dependence on fuel concentration exists up to a relatively low threshold value, beyond which it is insensitive to the amount of fuel. Oxygen, even when saturating the electrolyte, causes only a very small performance loss. Nitric acid, however, increased the polarization by as much as 200 mv.

A surface redox system, based upon the addition of a soluble rhenium salt to the electrolyte, was found to significantly improve the performance of a Pt black electrode. Mechanism studies showed this system to be analogous to, although more active than, the Pt-MoO_3-fuel redox system.

2.2 Task B, Air Electrode

A new C-type electrode structure was tested with the HNO_3 redox couple and found to improve upon the performance obtained from Pt screen electrodes by as much as 70 mv. Studies on direct O_2 electrodes were carried out using mixtures of Pt black and Teflon as the catalyst. When applied to Pt screen supports these mixtures gave high activity. They were found to be sensitive to the amount of Teflon present, as well as the H_2SO_4 concentration, but were independent of the flow rate of O_2 beyond about twice the stoichiometric value. In other work, the incorporation of different metals into Pt was found to alter its properties as an O_2 catalyst, but no significant improvements were obtained.

2.3 Task C, The Total Cell

An improved compact Teflon cell has been developed and used to test both half-cell and complete cell performance. A Pt fuel electrode was operated for over

1000 hours, increasing only slightly in polarization over this time. Furthermore, a fuel electrode chamber as small as 25 mils thick could be used without impairing fuel electrode performance. When assembled as a complete CH_3OH-HNO_3-air fuel cell, efficient, compatible operation was demonstrated in a 131 hour test. Methanol and HNO_3 losses could be minimized by operating with either low electrolyte circulation rates or at high current densities. Further improvements in performance were obtained using the C-type electrode structure as the cathode.

Other complete cell experiments were run to evaluate the compatability of the P-type fuel and direct O_2 electrodes. These showed that the P-type catalyst is able to operate at its expected level in such a system and that the operation of two cells with a common air chamber is feasible. Mathematical analysis of the heat and water transport in a total cell indicated that maintenance of the proper water balance should be possible by removing more water in the air stream than is produced and using the electrolyte level to control the return of water. The analysis also indicated that cell temperature and the rate of water removal will both be relatively insensitive to current density and would decrease inversely with air rate and cell voltage.

An electronic analyzer for CH_3OH has been developed for laboratory and eventual fuel cell use. It is compact and consumes little power.

A number of plastics have been investigated for use as construction materials. Polypropylene has looked particularly interesting, showing chemical and physical stability under the conditions of cell operation.

SECTION 3

PUBLICATIONS, LECTURES, REPORTS, AND CONFERENCES

3.1 Lectures

Heath, C. E. - Methanol-Air Fuel Cell, 17th Annual Power Sources Conference, Atlantic City, New Jersey, May 21, 1963.

3.2 Conferences

February 21, 1963 - Esso Research Center, Linden, New Jersey.

Organizations Represented: Esso Research and Engineering Company
United States Army Electronics Research and Development Laboratory
Mr. C. Daniel, Technical Consultant to USAELRDL

The meeting was held to review the research program with particular emphasis on experimental design. It was concluded that consideration be given to further exploring the use of various techniques of designing experiments in our catalyst development program.

March 26, 1963 - Princeton University, Princeton, New Jersey.

Organizations Represented: Prof. John Tukey, Consultant to Esso Research and Engineering Company
Esso Research and Engineering Company

The meeting was held to further discuss the use of statistics in the catalyst development program. It was decided that increased random replication and the use of chained blocks be incorporated into the program.

April 11, 1963 - Esso Research and Engineering Company, Linden, New Jersey.

Organizations Represented: Esso Research and Engineering Company
United States Army Electronics Research and Development Laboratory

The purpose of the meeting was to brief Dr. H. Hunger, official representative of the contracting officer, on our progress and future plans.

April 30, 1963 - Esso Research and Engineering Company.

Organizations Represented: Esso Research and Engineering Company
General Motors Corporation, Research Laboratory-Defense Systems Division

The meeting was held at the request of GM to discuss the possibility of using a methanol fuel cell battery in vehicular propulsion.

3.3 Reports

This report is written in conformance with the detailed reporting requirements as presented in the Signal Corps Technical Requirement on Technical Reports (SCL-2101N, 14 July 1961) under the terms of our contact; these requirements differ from the usual requirements for reports issued within Esso Research and Engineering Company.

SECTION 4

FACTUAL DATA

4.1 Task A, Fuel Electrode

Work has continued on the development of combinations of noble metals with other noble or base metals in an effort to enhance catalytic activity without sacrificing acid stability. Further investigations have been made on the recently developed P-type and modified P-type catalysts. These have continued to show outstanding performance. Particular emphasis has been placed on preparation and performance variables and their effect on catalyst activity and stability. Finally, performance and mechanism studies have been made with a new active homogeneous catalyst system.

Phase 1 - Performance And Preparation Of New Catalysts

The study of catalysts prepared by the reduction of mixed salt solutions of noble metals with other noble or with base metals, reported previously (1,2), has continued. In addition to the preparation of new catalysts, tests have been carried out to determine if more active catalysts can be prepared by using reducing agents other than $NaBH_4$, or by using $NaBH_4$ in various solutions. Other variables in the catalyst and electrode preparation procedures have also been investigated in the search for higher performance catalysts.

Part a - Performance Of $NaBH_4$ Reduced Catalysts

A number of new catalyst systems were prepared by the $NaBH_4$ reduction of mixed salt solutions. Combinations of Pt with Ag, U, Cr, Zn, Sn and Ru were tested, as well as Au with Fe and Re, Re with Ru, with Zn, and with Sn, and finally Ir with Ni. In addition, a mixture of Pt black and Teflon powder was tried, as was a ternary Pt-Au-Fe catalyst. The reduction technique as well as the manufacture of pressed electrodes for testing purposes have been described previously (1, 2).

The new catalysts fell into three categories when tested in 3.7 M H_2SO_4 and 1 M CH_3OH. Those with no activity were Pt-Ag, Au-Fe, Au-Re, and Re with Ru, Sn and Zn. A number of the binary catalysts were approximately as active as Pt black. These were Pt with U, Cr, Zn and Sn, and Ir with Ni. As shown in Table A-1, they all exhibited higher exchange currents and Tafel slopes than the pure noble metals. Earlier results obtained with Pt and with Ir are included for comparison. This effect of combining noble and base metals to produce catalysts of similar activities to the pure noble metals but of different kinetic parameters has been described previously (2).

Table A-1

Performance Of $NaBH_4$ Reduced Noble-Base Metal Catalysts

Catalyst	Polarization* at Indicated ma/cm^2			Kinetic Parameters	
	1	10	50	b	-Log I_o
Pt	0.52	0.56	0.60	0.049	10.6
Pt-U	0.52	0.58	0.62	0.062	8.3
Pt-Cr	0.53	0.60	0.64	0.069	7.7
Pt-Zn	0.47	0.53	0.57	0.058	8.7
Pt-Sn	0.49	0.57	0.63	0.084	5.8
Ir	0.53	0.58	0.62	0.053	9.9
Ir-Ni	0.55	0.62	0.66	0.070	7.9

Several catalysts showed better performances than Pt. These included Pt-Ru alloys,[a] Pt-Ru-Fe alloy, a mixture of Pt and Teflon powders, and a Pt-Au-Fe alloy. The Pt-Ru and Pt-Ru-Fe catalysts were tested at 60°C and 10 ma/cm^2 in 3.7 M H_2SO_4 and 1 M CH_3OH, and also at 90°C and 50 ma/cm^2 in 1 M H_2SO_4 and 0.5 M CH_3OH. Under both conditions the Pt-Ru catalysts averaged about 70 or 80 mv better than Pt, although displaying a slight dependence on Ru concentration. Alloy formation was necessary for improved activity, as shown by the performance of a Pt+Ru physical mixture which was only as good as pure Pt. The best performance was shown by a Pt-Ru-Fe combination, which was 160 mv less polarized than Pt at 60°C and 120 mv less at 90°C. The Pt-Teflon catalyst, tested at 52°C, was 70 mv better than pure Pt at 60°C. The Pt-Au-Fe sample was also 70 mv better than Pt at its test temperature of 60°C. Table A-2 presents more complete performance data, with pure Pt results included for comparison. Details of preparation and composition of all catalysts discussed in Part a are given in Appendix A-1.

* Polarization, unless otherwise noted, is defined here and elsewhere as the difference between observed voltage as measured by a calomel reference electrode and the voltage of a reversible electrode operating with the same reactant, temperature, pressure, and electrolyte. It is not the difference between observed and open circuit or standard reference electrode voltages. However, no attempt has been made to correct the voltage measurements for liquid junction and thermal potentials, the magnitude of which may be significant at elevated temperatures, about 50 to 100 mv.

Table A-2

Performance Of Highly Active $NaBH_4$ Reduced Catalysts

Catalyst	T, °C	Current Density, ma/cm^2	Polarization, Volts
Pt	60	10	0.56
Pt	90	50	0.49
Pt-Ru	60	10	0.49*
Pt-Ru	90	50	0.41*
Pt-Ru-Fe	60	10	0.40
Pt-Ru-Fe	90	50	0.37
Pt-Teflon	52	50	0.53
Pt-Au-Fe	60	10	0.49
P-Type	60	10	0.35*

* Average of all electrodes tested.

Part b - Effect Of Various Reducing Solutions On Catalyst Performance

Continuing the study initiated during the last reporting period of reducing systems other than simple aqueous $NaBH_4$ solutions, several catalyst types were prepared in various nonaqueous solutions using $NaBH_4$, $LiBH_4$ or an L-type proprietary reducing agent. The catalysts tested were Pt, Pt-Au, Pt-Fe, and Pt-Au-Fe, while the organic solvents were CH_3OH, heptane, ethyl ether, or diglyme. In addition, several preparations were made in the ordinary way with $NaBH_4$ in aqueous solution and also with $NaBH_4$ in acetate and phthalate buffered aqueous solutions. Performance tests were run under the standard conditions of 3.7 M H_2SO_4 and 1 M CH_3OH at 60°C using the pressed electrode structure.

Although their reducing solutions varied widely, the four Pt samples tested differed little from each other in activity. The only difference observed was a slightly larger Tafel slope and exchange current for Pt reduced with the L-type reducing system. A Pt-Au catalyst, made in acetate buffered $NaBH_4$ solution, had an activity similar to earlier Pt-Au electrodes, although it did exhibit a somewhat larger Tafel slope and exchange current than previously observed with Pt-Au. The only significant activity variations were found in the Pt-Fe system, where reduction with $NaBH_4$ in ethyl ether produced a very poor catalyst, while $NaBH_4$ in CH_3OH and especially $LiBH_4$ in diglyme gave rather active catalysts. In addition, the kinetic parameters of these three samples were not similar. The final system examined, Pt-Au-Fe, was not affected by changes in the reducing solutions. Table A-3 summarizes these results while complete details are found in Appendix A-2.

Table A-3

Performance Of Catalysts Reduced In Various Solutions

Catalyst	Reducing Agent	Solvent	Polarization, Volts, at Indicated ma/cm^2			Kinetic Parameters	
			1	10	100	b	-Log I_o
Pt	$NaBH_4$	H_2O	0.49	0.53	0.59	0.05	9.3
Pt	$NaBH_4$	H_2O+Acetate	0.45	0.51	0.57	0.05	9.4
Pt	$NaBH_4$	CH_3OH	0.46	0.52	0.61	0.05	9.3
Pt	L-Type	Heptane	0.46	0.52	0.58	0.06	7.3
Pt-Au	$NaBH_4$	H_2O+Acetate	0.43	0.50	0.58	0.07	5.6
Pt-Fe	$NaBH_4$	CH_3OH	0.38	0.48	0.62	0.10	3.8
Pt-Fe	$NaBH_4$	Ethyl Ether	0.42	0.56	0.64	0.14	3.0
Pt-Fe	$LiBH_4$	Diglyme	0.41	0.48	0.55	0.07	5.9
Pt-Au-Fe	$NaBH_4$	H_2O	0.45	0.52	0.59	0.07	6.7
Pt-Au-Fe	$NaBH_4$	H_2O+Acetate	0.42	0.50	0.57	0.08	5.2
Pt-Au-Fe	$NaBH_4$	H_2O+Phthalate	0.44	0.51	0.59	0.07	6.3

Part c - Other Reducing Agents

Magnesium was tested as a reducing agent by adding the powdered metal to a number of aqueous salt solutions of other metals. Platinum and Au were reduced to the metallic state, but V, Re and Mo only formed oxides. In all cases, even with Pt and Au, the reactions were much slower than when $NaBH_4$ was the reducing agent.

Part d - Effect Of Preparation Variables On Performance

In addition to the study of reducing agents, other variables in the $NaBH_4$ preparation of catalysts were investigated. These were temperature, reactant concentrations, stirring, exposure to the atmosphere and finally the use of small amounts of additives. All reductions were carried out with aqueous acetate buffered solutions or, in the case of the additive studies, in CH_3OH.

It was found that preparation of the Pt-Au-Fe catalyst at 0, 30, 60 and 90°C produced no meaningful change in activity and only a small trend in kinetic parameters, with the highest temperature sample showing the largest Tafel slope and exchange current. Other tests with pure Pt reduced from solutions of H_2PtCl_6 ranging from 0.001 to 0.066 M and with $NaBH_4$ solutions of 0.005 to 1.0 M showed no effect upon catalyst performance. There was also no effect when the reaction mixtures were vigorously stirred or when the reaction solutions were blanketed with argon or with O_2.

A distinct alteration in catalyst behavior was observed only when 2 wt % methylene blue was added to the CH_3OH reduction solution for a Pt-Fe sample. As shown in Table A-4, a large decrease in Tafel slope and exchange current was shown by this sample, compared to those prepared in the presence of lead acetate or with no additive present. As has been the case so often however, a compensation effect prevents these deviations in kinetic parameters from appearing also as variations in activity (1,2). These results are detailed in Appendix A-2.

Table A-4

Effect Of Additives On Pt-Fe Performance

Pt-10 atom % Fe 3.7 M H_2SO_4 - 1 M CH_3OH 60°C

Additive	Polarization at Indicated ma/cm^2			Kinetic Parameters	
	1	10	100	b	-Log I_o
None	0.38	0.48	0.62	0.10	3.8
1 wt % lead acetate	0.36	0.47	0.57	0.10	4.0
2 wt % methylene blue	0.44	0.50	0.59	0.06	7.6

Part e - Variables In Pressed Electrode Manufacture

Normally, pressed electrodes are made by the application of 2000 psi pressure to a catalyst slurry spread on a sandwich electrode structure (2). A number of electrodes were prepared at pressures of from 500 to 5000 psi however, to test the effect of this parameter on electrode performance. Several electrodes were also made at -78°C rather than room temperature, which is normally used. In addition, the effect of an argon blanket excluding atmospheric O_2 was looked at. In no case was a significant change in catalyst performance brought about by these alterations in the electrode preparation procedure.

Part f - Composition And Stability Studies Of The Pt-Au-Fe Catalyst Systems

A number of experiments were performed with a Pt-Au-Fe ternary catalyst directed toward the possibility of producing an active and relatively inexpensive catalyst. Equal molar amounts of Pt and Au were used and the Fe content was varied from 0.1 to 25 atom % in the original mixed salt solution. Reduction was performed with $NaBH_4$ in an aqueous acetate buffer solution at 0°C. The finely divided catalysts were washed alternately in H_2O, 3.7 M H_2SO_4 and once more in H_2O prior to fabrication into pressed electrodes. These structures were then tested in 3.7 M H_2SO_4 and 1 M CH_3OH at 60°C. In addition, the reaction solutions, wash liquids and electrolytes were tested for dissolved Fe to determine at what stage any Fe losses might have occurred. The catalysts themselves were also analyzed after testing.

It was found, as shown in Table A-5, that catalysts containing approximately 5 atom % of Fe were somewhat more active than those of higher or lower Fe content. Thus a sample with a final concentration of 5.15 atom % Fe was polarized 0.55 volts at 100 ma/cm^2 while catalysts containing 0.14 and 7.40 atom % were polarized 0.60 and 0.57 at the same current density. This more active catalyst also showed the largest exchange current. Complete details of preparation and performance are found in Appendix A-2.

Chemical analysis revealed that of the original amounts of Fe present in the mixed salt solutions, 30 to 60% was lost to the 3.7 M H_2SO_4 wash liquid in most cases. About another 10% was usually found in the electrolyte while only traces were detected in the H_2O washes or in the reaction solutions themselves.

Table A-5

Performance And Fe Content Of Pt-Au-Fe Catalysts

3.7 M H_2SO_4 - 1 M CH_3OH - 60°C

Initial Fe Conc, Atom %	Actual Fe Conc, Atom %	Polarization at Indicated ma/cm^2			Kinetic Parameters	
		10	50	100	b	-Log I_o
0.1	0.14	0.52	0.57	0.60	0.07	5.0
1.0	1.04	0.51	0.56	0.59	0.07	6.4
5.0	3.08	0.49	0.54	0.57	0.08	5.5
7.5	4.75	0.48	0.53	0.56	0.07	6.2
10.0	5.15	0.46	0.52	0.55	0.08	4.8
12.5	5.80	0.46	0.52	0.55	0.07	5.7
15.0	6.30	0.49	0.55	0.57	0.08	6.0
25.0	7.40	0.49	0.54	0.57	0.07	6.0

Part g - Stability And Drying Of Pt-Au-Fe Catalysts

Several other tests were performed with the Pt-Au-Fe system to study the storage, drying and long term stability of electrodes. Keeping samples in H_2O or 3.7 M H_2SO_4 at room temperature for 16 hours caused no change in performance, while heating the acid to 60°C for the same period produced only a 10 to 20 mv loss. Drying electrodes at 160°C in air also did not change the activity, but drying at 200°C caused a loss of performance. Life tests in 3.7 M H_2SO_4 and 1 M CH_3OH at 60°C and current densities of 50 to 100 ma/cm^2 resulted in gradual polarization increases of 60 to 80 mv over a 2 week period.

Phase 2 - Preparation Of P-Type And Modified P-Type Catalysts

The last report discussed the discovery of the highly active P-type and modified P-type catalysts (2). To further improve the performance and stability of these catalysts, studies were carried out on the influence of preparation conditions on activity. The use of $NaBH_4$ in various media as well as other reducing agents was also examined. In addition, the storage of these electrodes has been investigated.

Part a - Variable Studies Of $NaBH_4$ Reduction Of P-Type Catalysts

A program was initiated to determine if more active P-type catalysts could be prepared by modifying the standard $NaBH_4$ aqueous solution preparation technique. Therefore experiments were performed to study the effects of temperature, $NaBH_4$ concentration and order of addition of the reacting solutions. Two P-18 catalysts were reduced at 2 and 60°C and compared with the standard 25°C reduction. The same tests were made with P-6 type electrodes, using 0 and 50°C. The concentration of $NaBH_4$ was studied over the range of 0.5 to 10 wt % at 25°C reduction temperature with P-18 catalysts. Finally, several P-18 electrodes were made by reversing the usual procedure of adding the salt solution to the $NaBH_4$ solution.

It was found that reduction at close to 0°C produced slightly less active catalysts than at the higher temperatures in the case of the P-18 samples. With the P-7 catalysts, as shown in Table A-6, there was little difference between reductions carried out at 0 or 25°C, but at 50°C the electrode produced was approximately 100 mv less polarized.

Table A-6

Effect Of Reduction Temperature On Catalyst Activity

3.7 M H_2SO_4 - 1 M CH_3OH - 60°C

Catalyst	Temp, °C	Polarization at 50 ma/cm^2
P-18	2	0.45
P-18	25	0.41
P-18	60	0.42
P-7	0	0.54
P-7	25	0.53
P-7	50	0.45

The $NaBH_4$ concentration studies indicated, as shown in Table A-7, that a slight advantage existed in favor of catalyst samples reduced with approximately 5 wt % $NaBH_4$. These tests were run with the P-18 catalyst.

Table A-7

Effect Of $NaBH_4$ Concentration On Performance

3.7 M CH_3OH - 1 M CH_3OH - 60°C

$NaBH_4$, wt %	1.0	2.5	4.0	5.0	7.5	10
Polarization at 10 ma/cm^2	0.40	0.38	0.37	0.34	0.35	0.39

The final result of this series of experiments showed that catalyst activity did not depend upon the order in which the reacting solutions were mixed. Full details of all these tests are found in Appendix A-3, as well as the activities of a number of P-type catalysts prepared by the standard $NaBH_4$ reduction technique.

Part b - Reduction Of P-Type
Catalysts With Other Solutions

In addition to the aqueous $NaBH_4$ solution work just described, a number of other reducing solutions were tried. Thus $NaBH_4$ was used in acetate buffer and in CH_3OH while KBH_4 was also tested in CH_3OH. In addition, catalysts were made by an L-type reducing system. It was found that in all but one case catalysts of lower activity were obtained than from simple aqueous $NaBH_4$ reduction. The exception was a P-6 sample reduced in acetate buffer at 0°C, which was polarized 30 mv less than a similar catalyst made in an unbuffered system, also at 0°C. These runs are shown fully in Appendix A-4.

Part c - Storage Of P-Type Catalysts

A study was made of the effects of storage conditions on the performance of P-type catalysts. Thus, their performances were measured following storage in H_2O or H_2SO_4 and solutions of CH_3OH or HCHO in these solvents for periods of from 1 hour to 10 days at room temperature. Table A-8 shows the polarizations obtained at 10 ma/cm^2 in 3.7 M H_2SO_4 + 1 M CH_3OH electrolyte at 60°C following storage in the solutions and for the periods indicated.

Table A-8

Effect Of Storage Conditions On Performance

Storage Solution	Polarization After Indicated Days Storage			
	2	4	6	10
H_2O	0.34-0.47	--	0.41-1.4	0.34
3.7 M H_2SO_4	0.34	0.47	0.47	--
1 M CH_3OH in H_2O	0.37	0.35	0.36	--
1 M HCHO in H_2O	0.32	--	0.34	0.34
1 M CH_3OH in H_2SO_4	0.39	--	0.40	--

It can be seen that H_2SO_4 alone caused a decay in activity. Water by itself gave anomalous results, sometimes producing a complete loss in activity and sometimes not affecting performance at all. The cause of this strange behavior is not yet clear. Solutions of CH_3OH or HCHO gave the most consistent and active electrodes, even after as much as 10 days storage. In the case of HCHO, performance tests were run for sufficient time to insure that the increased activity observed was not due to residual HCHO in the system. Further details of these experiments are in Appendix A-3.

Part d - Washing Of P-Type Electrodes

Following the reduction of catalysts with $NaBH_4$, they are usually given several rinses in H_2O and 3.7 M H_2SO_4. In order to determine the effect of these wash steps on the activity of the catalyst, a number of P-type catalysts were prepared identically and then subjected to various degrees of washing. These conditions varied from single H_2O or acid rinses up to combinations of as many as five H_2O and acid washes in different sequences. A total of ten runs were made and an average deviation of only $\pm$ 20 mv was found among the performances of all these catalysts. Apparently then, the activity of P-type catalysts is not sensitive to the severity of washing. Additional data on these experiments is found in Appendix A-3.

Part e - Modified P-Type Catalysts

Several modified P-type catalysts were prepared by reduction in H_2O or acetate buffer solutions by $NaBH_4$ at 0°C. As shown in Appendix A-4, catalysts P-74 and P-75 were approximately as active as ordinary P-type catalysts, while P-76 and P-77 compositions were considerably poorer in performance. In the case of the P-77 samples, reducing conditions had no effect upon their activity.

A number of other modified P-type catalysts were prepared by the standard $NaBH_4$ reduction technique and performance tested. Appendix A-5 shows that catalysts of greatly varying activity were obtained, although none improved upon the ordinary P-type.

Phase 3 - Variable Studies
Using P-Type Catalysts

Studies were directed toward evaluating the performance of P-type catalysts at varying temperature; and fuel concentrations, and in the presence and absence of O_2 and in the presence of HNO_3. Additional tests were made to evaluate the long-term stability of this catalyst under typical operating conditions.

Part a - Effect Of Temperature

The effect of temperature on performance of the P-type catalyst using CH_3OH fuel was evaluated over the range of 25-90°C. A P-type electrode was potentiostatted at 0.4 volts polarization at 25°C in 1 M CH_3OH - 3.7 M H_2SO_4, and current measurements made as the temperature was slowly raised to a final level of about 90°C.

The data gave a reasonably linear plot of current density versus reciprocal absolute temperature, as shown in Appendix A-6, indicating an activation energy of $\sim$ 10.2 kcal/mole for the electrochemical reaction. Energy values of this magnitude are commonly obtained when electron discharge is the limiting step and are associated with an increase in current by a factor of about 1.6 for every 10°C rise in temperature over this range.

Part b - Effect Of CH_3OH Concentration

The effect of CH_3OH concentration was studied at temperatures from 40-80°C, both with and without sparged O_2. A P-type electrode was potentiostatted at 0.4 volt polarization at a given temperature in 3.7 M H_2SO_4. Methanol additions were made in increments to cover the concentration range from 0.14 to 1.32 molar. Identical sets of experiments were carried out in systems with and without the added O_2.

The performance, without O_2, was shown to become less dependent on CH_3OH concentration as the temperature was raised from 40°C to 80°C. At 80°C, performance was relatively insensitive to CH_3OH concentration at levels beyond about 0.4 M. By contrast, at 40°C, a CH_3OH concentration of 0.7 M was required to reach an insensitive level, as shown in Figure A-1.

Figure A-1

Effect Of CH_3OH Concentration
On Performance Of P-type Catalyst

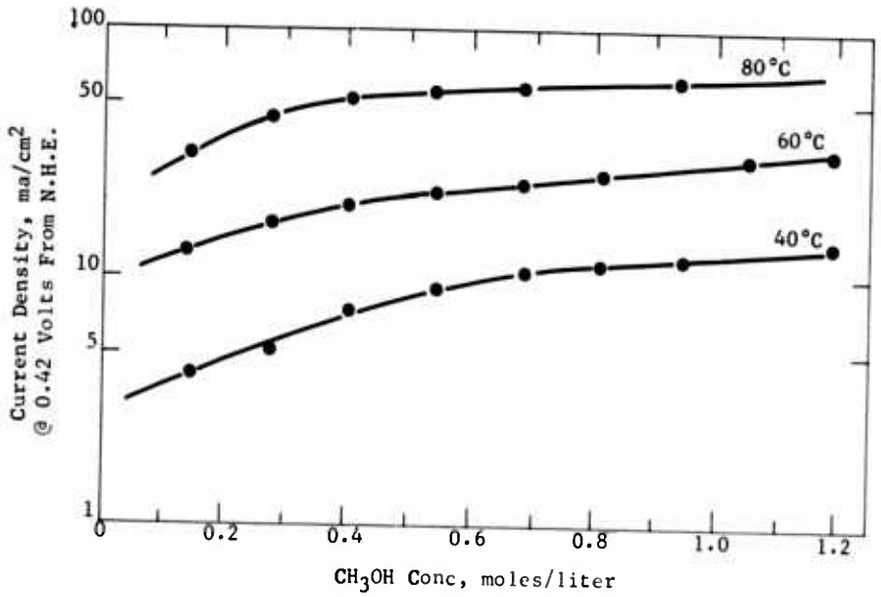

The data obtained in O_2-sparged systems showed comparable dependence, with the additional factor that current at a given concentration level was reduced by 5-15%, depending on temperature. The data for both these systems are shown in Appendix A-7.

Part c - Stability Of P-Type Catalysts

The long term stability of the P-type catalyst was investigated in a series of tests of up to 1000 hours under fixed operating conditions. Representative electrodes were operated in 1 M CH_3OH, 3.7 M H_2SO_4 at 60 or 82°C with fixed current density loads of 40-50 ma/cm^2. In all cases the electrodes were operated against a smooth platinum "driven" electrode, power being supplied by low voltage constant current sources. As a routine procedure, the cells were open-circuited once each 24 hours, generally for 30 seconds.

Since it was discovered in a routine screening procedure that in some cases saturation of the 3.7 M H_2SO_4 electrolyte with Na_2WO_4 seemed to improve the long-term stability of P-type catalysts, several of the long term tests were conducted in Na_2WO_4-containing electrolyte.

The results, summarized in Appendix A-8, indicate that P-type catalysts can be made to operate with considerable stability for over 1000 hours. The best electrodes at the end of this period were polarized about 0.4 volts from CH_3OH theory at 50 ma/cm^2 and 82°C, having lost about 50 mv from their original performance. Although electrodes in H_2SO_4 both with and without Na_2WO_4 successfully withstood the 1000 hour test at 82°C, there exists a slight indication that electrodes in Na_2WO_4 - containing electrolyte may polarize less over the 1000 hour period. Two other electrodes, operated without Na_2WO_4 at 50 ma/cm^2 at 60°C for

380 and 310 hours, respectively did not lose any activity over these intervals, being polarized 0.44 and 0.41 volts respectively under these conditions.

Part d - Effect Of HNO_3 On P-Type Catalysts

Two modified P-type catalysts were exposed to HNO_3 to test their resistance to poisoning by this material. The addition of 0.2 wt % HNO_3 to electrodes operating in 3.7 M H_2SO_4 and 1 M CH_3OH at 10 ma/cm^2 caused polarization increases of 40 and 160 mv at 60 and 80°C. At the 1 wt % level, these increases amounted to 140 and 250 mv. However, upon continued operation, performances improved back towards their original levels, particularly at the higher temperature. After rinsing and replacement into fresh solutions both electrodes regained the same activities as before exposure to HNO_3.

Catalyst type P-18 was also tested with HNO_3 while operating in 3.7 M H_2SO_4 and 0.5 M CH_3OH at 90°C at a current density of 50 ma/cm^2. The addition of 0.2 wt % HNO_3 caused a 90 mv increase in polarization, which leveled off at that value.

Phase 4 - Performance Of Pt Electrodes In Rhenium Containing Electrolytes

It was previously shown that the addition of MoO_3 to the electrolyte produces an improvement in fuel electrode performance. Therefore, a study was conducted to see if this effect could be caused by other metal oxides. It was found that Re_2O_7 could improve fuel electrode performance when added to the electrolyte.

Part a - Performance Of Pt-Re_2O_7 Systems

A $NaBH_4$ reduced Pt black electrode was operated in 0.002 M Re_2O_7 - 3.7 M H_2SO_4 electrolyte. This addition of a soluble Re compound resulted in improvements in performance with both CH_3OH and HCHO fuels. Typical performance data for both is shown in Figure A-2.

A study of the effect of Re_2O_7 concentration in the electrolyte indicated that a rough optimum in Re_2O_7 content occurred at about 10^{-3} moles/liter of Re_2O_7 as shown in Figure A-3.

Figure A-2

Typical Performance Of CH_3OH And HCHO
In Rhenium Containing Electrolyte

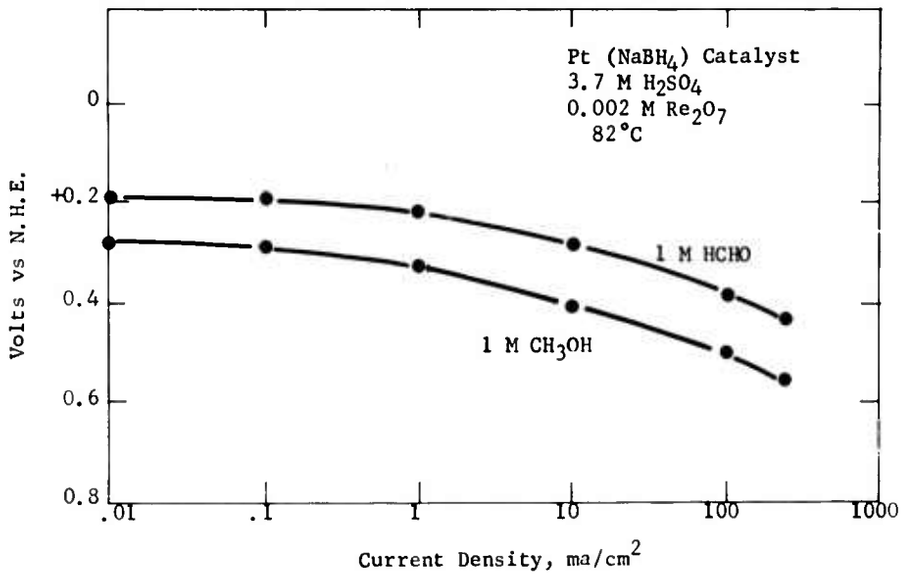

Figure A-3

Effect Of Electrolyte Re_2O_7 Content On
Performance Of Pt - CH_3OH Electrode

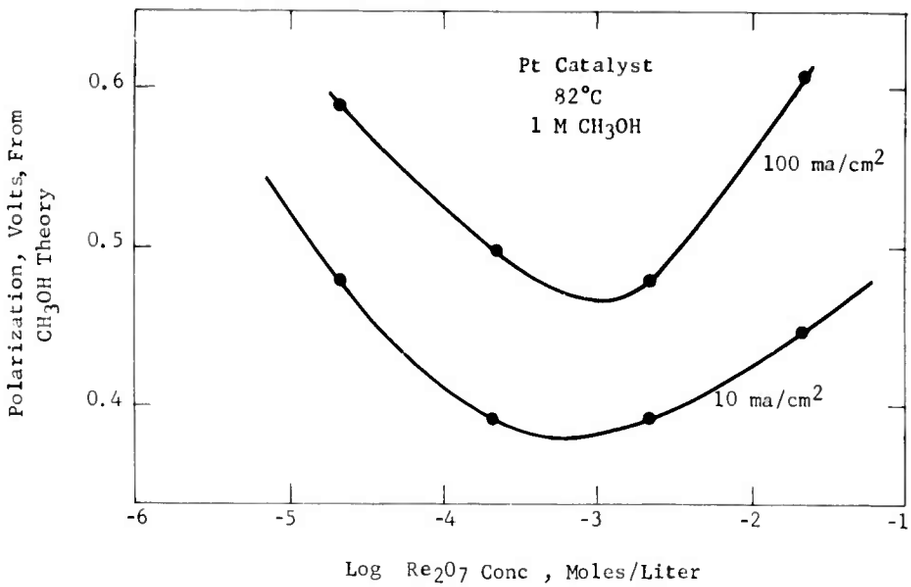

It was also discovered that the performance improvements could be realized by simply dipping the Pt electrode into a Re_2O_7-H_2SO_4 solution before placing it into the fuel-containing electrolyte. Electrodes of this type, however, lost activity after being subjected to high current densities. Typical performance data for CH_3OH and HCHO is shown in Appendix A-9.

Part b - Catalysts In Re_2O_7-Containing Electrolytes

In common with the molybdate redox system previously reported (2), it was found that the electrochemical reaction of Re_2O_7 could be carried out on other metal electrodes, particularly Au. For this reason several electrodes of mixed powders of Pt and Au in a 1:1 ratio were prepared and tested in the Re_2O_7-H_2SO_4 electrolyte. While these electrodes were in general as good as those prepared from Pt alone, no increases in CH_3OH performance of the electrode were observed.

Other experiments indicated that performance of commercial Pt black (Engelhard) was comparable to that obtained from borohydride reduced Pt. Electrodeposited Pt, however, was shown to be inferior in all cases tested. Typical performance data for these catalysts are summarized in Appendix A-9.

Phase 5 - Mechanism Of Pt-Re_2O_7 Catalysis

Based on the similarity of this soluble catalyst with the molybdate systems previously investigated (2), the mechanism and variables in the Pt-Re_2O_7 system were studied along the same lines as those previously developed in the Pt-Mo systems. Experiments were performed to ascertain if a redox mechanism was operative in the Re_2O_7 system, and attempts were made to determine characteristics of chemical and electrochemical behavior. The techniques of constant potential coulometry and galvanostatic chronopotentiometry were applied in evaluating the electrochemical behavior of the system.

Part a - Electrochemical Behavior

The initial step in assessing the possibility of Re_2O_7 redox reaction was to determine if reduction of the heptavalent Re species occurred in the voltage region accessible to the fuel electrode. Galvanostatic transients obtained on a platinized Pt electrode in 3.7 M H_2SO_4 - 0.002 M Re_2O_7 indicated that anodization from initial potential levels of +0.15 volts vs NHE resulted in the production of a well defined anodic reaction wave with a half wave potential about 0.55 volts positive to NHE. This response is shown in Figure A-4.

Figure A-4

Typical Transient Showing Oxidation
Of Adsorbed Rhenium

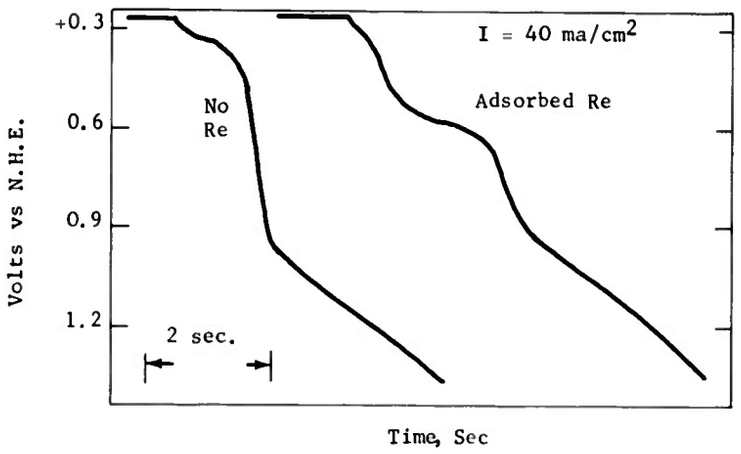

Since the original potential level is easily accessible to the CH_3OH or HCHO fuel electrodes, reduction of Re_2O_7 by these fuel components can be expected. Electrochemical reoxidation of the Re species would then complete the cycle.

Part b - Coulometric Studies

Two types of coulometric analysis were employed in the Re_2O_7-H_2SO_4 system in order to determine the probable valence change involved in the redox reaction. The first of these was a conventional measurement of the coulombs required for the potentiostatic reduction and/or reoxidation of a standard sample of Re_2O_7 in H_2SO_4 on a platinized electrode. The reduction potential was set at +0.15 volts vs NHE; reoxidation was carried out at +0.95 volts vs NHE.

The second type of experiment involved a constant potential reduction under flow conditions, wherein all of the reactive species flowing through a platinized porous medium is reacted. This type of "flow coulometry", (2), was designed to facilitate the distinction between pure electrochemical reduction steps and possible coupling with chemical reactions or disproportionations. Thus, in the flow system, a downstream deficiency of oxidized species lessens the possibility of chemical reactions with the reduced component.

The two types of experiments gave different results. Conventional coulometry indicated the reaction to be a three-electron change to the tetravalent state, ReO_2. Flow coulometry, by contrast, indicated an average change of 1.3 electrons, as shown in Table A-9.

Table A-9

Coulometry Of Re_2O_7 Solutions

Condition	Coulombs Calc (1 Electron)	Coulombs Found
Flow	7.96	10.70
Flow	6.38	8.90
Static	3.44	10.39

These observations indicate that the true electrochemical reaction on Pt is probably the one-electron reduction to the purple +6 state, this reaction in bulk solution being followed by a relatively slow disproportionation to the tetravalent ReO_2.

$$3ReO_3 \rightleftharpoons ReO_2 + Re_2O_7$$

Literature sources indicate that this reaction is well known (3).

Part c - Analysis Of Transients

In order to test the electrochemical behavior of the intermediate valence state of Re, an attempt was made to isolate this species by electrochemical reduction of Re_2O_7 in H_2SO_4 on electrodes other than Pt. Reduction on a large mercury cathode at -0.6 volts vs NHE was successful, producing a bright purple solution believed to contain only the intermediate +6 species.

Due to possible long term effects of chemical disproportionation in this system the electrode kinetics of the species was observed only under transient conditions. Several chronopotentiometric transients were recorded during galvanostatic pulsing of a platinized Pt electrode in this Re +6 solution. These voltage-time transients were analyzed by fitting them to the expected mathematical relationship for diffusion controlled irreversible reaction of a species.

The expected half-wave slope for the irreversible diffusion controlled reaction is, (4),

$$\left[\frac{\partial \Delta E}{\partial (t/\tau)} \right]_{t = \tau/2} = 2.41 \frac{RT}{\alpha n_a F}$$

where τ is the wave transition time, and all other symbols have their usual significance. Half-wave slopes obtained from four transients are shown in Table A-10 together with the calculated αn_a values.

The values of $\alpha n_a = 0.5$ obtained are consistent with a one-electron irreversible limiting step, and would be expected to yield E-log I curves for the redox reaction with Tafel slope, b, of about 0.12 volts/decade current. This value is consistent with the experimental slopes found during CH_3OH reaction on Pt black in Re_2O_7 containing electrolytes.

Table A-10

Analysis Of Re^{+6} Transients

Transient	Half Wave Slope mv/unit t/τ	Calculated n_a
I	135	0.46
II	132	0.47
III	111	0.56
IV	127	0.49

Part d - Chemical Reaction Of Re_2O_7

An attempt was made to evaluate the possible chemical reaction between fuel and Re_2O_7 by monitoring the CO_2 production from a reaction vessel in which HCHO fuel, dissolved Re_2O_7, and powdered platinum black were stirred in 3.7 M H_2SO_4 at 80°C. In contrast to the molybdate-fuel system, no measurable CO_2 production was observed in the Re system.

Part e - Adsorption Of Rhenium

Studies were made to define the conditions necessary for the adsorption of suitable quantities of Re_2O_7 and fuel on Pt black electrodes. The information was obtained through the analysis of anodic stripping transients on electrodes containing preadsorbed layers of Re_2O_7 and fuel. Thus, a Pt microelectrode was allowed to equilibrate with a solution of Re_2O_7 and/or fuel, removed, rinsed and the adsorbed material removed by a constant anodic current. Voltage-time transients were displayed on an oscilloscope and photographed.

It was found that a few seconds immersion of the Pt black electrode in 0.002 M Re_2O_7 - 3.7 M H_2SO_4 resulted in coverage of the surface with a quantity of Re_2O_7 which thereafter did not increase appreciably with immersion time. Application of the same procedures using 0.002 M Re_2O_7 - 1 M CH_3OH - 3.7 M H_2SO_4 solution however produced a surprising interaction. Anodic transients on these electrodes indicated the presence of three to four times more Re than those electrodes treated with Re_2O_7 alone. In addition, the size of the CH_3OH reaction wave was greatly diminished. These results are shown in Figure A-5. Solutions of Re_2O_7-HCHO-H_2SO_4 however did not show a significant change in Re_2O_7 adsorption or in the size of the HCHO wave.

Figure A-5

Increase In Re_2O_7 Adsorption From Solutions Containing CH_3OH

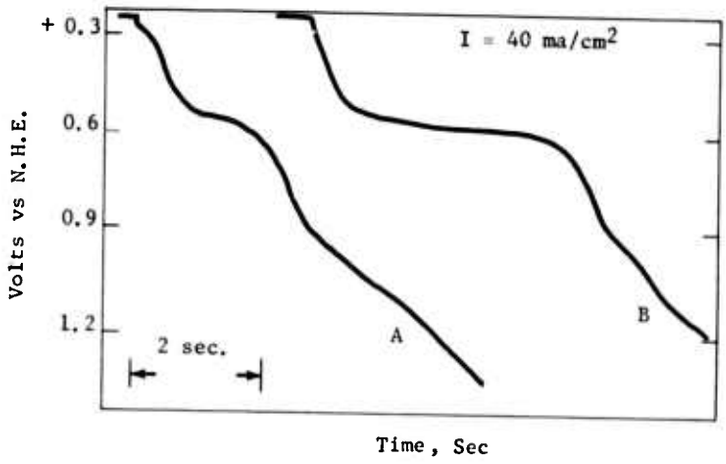

A. 2 min adsorption in 0.002 M Re_2O_7 in H_2SO_4

B. 2 min adsorption in 1 M CH_3OH - 0.002 M Re_2O_7 in H_2SO_4

The Re species was shown to be adsorbed on the electrode surface in experiments involving repeated anodizations of co-adsorbed layers of fuel and Re_2O_7. With HCHO-Re_2O_7, individual reaction waves were observed in the initial transient corresponding to reaction of each component at a different voltage level, identical to the result reported in the previous paragraph. The subsequent anodic transient then indicated the continued presence of most of the initial adsorbed Re_2O_7. A fuel reaction wave was absent in this second transient. These effects are shown in Figure A-6.

Figure A-6

Consecutive Transients On Platinum Electrode
With Both Re_2O_7 And HCHO Adsorbed

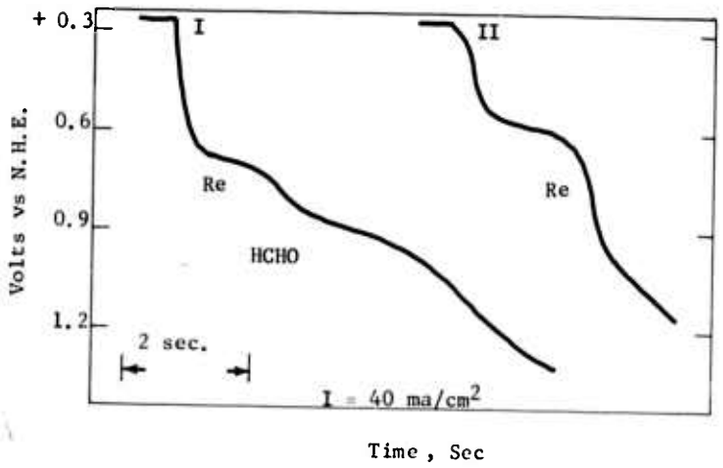

Continued anodic pulses on this electrode indicated a gradual diminution of the amount of Re_2O_7 on the electrode. Similar behavior during repetitive anodization was observed with Re_2O_7 layers adsorbed from CH_3OH - Re_2O_7 solutions.

Part f - Proposed Mechanism

Based on the observations to date, the Pt-Re_2O_7-fuel interaction seems to be governed by a surface redox process quite analogous to the molybdate redox investigated earlier. The reactions involved may be summarized as follows:

Chemical Reaction:

$$Re^{+7}\ (ads) + Fuel \longrightarrow Re^{+6}\ (ads) + CO_2 + H_2O$$

Electrochemical Reaction:

$$Re^{+6}\ (ads) \longrightarrow Re^{+7}\ (ads) + e^-$$

4.2 Task B, Air Electrode

The unique HNO_3 redox system developed for use at the fuel cell cathode offers low polarization at practical current densities and can be run with very efficient regeneration of HNO_3 (2). Further laboratory studies have been carried out with new electrode structures in an effort to further improve the performance of this system. In addition, because of the possibility that the P-type catalysts used at the fuel electrode may be harmed by the presence of HNO_3 or its reduction products, investigations of direct O_2 electrodes have been made. Thus Pt has been studied with several bonding agents and also combined with other metals.

Phase 1 - HNO_3 Redox Performance Using C-Type Electrodes

To increase the efficiency and power output of the CH_3OH-HNO_3 cell, a proprietary (C-type) electrode structure was tested as a cathode. The electrode contained 8 mg/cm^2 of electrodeposited Pt black as the catalyst. These laboratory studies were necessary to determine whether improved performance was attainable and whether this new structure was electrochemically stable.

Part a - Experimental System

Tests were made in a 4 inch diameter glass cell with an external circuit as described previously (1). The driven anode was a Pt screen and the anolyte and catholyte were separated by a membrane. The cell arrangement is shown in Appendix B-1.

The cell was first heated to 82°C with 30 wt % H_2SO_4. Nitric acid was then added to the catholyte. The reaction was initiated by drawing 0.5 amp for 30 seconds, following which the cathode polarization was measured as a function of current density. No attempt was made to regenerate HNO_3 consumed in the electrochemical reduction. Instead, the HNO_3 concentration was maintained constant by addition of the coulombic equivalent of HNO_3 consumed during the experiment.

Part b - Electrode Performance

Most of the new electrode structures demonstrated improved performance over conventional Pt screens in these half-cell tests. Several electrodes gave outstanding performances. For example, the best activity obtained with 1 wt % HNO_3 was 0.21 volts polarization from theoretical O_2 at 100 ma/cm2. A comparison of the best performance on these new structures with that obtained on 80 mesh screens is given in Figure B-1. Additional data for 2 wt % HNO_3 is given in Appendix B-2.

Figure B-1

Electrochemical Performance Of HNO_3 Cathode

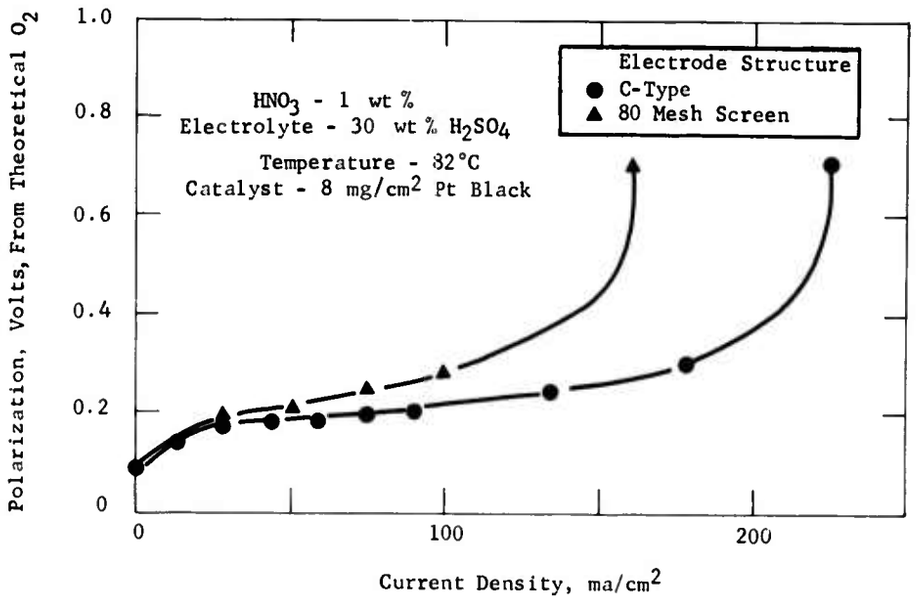

Some of the new structures proved to be electrochemically unstable and gave poor performance. However, the better electrodes were inert during intermittent tests of up to 100 hours.

During these half-cell tests, it was observed that some of the NO gas from the electrochemical reduction at the electrode catalyst surface appeared on the anolyte side of the membrane. This apparently resulted from solution and diffusion of the NO through the electrolyte in the membrane pores.

Phase 2 - Direct O_2 Electrodes

Although the HNO_3 redox system allows high performance to be obtained at the cathode, it has been shown that there are compatibility problems with the active P-type catalysts used at the fuel electrode. For this reason, work with direct O_2 electrodes was initiated. Thus Pt has been studied as a catalyst by bonding it with Teflon or combining it with other metals. The effects of O_2 flow rate and H_2SO_4 concentration on the performances of some of these catalysts have been checked.

Part a - Platinum-Teflon Electrodes

A number of electrodes were prepared by spreading a mixture of Pt and Teflon powders on a Pt screen. Sufficient mechanical stability was imparted by the Teflon so that pressing was not necessary. The electrodes, which contained 20 to 50 wt % Teflon, were tested in 3.7 M H_2SO_4 at temperatures of 38 and 60°C in the glass cell described in Appendix B-3.

An optimum Teflon content in the vicinity of 30 wt % was found. Thus, as shown in Figure B-2, at the typical operating conditions of 60°C and 100 ma/cm^2 the best electrodes contained 25 or 30 wt % Teflon. A similar result was found at 38°C. Complete performance data for these runs is given in Appendix B-4.

Figure B-2

Performance Of Pt-Teflon Electrodes

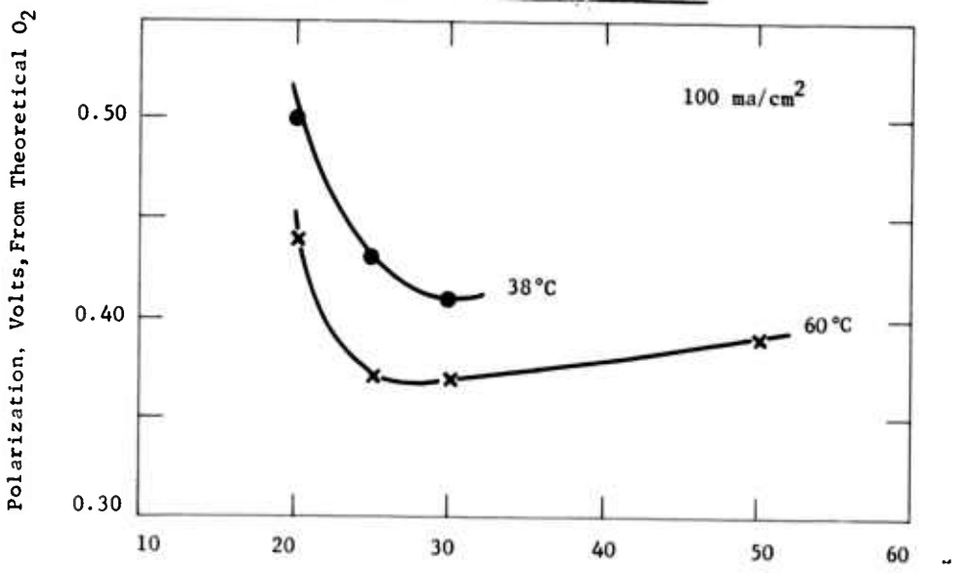

Part b - Platinum-Carbon-Teflon Electrodes

In addition to the Pt-Teflon unpressed electrodes, some carbon containing catalysts were pressed onto Pt gauze structures at 1000 psi and tested under similar conditions. In these systems the Teflon content was maintained at 20 or 33 wt % and the carbon and Pt proportions varied. It was found that these carbon containing electrodes were considerably less active than the Pt-Teflon mixtures. For example, at 100 ma/cm^2 at 62°C, the most active carbon sample was polarized 140 mv more than the most active Pt-Teflon electrode. Full performance details are presented in Appendix B-5.

Part c - Oxygen Flow Rate Studies

The effect of O_2 flow rate on the performance of the direct O_2 electrode was investigated to determine the optimum operating rate. A Pt-10 wt % Teflon electrode was used for these tests, which were carried out at 20 and 50 ma/cm^2 and at ambient, 60°C, and 82°C temperatures. It was found, as shown for a typical case in Figure B-3, that polarization decreased rapidly with increasing flow rate until about twice the stoichiometric value. Beyond this point constant polarizations were obtained. Further details of performance are shown in Appendix B-6.

Figure B-3

Effect Of Oxygen Flow Rate On Performance

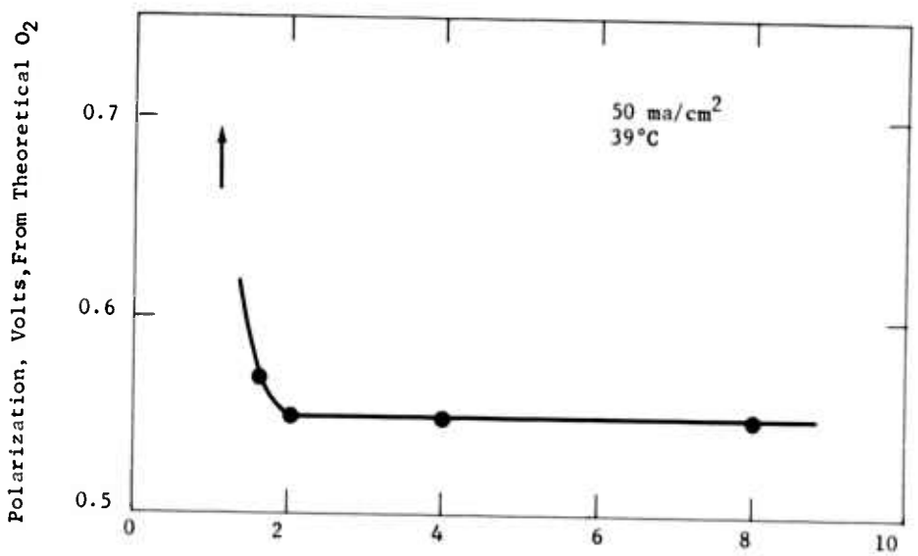

Part d - Storage Of Pt-Teflon Electrodes

One problem in the development of Pt-Teflon direct O_2 electrodes has been a deterioration in performance occurring between tests while the electrode was stored in electrolyte. However, it was found that by draining the bulk electrolyte from the half-cell and leaving the catalyst only moist rather than completely immersed during storage, the initial activity could be maintained even after long idle periods. Thus a 25 wt % Teflon electrode did not lose any activity after storage for 86 hours under the new conditions. Further test details are shown in Appendix B-7.

Part e - Sulfuric Acid Concentration Studies

An investigation was carried out on the change in performance of the Pt-Teflon direct O_2 electrode with varying H_2SO_4 concentrations. Thus 20 and 25 wt % Teflon electrodes were run at temperatures from 38 to 60°C in an acid range of 0.5 to 3.7 M. In all cases, the observed polarizations, when corrected for the change in theoretical potential with pH, showed an optimum acid concentration of less than 3.7 M. Table B-1 illustrates a typical set of results obtained with the 20 wt % Teflon electrode operating at 50 ma/cm^2 at 50°C. Polarizations both before and after the pH correction are shown. Additional results are found in Appendix B-8.

Table B-1

Effect Of Sulfuric Acid Concentration On
20 wt % Teflon Electrode Performance

H_2SO_4 Concentration M/L	Polarization at 50°C and 50 ma/cm^2	
	from O_2 potential for 3.7 M H_2SO_4 electrolyte	from theoretical O_2 potential for indicated H_2SO_4 concentration
0.5	0.41	0.34
0.75	0.42	0.36
1.5	0.40	0.36
3.7	0.43	0.43

Although a definite half-cell performance advantage is indicated for acid concentrations lower than the normal 3.7 M value, the improvement is not sufficient to overcome the additional IR losses introduced by the more dilute electrolyte. Until unit cells of lower resistance are designed, 3.7 M H_2SO_4 continues to be the optimum concentration.

Part f - Performance of Pt-Base Metal Catalysts With O_2

Several binary systems were prepared by $NaBH_4$ reduction of mixtures of a Na_2PtCl_6 solution, and salt solutions of the second metal. The metals tested were Ni, Pb, Cr, and Mo. Performance tests were run in 3.7 M H_2SO_4 electrolyte at 60°C. Oxygen was passed over the surface of the catalyst which was supported at the O_2 - electrolyte interface.

The performance of the electrodes tested varied considerably. Thus Pt-Ni performed essentially the same as Pt alone, but Pt-Mo and particularly Pt-Pb gave much poorer performances. Only Pt-Cr gave any indication of improvements in performance over Pt, and at 100 ma/cm^2 the difference between these two was only 20 millivolts. Details of these runs are shown in Appendix B-9.

4.3 Task C, The Total Cell

Further work was carried out on improving the design of the methanol-HNO_3-air fuel cell so as to increase over-all cell performance in sustained operation. Since the P-type catalyst could not be effectively used together with HNO_3, studies were also made of total cell operation using direct oxygen or air electrodes and P-type catalyzed methanol electrodes. In addition, an analysis was made of the effects of design and operating conditions on water removal. Also included are development work on a methanol analyzer and a study of possible materials for use in fuel cell construction.

Phase 1 - Cell Design Studies: CH_3OH - HNO_3 - Air Fuel Cell

A compact Teflon cell was set up as a methanol half cell using a driven cathode. Its purpose was to improve cell design and operability by assessing long term methanol electrode performance independently of effects attributable to total cell interactions. In addition, these tests would be useful in distinguishing between these additional effects and those present only at the methanol electrode. Tests were also made to determine the minimum fuel chamber size.

Part a - Long Term Methanol Electrode Performance

The cell used in this study was described in a previous report (2). Several modifications made during this work are described in Appendices C- 1, C-2 , and C-3 . The main test of the methanol electrode was a 1029 hour run. The experiment was conducted with a platinum black catalyst on an 80 mesh platinum-rhodium screen at 50 ma/cm^2 and 82°C using commercial grade methanol in 30 wt % H_2SO_4. The cell was open-circuited for several seconds about once a day to maintain performance. The methanol concentration varied between 0.8 and 3 vol % and averaged 1.9 vol %.

At the end of 1029 hours, the methanol electrode polarization had increased from 0.58 to 0.61 volts. The lost performance was largely restored by adding fresh electrolyte, indicating that this slight increase in polarization was due to accumulation of impurities in the recycled electrolyte (see Table C-1).

Table C-1

Life Study Of CH_3OH Electrode

Operation	Total Hours on Catalyst	Current Density, ma/cm^2	Polarization, Volts
Long term run with electrolyte recycle and methanol-water addition	Start	50	0.58
	1029	50	0.61
Fresh electrolyte	1080	50	0.59
Increased current	1149	105	0.69

At the end of the long term test, the current was increased to 105 ma/cm^2 and the cell operated for 69 hours without any serious difficulties. At the higher current, voltage oscillations due to CO_2 rejection from the 80 mesh electrode surface were less than 6 millivolts. The polarization, however, was about 90 millivolts higher than expected, attributable to poor methanol distribution resulting from a single point feed system. Thus, with proper control, the methanol activity on a platinum black catalyst can be maintained. Some of the initial results were given in an earlier report (2). Therefore, only the additional data are given in Appendix C-4.

During this long term methanol electrode performance run, material and electrochemical balances were made to validate the cell reactions. Measurements of feed reactions and products in and out of the cell were made at frequent intervals throughout the run. The over-all weight balance for the run was 100.1%. Detailed data are presented in Appendix C-5. The logs of methanol and water fed and gases produced are shown graphically in Appendix C-6. The over-all balances for the 1029 hour run, summarized in Appendix C-5, confirmed the fact that the methanol is electrochemically oxidized completely to CO_2. The 31.8 gram moles of CO_2 produced were coulombically equivalent to 100.0% of the current.

Part b - Fuel Chamber Design

The composition of the CO_2 exhaust obtained in tests with various sized electrolyte chambers was examined in runs at currents ranging from 25 to 105 ma/cm^2. The tests were made at 85°C with 1 vol % methanol in 30 wt % H_2SO_4 electrolyte to determine whether efficient CO_2 release was possible in these chambers.

The exhaust CO_2 was found to be saturated with water and methanol in the large, 225 mil thick, chamber. Surprisingly, the degree of saturation decreased to about 90% and 50% in the 100 and 25 mil chambers respectively. The degree of saturation was further reduced at lower current densities. These results are summarized in Figure C-1. Detailed data are given in Appendix C-7.

Figure C-1

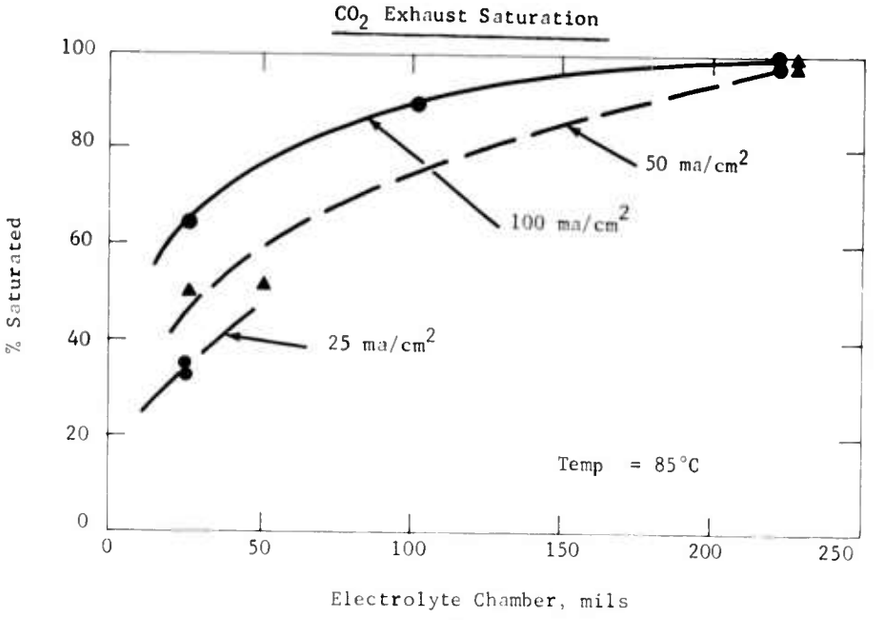

Phase 2 - Life Studies In The
CH_3OH - HNO_3 - Air Fuel Cell

The compact Teflon cell was assembled for testing the over-all performance of the methanol electrode and the air-HNO_3 redox system in sustained operation. The equipment used in these experiments was described in a previous report (2). The coulometric timer used to control CH_3OH and HNO_3 feed rates was modified for better control and an air rate controller was added. These are described in Appendices C-1 to C-3.

Part a - Long Term Testing

The methanol-air-HNO_3 system was operated in a long term test. The cell used 80 mesh screens for both electrodes and a CR-61 membrane separator. Platinum was used exclusively as the catalyst. The test was carried out at 82°C using 1 to 2 vol % methanol in 30 wt % H_2SO_4 anolyte, and 1 wt % HNO_3 in 30 wt % H_2SO_4 catholyte. The cell was operated continuously for 181 hours at current densities varying from 2 to 112 ma/cm^2. The maximum power level at the cell terminals amounted to 19 milliwatts/cm^2 at 0.40 volts. The IR losses amounted to 0.20 volts at 100 ma/cm^2. During the run, although feed was controlled by the modified coulometric timer, periodic manual adjustments were necessary. The catalyst activity was found to be normal when tested at the end of the run. A log of procedures during the run, a tabulation of electrical performance data, and a graphical presentation are given in Appendices C-8, C-9, and C-10, respectively.

Part b - Improved Cell Performance

Based on the experience obtained in the above test, a number of assembly arrangements were tried in an effort to improve the electrical cell output. The assembly arrangements included variation in the number and mesh of screen electrodes, as well as spacing between electrodes. The tests were made at 82°C using 1 vol % methanol in 30 wt % H_2SO_4 and 1 to 2 wt % HNO_3 in 30 wt % H_2SO_4 as anolyte and catholyte, respectively. Methanol losses and HNO_3 regeneration efficiencies were measured. Detailed data are given in Appendices C-11 through C-22.

During these tests the methanol losses due to chemical reaction with NO were largely dependent on the electrode acting as a barrier to methanol diffusion to the opposing compartment. Essentially no methanol was lost when the electrochemical conversion of methanol was greater than 60%. However, decreasing the conversion to 55% resulted in losses as high as 54 lbs/100 lbs of methanol reacted. This use of the electrode as a methanol barrier was discussed in an earlier report (1).

No attempt was made to use an efficient HNO_3 regeneration system. The nitric acid regeneration was accomplished externally in a simple 1" diameter glass column packed with 3/32" glass helices. Air for NO oxidation was fed to the regenerator at about two times the stoichiometric requirement. Electrolyte solution flowed down the column to the cell to furnish water for NO_2 hydrolysis to HNO_3. The HNO_3 regeneration efficiency in this column varied from 1.5 to 9 coulombs measured per coulomb equivalent to HNO_3 consumed or lost from the column exhaust, depending on the amount of NO produced in the cell. Since NO is produced electrochemically as well as by chemical oxidation of diffusing methanol, the regeneration efficiency depended on the current density and methanol conversion per pass. Low currents and high conversion produced less NO and consequently resulted in the highest regeneration efficiencies.

The biggest improvement in electrical performance was obtained by providing escape routes for CO_2 between the membrane and screen electrode. This modification also resulted in a steady electrical output without any evidence of oscillations observed in other assemblies. The maximum power output at the terminals was 23 milliwatts/cm^2 over the range of 70 to 100 ma/cm^2 current density and 0.30 to 0.24 volts. Excluding the IR loss, which amounted to 0.13 volts at 100 ma/cm^2, the maximum power was 40 mwatts/cm^2. The best previously reported (2) performance was about 15 mwatts/cm^2. The power performance data are compared in Figure C-2.

Figure C-2

Cell Power Versus Current Density

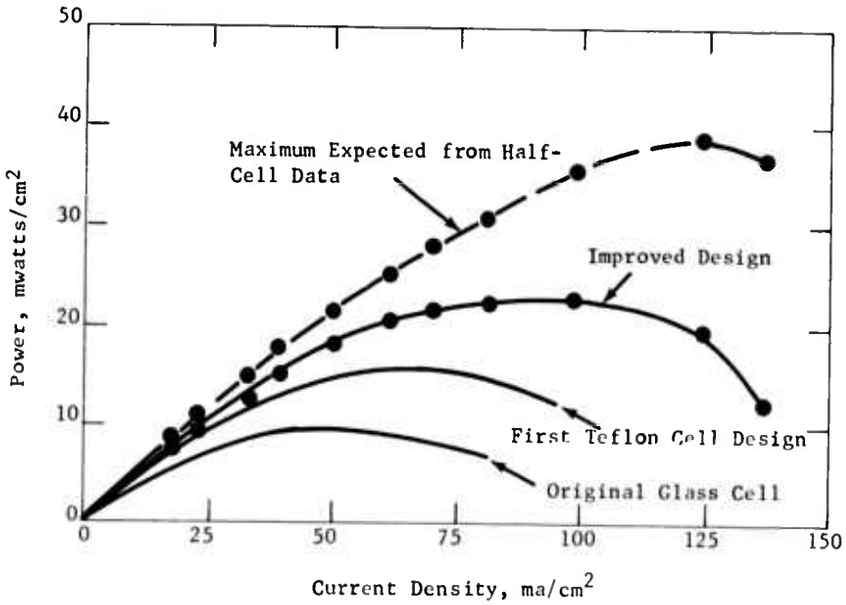

Phase 3 - Performance Of New Electrode Structures In The CH_3OH - HNO_3 Fuel Cell

Because of the outstanding HNO_3 half cell performance of some of the new electrode structures described in Task B, tests were made to evaluate these structures in total cell operation, using platinum black catalyst.

Part a - Experimental System

The tests were made with 4 inch diameter electrodes and gold current collectors in a glass cell described in a previous report (1). Auxiliary platinum screen electrodes were installed in each reactant chamber to permit independent operations, such as activation and half-cell measurements. The external circuit consisted of only resistive elements, including a rheostat, ammeter, and voltmeter. The cell arrangement is shown in Appendix Figure C-3.

After a variety of electrode pretreatments, the cell was filled with 30 wt % H_2SO_4 and heated to 82° C. The reactants, CH_3OH and HNO_3, were added and the performance was determined by measuring the individual electrode polarizations and cell voltage at each current density. Both CH_3OH and HNO_3 were added manually during the test to replace the coulombic equivalent consumed by the electrochemical reaction. No attempt was made to regenerate HNO_3.

Part b - Compatibility Problems

Initial performance, using C-type electrode structures at both the anode and cathode, was limited to 6.6 mwatts/cm^2 at 0.2 volts. Considerable gas accumulation was observed between the electrodes making continuous operation impossible. This was attributed to NO solution at the cathode and diffusion toward the anode. This had been observed previously in HNO_3 half-cell tests with this type of electrode.

To eliminate this gas accumulation, the C-type structure at the anode was replaced with either 80 or 150 mesh platinum screens. No gas pockets formed with this type of unit cell consisting of a screen anode and the C-type cathode.

Although the cell performance increased to 29.2 mwatts/cm^2 at 0.39 volts there were losses due to incompatibility of HNO_3 and CH_3OH at each of the electrodes. These losses were determined by comparing each electrode's performance during total cell operation with previous half-cell data for that electrode. The degree of compatibility at an electrode was found to be dependent on the treatment of the electrode before exposure to the opposing reactant in the total cell. For example, in cases where CH_3OH was pre-adsorbed on the anode and absorbed in the pores of the separator, HNO_3 performance was less than expected. This is shown in Figure C-3.

Figure C-3

CH_3OH-HNO_3 Cell Performance Following CH_3OH Pretreatment

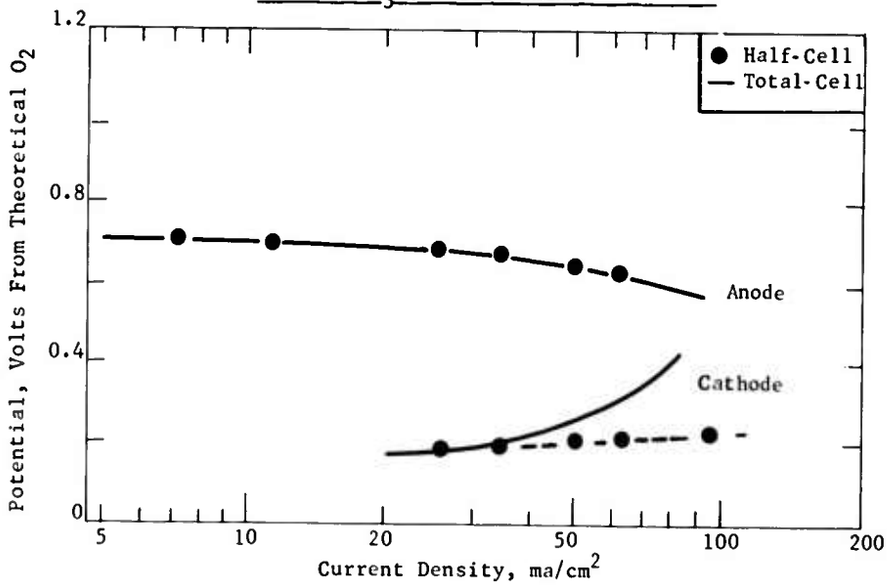

The reverse situation is shown in Figure C-4, where HNO_3 was introduced in the catholyte of the cell before CH_3OH, permitting its absorption in the separator.

Figure C-4

CH_3OH-HNO_3 Cell Performance Following HNO_3 Pretreatment

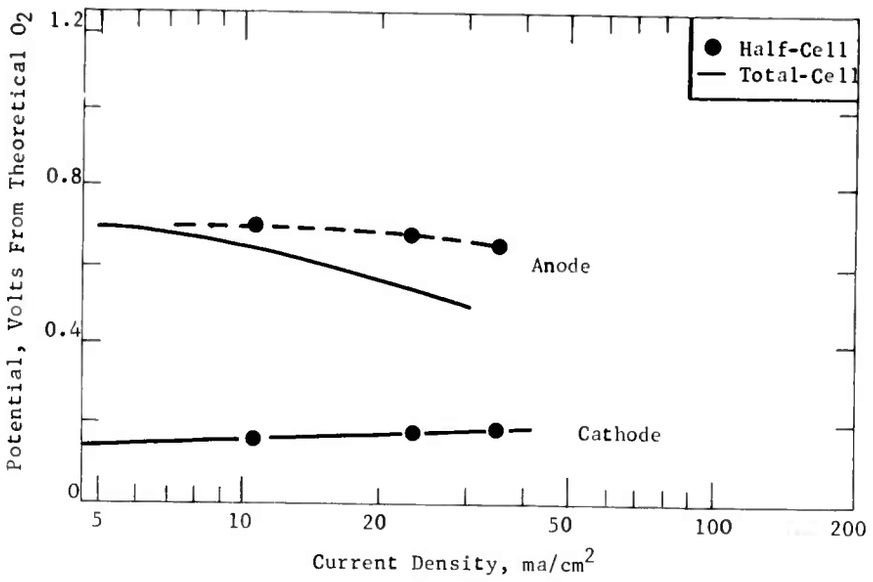

An improved start-up procedure, which improved compatibility during the nominal 3 to 4 hour test period, was devised. In this technique each reactant was adsorbed on its electrode prior to installation in the cell. The cathode was then anodized to remove CH_3OH and the anode was cathodized to remove HNO_3. The electrode potentials were maintained near H_2 at the anode and near O_2 at the cathode. CH_3OH and HNO_3 were then added to the anolyte and catholyte, respectively. Cell operation was initiated immediately. Performance improved to 31.6 mwatts/cm^2 at 0.22 volts with 1 vol % CH_3OH and 2 wt % HNO_3. The individual electrode performances agreed with measurements in half-cells of each electrode. This is summarized in Figure C-5.

Figure C-5

CH_3OH-HNO_3 Cell Performance Following CH_3OH And HNO_3 Pretreatment

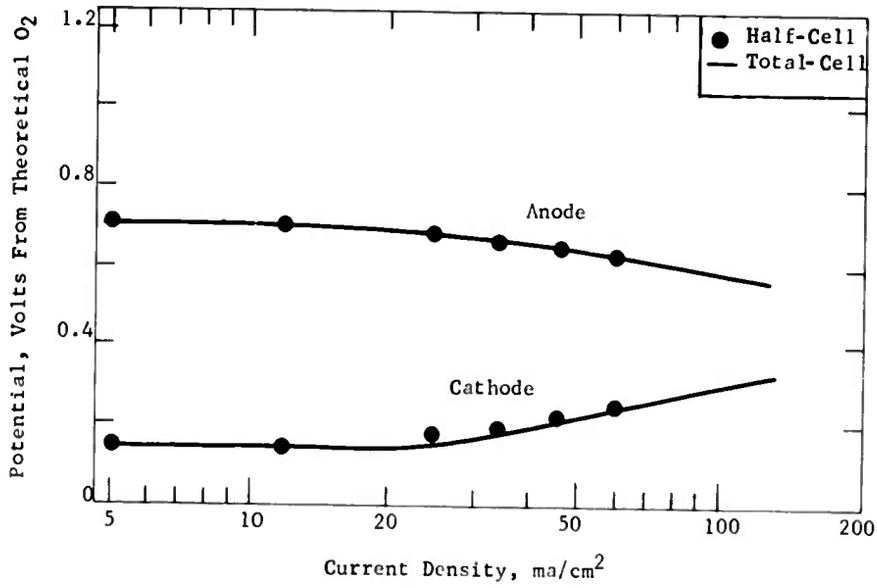

Part c - Cell Performance With Improved Cathode

With the improved start-up technique, high power levels were achieved from the CH_3OH-HNO_3 cell. With 1 vol % CH_3OH and 1 wt % HNO_3, up to 33.8 mwatts/cm^2 at 0.30 volts was maintained. The reactant concentrations were increased to 3 vol % CH_3OH and 2 wt % HNO_3 without additional losses due to incompatibility. The power output also increased to 44 mwatts/cm^2 at 0.34 volts. Furthermore, internal electrolyte IR losses were reduced to a negligible level. These performance levels were maintained during test periods of up to 8 hours of continuous operation. The results are summarized in Figure C-6 and all data is presented in Appendix C-23.

Figure C-6

CH_3OH-HNO_3 Fuel Cell Performance

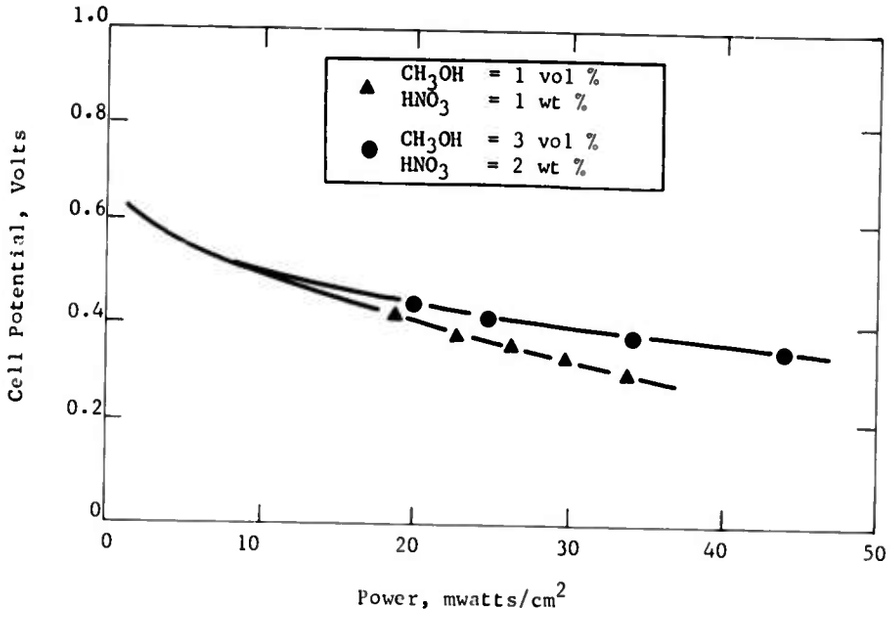

Phase 4 - Laboratory Studies Of The CH_3OH - Direct Oxygen Fuel Cell

Because of the difficulties in using a P-type catalyst in the presence of HNO_3, studies with this catalyst were carried out in total cells using direct oxygen electrodes instead of the HNO_3 redox electrode. The purpose was to check whether the improved performance attainable with the P-type catalyst will more than offset the lower performance of a direct oxygen electrode operating on air.

Part a - Experimental Systems

The experiments were carried out in the 4 inch diameter glass cell described in Appendix C-24. The cathode chamber was reduced in size to a thickness of only 68 mils. Unless otherwise noted, the P-5 catalyst was used at the anode and a 72 wt % Pt-28 wt % Teflon mixture was used at the cathode. The electrolyte generally contained 1.5 M CH_3OH in 30 wt % H_2SO_4. Experiments were carried out at temperatures ranging from ambient conditions to 82°C and generally with oxygen. Experiments with air have only recently begun. The results of these experiments are detailed in Appendices C-25 to C-26.

The major variable in these tests was the membrane used as the separator. The membrane is especially important in a methanol-direct oxidant fuel cell because it can control the rate at which electrolyte flows into the cathode from the fuel electrode electrolyte reservoir chamber.

Part b - Cell Performance

Cell performance with the Ionics CR-61 membrane proved to be the most stable and reproducible. At 61°C, using oxygen, net power outputs of 26 milliwatts/cm^2 at 0.26 volts were achieved at the terminals. Neglecting IR, power levels of 35 milliwatts/cm^2 at 0.35 volts were obtained. These data are illustrated in Figure C-7.

Figure C-7

Cell Performance - Ionics Membrane

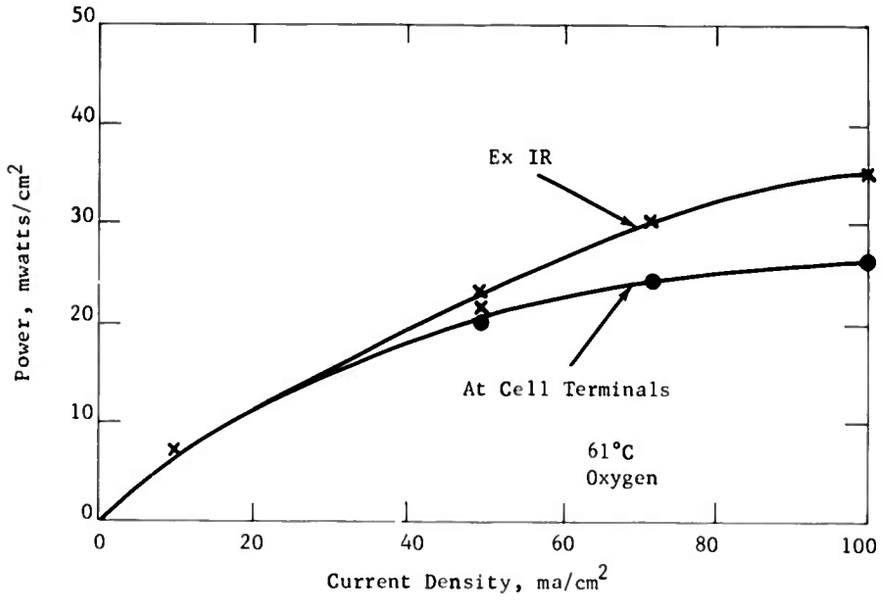

The fuel electrode performance was in close agreement with the results obtained in half cell studies. The oxygen electrode was polarized only 30 mv more than that expected from half cell studies, indicating little difficulty due to interactions with methanol.

Further increases in temperature with this membrane resulted in an irreversible increase in IR, possibly caused by partial drying of the membrane on the cathode side. Therefore a dual combination of an Ionics CR-61 and an A-type membrane was tested at 82°C. This cell, using O_2, produced 28 milliwatts/cm^2 at 0.28 volts at the terminals and 40 milliwatts/cm^2 at 0.40 volts neglecting IR losses. The performance of this system is presented in Figure C-8.

Figure C-8

Cell Performance-Dual Membrane

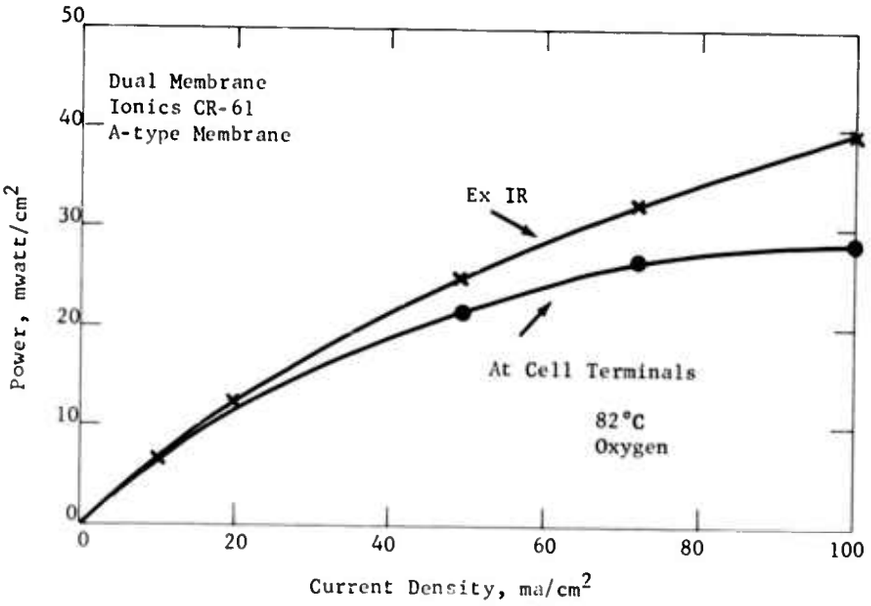

Tests using other membranes were less successful. These included Nalfilm D-30 membrane which appeared to be too porous, and an AMFion C-313 membrane whose IR loss proved to be too large.

Part c - Bi-cell Tests

Several tests were also carried out to evaluate the performance of two cells having a common 80 mil cathode chamber. Both cells in the package used P-5 catalyzed fuel electrodes, Pt-Teflon oxygen electrodes, and Ionics CR-61 membranes. The experiments were run at 50°C with oxygen and 54°C with air.

Performance of the two cells in series was in excellent agreement with the results expected from single cell tests. This was true for both oxygen and air. These results are summarized in Appendix C-27 and shown for oxygen in Figure C-9.

Figure C-9

Bi-cell Performance Vs Single Cell Results

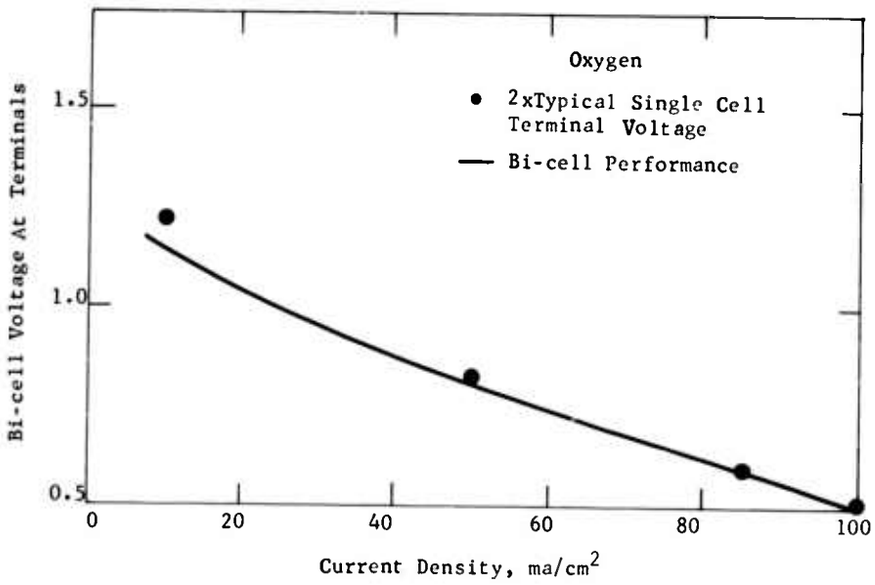

Phase 5 - The Water Balance

The balance between water production and water removal is particularly important for successful operation of a cell for extended periods of time. An improper balance can result in decreased or increased acid concentrations and flooding or drying of direct air electrodes. As a consequence, electrode performance would decrease, electrolyte IR would increase, and the over-all cell efficiency would be lowered. Therefore, a mathematical analysis was made of the effects of the major design and operating variables on the water balance in a methanol-direct air fuel cell.

Part a - Design Basis

The analysis was based on a single cell. However, its operation was also related by assuming a single air chamber that would service two air electrodes. Thus a multicell array would consist of a repeating pattern of the basic 2-cell module shown in Figure C-10. The end modules would be single cells with air chambers on the outside. Such modules are essentially isolated from each other and therefore can be treated independently.

Figure C-10

Simplified Fuel Cell Schematic

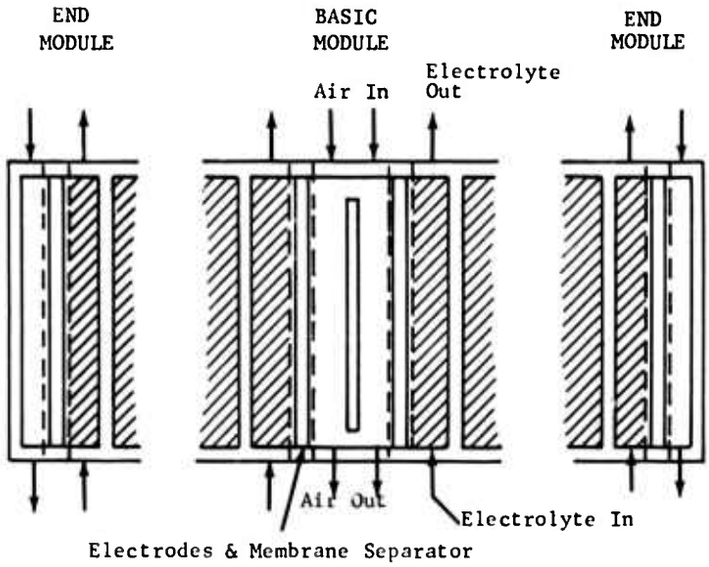

From previous considerations, it was assumed that the cells would operate in the temperature range of 60 to 80°C, electrolyte would be circulated upwards through the cells from a common reservoir, and the air, passing downward, would be used to remove water. The design further assumed that the air flow rate and its inlet temperature could be adjusted so that more water is removed than is generated. In this situation, the liquid level in the electrolyte reservoir could be used to control the amount of water in the air exhaust that is returned to the reservoir. Figure C-11 presents a schematic of this system.

Figure C-11

MULTIPLE FUEL CELL SCHEMATIC

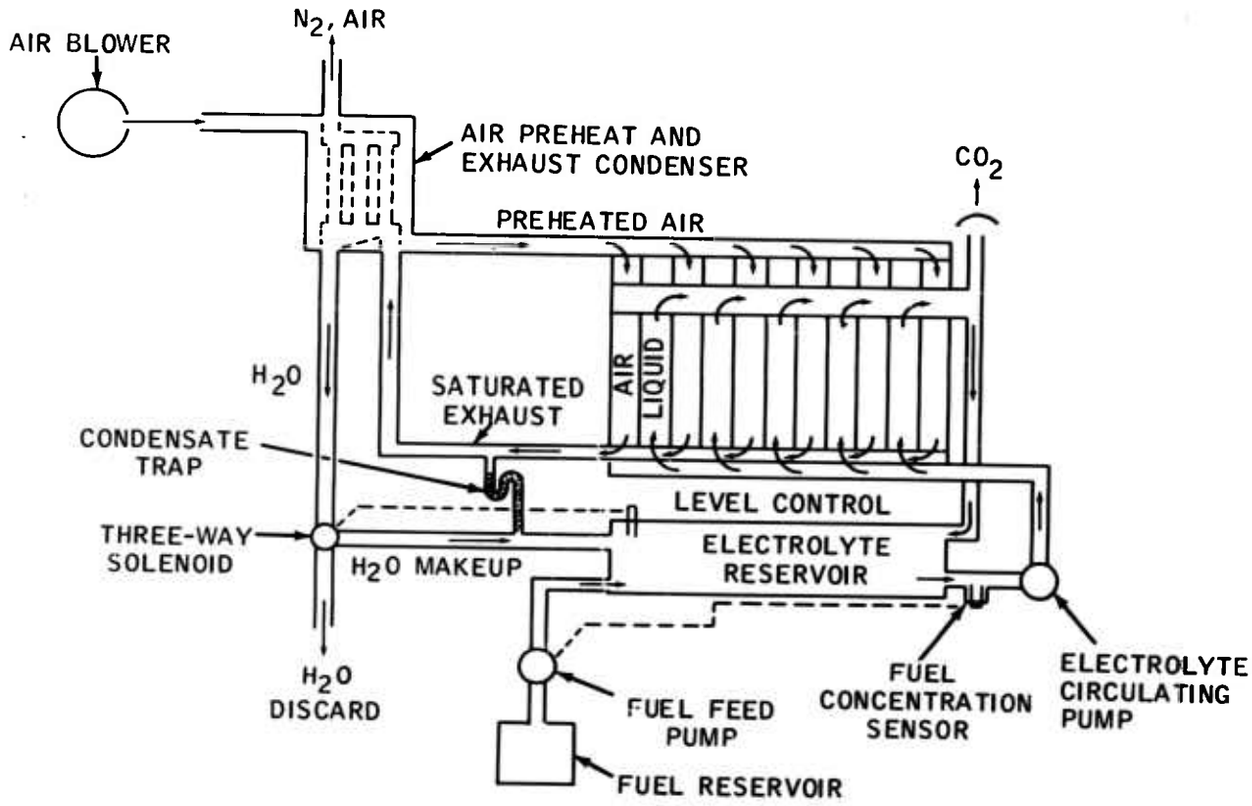

Part b - Effect Of Cell Design
On Exit Air Water Content

Since the air flow through the air chamber will be laminar, the amount of water removed will be controlled by the combined convective and diffusional transport of water within the air stream. On this basis, the average water content of the exit air (X_L) is related to the inlet air water content (X_i) by the following equation:

$$\frac{X_L - X_i}{X^* - X_i} = 1 - \left(\frac{B^2 v}{4\pi DL}\right)^{1/2} \qquad (1)$$

where X^* = molal humidity at the electrode interface
B = half thickness of the air chamber
L = electrode height
D = diffusivity of water in air
v = air velocity

Appendix C-28 analyzes this problem in greater detail. This derivation assumes, and it has been verified (see Appendix C-29), that heat conduction is sufficiently rapid within the cell so that temperature is not limiting.

Using the above equation it was found that in a thin air chamber and over a wide range of operating conditions, air leaves the chamber essentially in equilibrium with the acid. This is shown in Figure C-12 (and Appendix Table $\overline{C}$-1) in which the percent saturation is examined for various air rates and chamber thicknesses. These results were checked for current densities ranging from 15 to 100 ma/cm^2 at cell voltages of 0.2 to 8 volts.

Figure C-12

Exit Air Moisture Content For Various Air Chamber Thicknesses

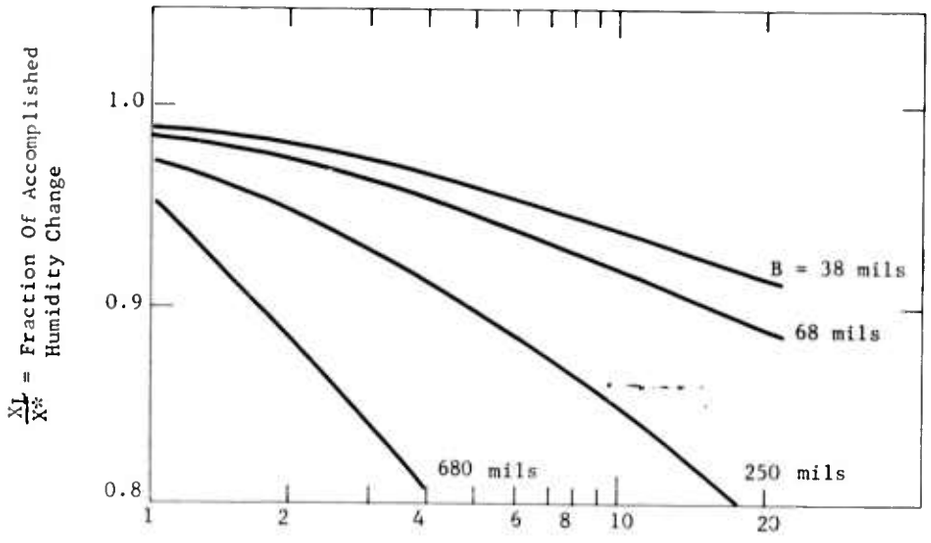

In this figure it is seen that in air chambers with half thicknesses of less than 100 mils, the air leaves the cell over 90% saturated. Since it is expected that half thickness of the air chamber will be about 68 mils, the saturation values will be used in further calculations.

Furthermore, the fact that the air stream leaves essentially at equilibrium permits evaluation of the rate of water removal and the exit air temperature under various conditions using only an over-all energy balance that takes into account the heat removed by both conduction and vaporization. In addition, it was assumed that all the heat generated is removed by the air stream. The validity of this assumption is discussed in Appendix C-29.

Part c - Dependence Of Water Removal On Air Rate

On this basis, it was calculated that the rate of water removal at constant current and voltage decreases slightly with increasing air rate. A twentyfold increase in air flow results in only a 20% change in the rate of water removal. This results from the fact that the exit air temperature decreases markedly with increasing air rate. Hence, the benefits of increased air capacity are offset by decreased temperature. This is illustrated graphically in Figures C-13 and C-14.

Figure C-13

Effect Of Air Rate On Water Removal

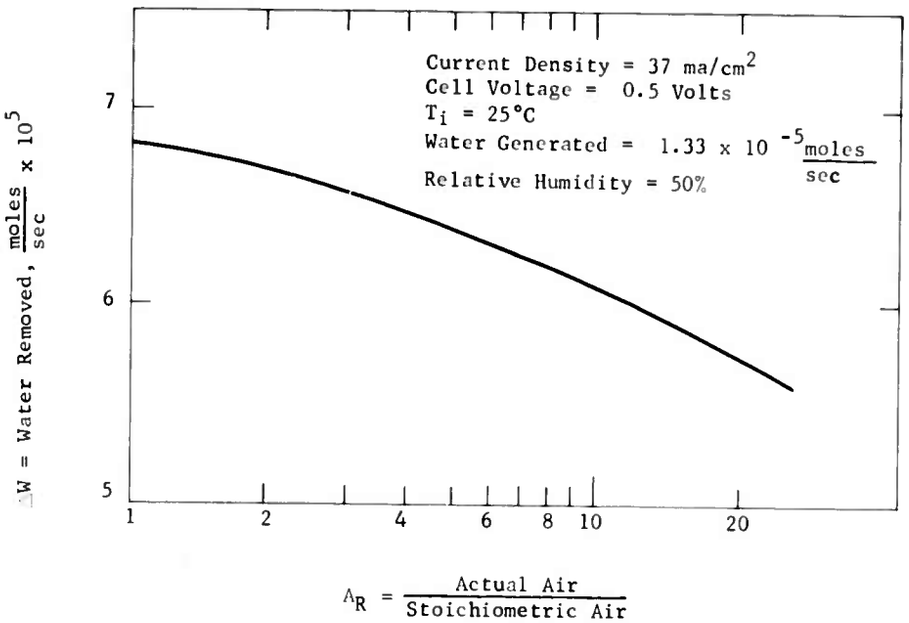

Figure C-14

Effect Of Air Rate On Air Temperature

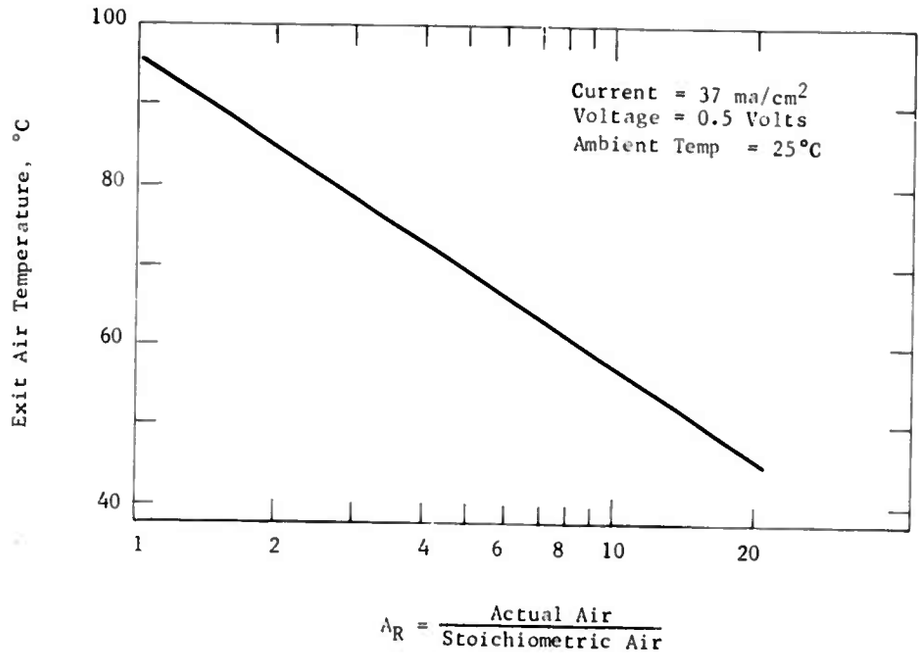

Part d - Dependence Of Water Removal On Current And Voltage

Similar analyses were made of the effect of varying current and voltage. These analyses showed that the rate of water removal should be relatively independent of current density, but markedly dependent on the output voltage. However, in all cases considered the rates of water removal were calculated to be substantially greater than the rates at which water is produced. This is shown in Figures C-15 and C-16.

Figure C-15

Effect Of Current On Water Removal

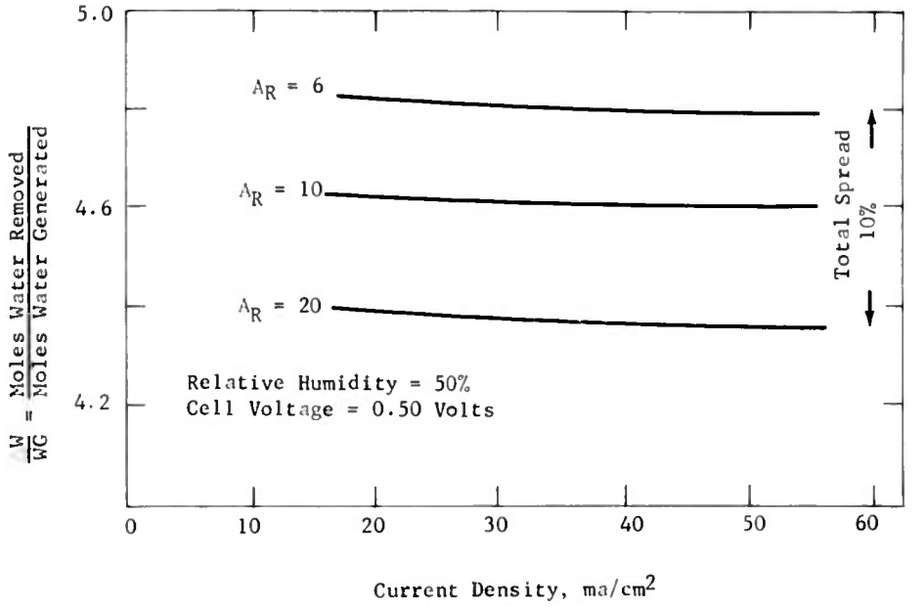

Figure C-16

Effect Of Efficiency On Water Removal

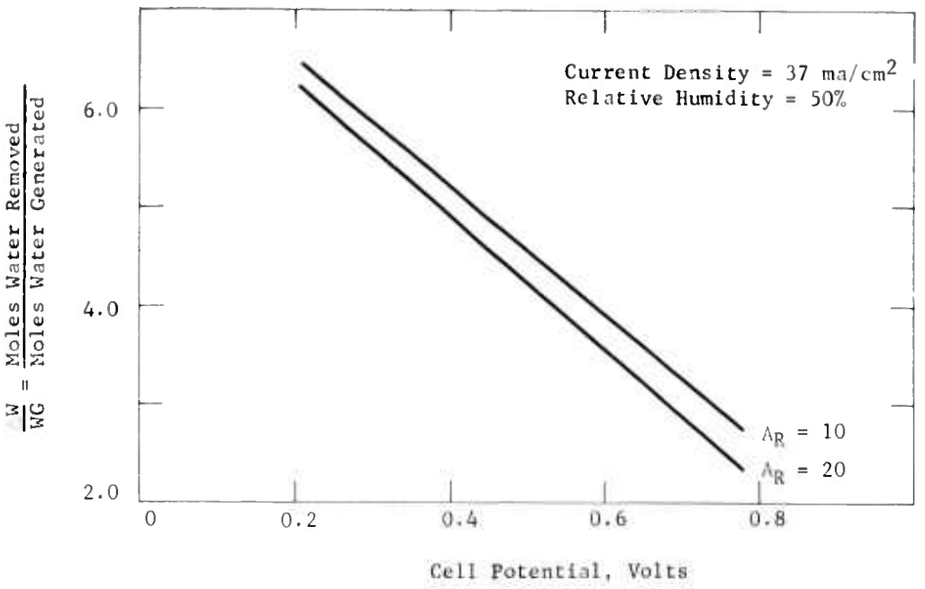

Similarly, as indicated in Figures C-17 and C-18, the exit air temperature changes markedly with cell voltage but is relatively independent of current density.

Figure C-17

Effect Of Current On Air Temperature

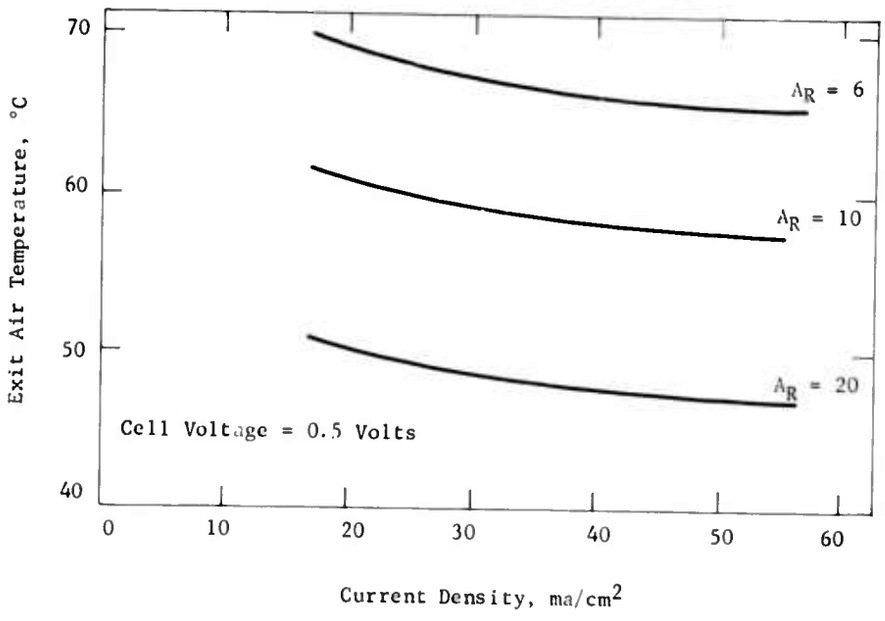

Figure C-18

Effect Of Cell Voltage On Air Temperature

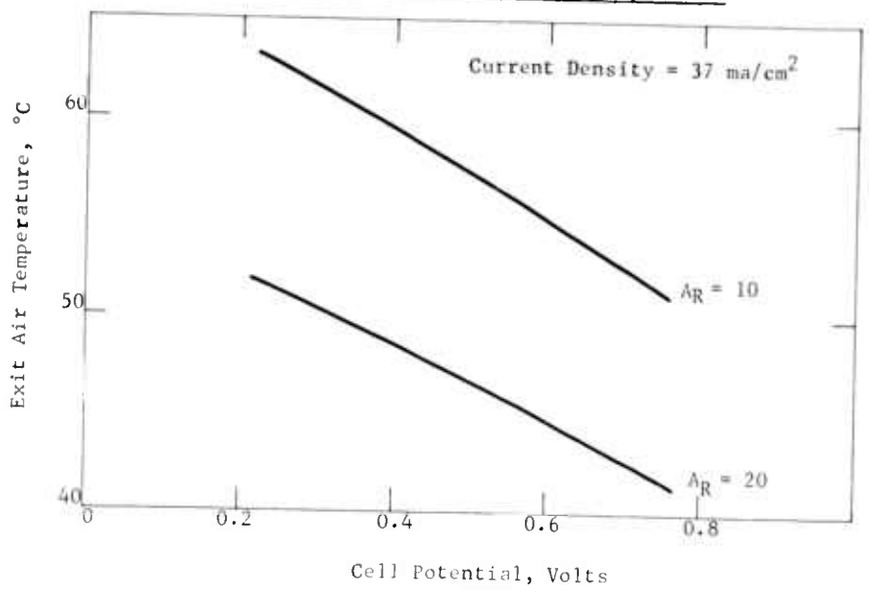

Part e - Effect Of Ambient Air
Temperature On Cell Operation

The previous analysis assumed that air entered the cell at 25°C. Therefore, additional calculations were made of the effect of varying the ambient air temperature on water removal and cell temperature. In this case, an air rate 10 times the stoichiometric requirement with a 50% relative humidity was assumed.

The calculations indicated that the air entering the system generally must be preheated by the air exhaust in order to attain the desired 60 to 80°C operating temperature range. This is shown in Figure C-19. It was also shown that the removal and condensation of excess water should not be a serious problem except at temperatures above 30°C where insufficient water would be condensed for maintaining the acid concentration of the electrolyte. (See Appendix Figure C-6). At these higher ambient temperatures, auxiliary cooling will be necessary.

Figure C-19

Effect Of Inlet Air Temperature On Mean Air Temperature

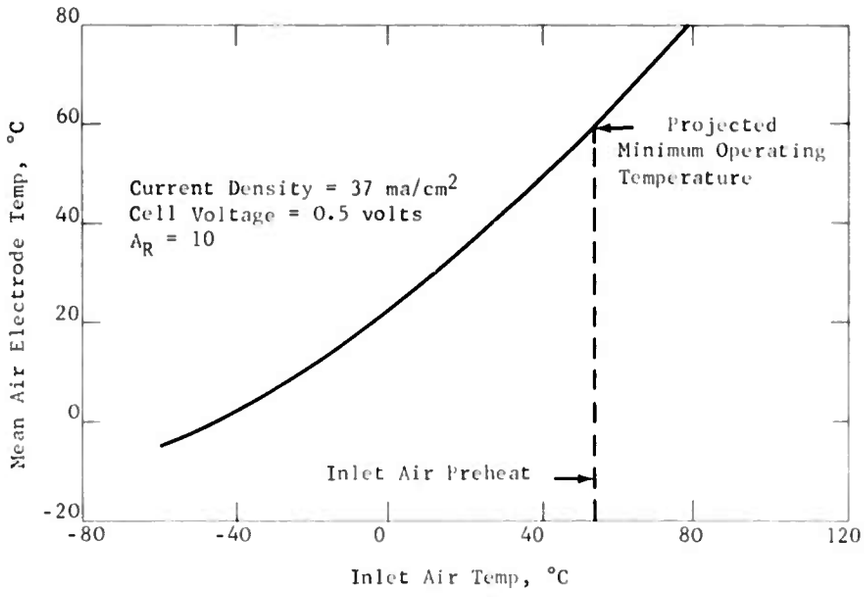

Phase 6 - Methanol Analyzer And Controller

A proprietary instrument has been evaluated as a means for monitoring the methanol concentration in the electrolyte in laboratory studies and for possibly controlling fuel addition to a fuel cell. In essence, the analyzer operates by measuring the peak current obtainable from a driven methanol microelectrode. Earlier studies indicated that the analyzer exhibited good electronic equipment stability with satisfactory short term electrode stability. Therefore, work has been directed toward selecting the best combination of analyzer cell electrodes and analyzer cycle conditions in terms of accuracy and long term performance.

Part a - Operating Conditions

The basic analyzer may be adjusted to provide a wide range of reaction severity conditions at the analyzer cell electrodes. Electrode performance studies were made under mild reaction conditions (designated as A), very severe reaction conditions (designated as B), and a compromise group of conditions, intermediate in severity (designated as C). The equipment was operated continuously with periodic checks of calibration stability and sensitivity to practical electrolyte system impurities.

Cell conditions included various concentrations of methanol up to a maximum of 4 vol % in 30 wt % H_2SO_4 electrolyte. All testing was carried out at room temperatures between 24 and 27°C. Continuous stirring of the electrolyte was used during part of the studies.

Part b - Cell Electrodes

Since the analyzer cell must be small and uncomplicated, simple platinum wire electrodes were chosen for the initial studies. The 0.05" diameter wire electrode surfaces were used as clean bright platinum or electrodeposited with platinum black at levels of 5 and 10 mg/cm^2. The working area was 1.2 cm^2 for the bright platinum and 0.8 cm^2 for the platinum black surface.

Part c - Electrode Performance

Bright Platinum Electrodes

The small surface area of the bright platinum electrodes produced low analyzer currents and was made even less effective by trace electrolyte impurities. Methanol calibration curves could be established in fresh electrolyte solutions but electrolyte from operating cells caused malfunctioning of the bright platinum electrodes. Analyzer response to the methanol in these solutions was very poor.

Platinum Black Electrodes -
Mild Analyzer Conditions "A"

Platinum electrodes with 5 mg/cm^2 of electrodeposited platinum black catalyst operating with mild analyzer conditions (condition A) provided a methanol concentration calibration curve as shown in Figure C-20. A peak current of 155 ma/cm^2 was produced by this analyzer condition at the 1.0 vol % methanol level.

Figure-20

Analyzer Calibration - Condition "A"

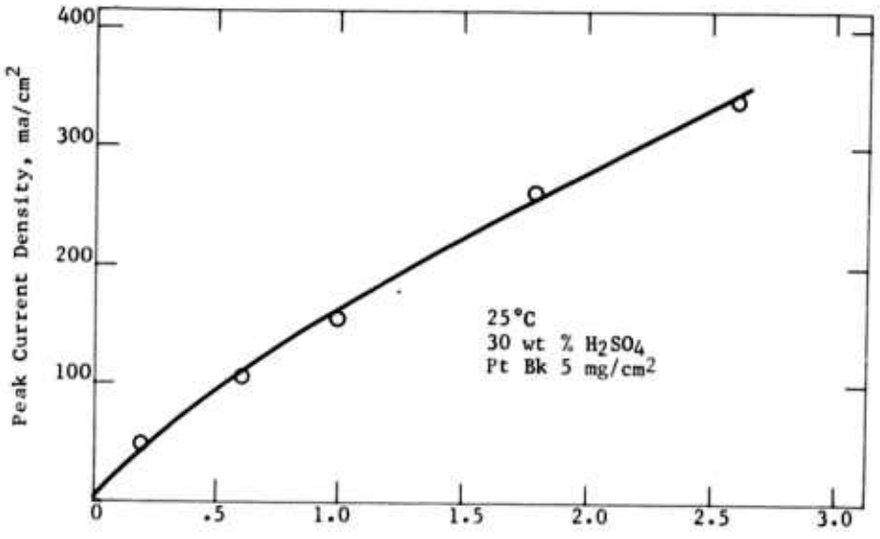

Under continuous operating conditions, the relationship between methanol concentration and analyzer current shown in Figure C-20 was maintained for part of one day and then began to change. After 72 hours the electrode performance had dropped so as to provide only 63% of the initial current response at 1.0 vol % of methanol. In addition to the decaying performance which started almost immediately under these operating conditions, response to changes in methanol concentration was slow. The methanol response of these electrodes improved to about 93% of the initial value by repeated cathodization and anodization. However, continued operation resulted in rapid loss of performance.

Platinum Black Electrodes -
Severe Analyzer Conditions "B"

Platinum electrodes with 5 mg/cm^2 of electrodeposited platinum black catalyst operating with severe analyzer conditions "B" provided a methanol calibration curve as shown in Figure C-21. Under these conditions 1.0 vol % of methanol provided an indicated analyzer peak current of 260 ma/cm^2.

Figure C-21

Analyzer Calibration - Condition "B"

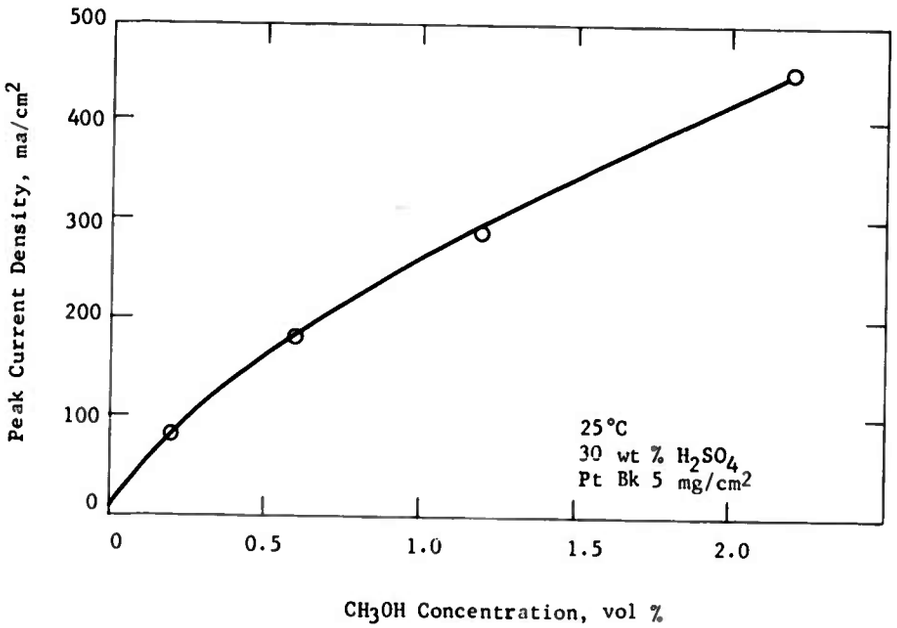

Response to changes in methanol concentration was rapid. After 48 hours of operation the response to 1.0 vol % of methanol was 97% of the initial value. This figure dropped to 89% at 72 hours and 73% at 96 hours.

Electrode performance continued to drop very sharply after 96 hours and considerable black debris was observed in the electrolyte. This was in the form of large pieces which dropped to the bottom of the analyzer cell and tiny particles which could be found on the wall of the glass cell by wiping with white paper. Inspection of the methanol electrode showed more than 40% of the surface to be free of catalyst. The remaining areas of catalyst were cracked and eroded.

Quite similar electrode performance was observed at a platinum black catalyst level of 10.0 mg/cm^2. Initial performance was about 8% higher than that obtained with 5.0 mg/cm^2. However, performance decay and physical loss of catalyst occurred over a period of about 100 hours.

Catalyst loss was not evident during a continuous oxygen evolution period of 36 hours. In addition, losses occurred under severe reaction conditions in an unstirred system.

Platinum Black Electrodes - Controlled
Sequence Analyzer Conditions "C"

Platinum electrodes with 10 mg/cm^2 of electrodeposited platinum black catalyst operating with analyzer conditions "C" provided a methanol calibration as shown in Figure C-22. A peak current of 175 ma/cm^2 was measured for 1.0 vol % methanol. Under these conditions, response to change in methanol concentrations is less rapid than conditions "B". However, long term stability appears excellent as evidenced by a continuing analysis period now approaching 300 hours of operation with no loss in electrode performance.

Figure C-22

Analyzer Calibration - Condition "C"

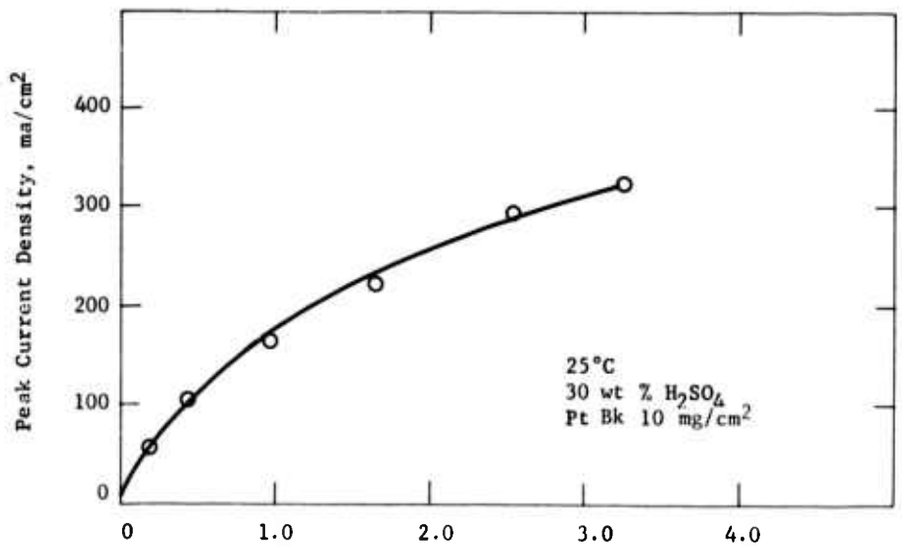

Part d - Methanol Analyzer As A
Laboratory Operations Monitor

During the electrode performance studies the analyzer has been used to determine methanol concentration levels in some of the half cell and full cell laboratory operations. Even though electrode stability difficulties were encountered on a long term basis, sufficient stability was obtained with severe analyzer conditions "B" to provide good analysis of unknown samples. To limit the amount of samples required from an operating unit, most unknown samples were run at one fifth their initial concentration rather than attempting to work at a sample cell volume of less than 100 ml. This required the establishment of a calibration curve in the 0.1 to 0.4 vol % methanol range as shown in Figure C-23.

Figure C-23

Analyzer Calibration - Condition "B"

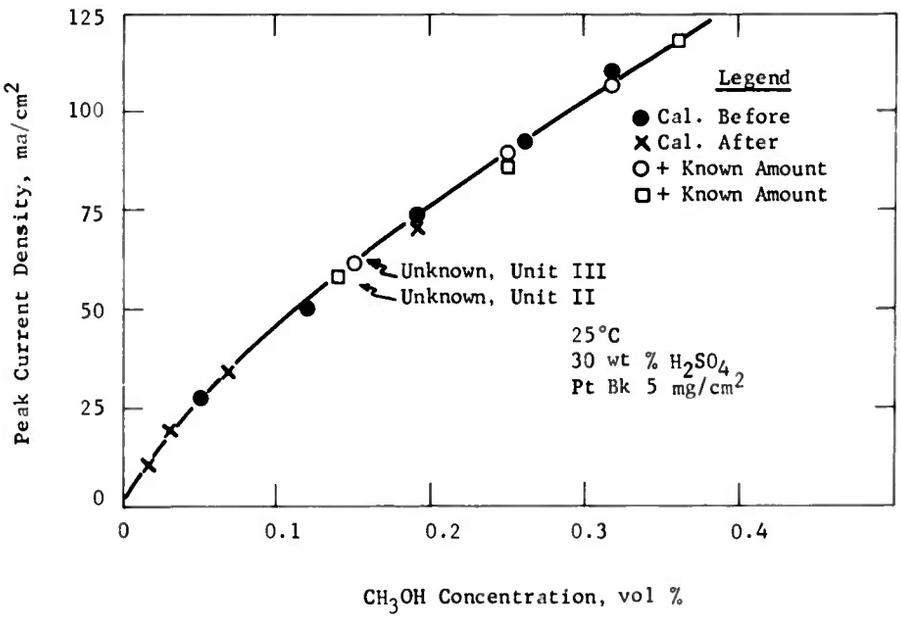

In addition to calibration points obtained before and after a series of unknowns, two unknown samples are shown at assigned values of 0.14 and 0.15 vol % methanol. The validity of these assignments was verified by adding known amounts of methanol to the unknowns and observing their relationship to the calibration curve. A number of unknowns were evaluated as shown in Table C-2.

Table C-2

Analyzer Performance - Sample Analysis

Sample	Analyzer Results, vol % CH_3OH	Corrected for Dilution, vol % CH_3OH	Known Concentration, vol % CH_3OH
1	1.25	--	1.2
Unit II	0.14	0.70	<1
Unit III	0.15	0.75	<1
Unit IV	1.3	6.5	>2
CHW I	1.05	5.25	>4
CHW II	0.2	1.00	<1
CHW III	0.39	1.95	2
3475-32	0.38	1.9	2

There appeared to be good agreement between the methanol concentration values as determined by the analyzer and known values established later. The analysis also confirmed suspected reasons for operating unit difficulties, i.e. fuel electrode failure due to low methanol concentration. Appendix C-30 presents a complete summary of these results.

Phase 7 - Materials Of Construction

The screening of possible plastics for use in multicell systems was initiated. Several materials were tested for both physical and chemical stability and for possible harmful effects to the fuel cell catalysts.

Part a - Initial Testing

Polypropylene, an epoxy resin, Viton, Penton, and Lustran were examined. In these initial tests, the materials were subjected to 4-hour treatments in 30 wt % H_2SO_4. Samples of the materials were also treated with 2 wt % HNO_3-30 wt % H_2SO_4 solutions followed by 30 wt % H_2SO_4. The resulting 30 wt % H_2SO_4 solutions were used as electrolyte in performance tests made at 60°C with 1 vol % CH_3OH using a platinum black on a 2 cm^2 platinum sheet electrode. The results were compared with standard solutions not subjected to testing materials.

Polypropylene, epoxy resin, Viton, and Penton proved satisfactory when tested for methanol performance. Lustran was unsuitable, showing a harmful influence on methanol performance. Physically, Lustran, Viton and epoxy resin showed weight gains evidencing chemical attack by the electrolyte. Penton and polypropylene were inert. Detailed data are given in Appendix C-31.

Part b - Further Testing

In view of these screening tests, a section of polypropylene was installed in a half cell for further testing its contamination influence on the methanol-H_2SO_4 system. The section of polypropylene, measuring 1/16" thick by 4" square, with circulation holes therein, was positioned in the electrolyte chamber. The half cell was operated at 50 ma/cm^2 and 82°C with 1 vol % methanol in 30 wt % H_2SO_4. The electrode consisted of platinum black on an 80 mesh platinum-rhodium screen. The polarization at this methanol electrode remained essentially unchanged for 313 hours, the duration of the test, showing polypropylene to be a suitable construction material. These data are highlighted in Table C-3.

Table C-3

Effect Of Polypropylene On Methanol Anode Performance

Run Hour	Polarization, volts
3	0.51-0.53
48	0.52-0.54
216	0.48-0.54
313	0.50-0.56

SECTION 5

CONCLUSIONS

5.1 Task A, Fuel Electrode

Phase 1 - Performance And Preparation Of New Catalysts

The compensating effect of changes in Tafel slope and exchange current upon each other, which acts to restrict the activities of a wide variety of catalysts to the same region, has again been observed. However, several exceptions, such as Pt-Ru-Fe, have been found and these are all more active than Pt. However, none is as active as the P-type catalyst.

The technique used to reduce Pt or binary catalysts does not appear to greatly influence the performance obtained. In a few cases slight improvements or decreases in activity occurred, but generally no significant changes were observed. Generally, there was also little effect upon the kinetic parameters of these catalysts. The influence of changes in other phases of the preparation procedure were also generally negligible.

It is possible to prepare catalysts with the same or slightly higher activity than Pt which are less expensive. This has been demonstrated by the incorporation into Pt of a large proportion of Au and a smaller amount of Fe. A considerable part of this Fe is leached from the catalyst and a Raney type structure may be responsible for the observed benefits. However, further improvements in performance and enhanced stability must be achieved before practical use can be made of this approach.

Phase 2 - Preparation Of P-Type And Modified P-Type Catalysts

The P-type and modified P-type catalysts continue to be the most active fuel electrode catalysts. No new preparation methods have been found which give higher activity than the original aqueous $NaBH_4$ reduction technique. Variations in reduction agents, solutions, and other conditions produced only catalysts of equal or inferior performance to the standard samples.

The method of storage of P-type electrodes prior to use is critical to the activity observed. The most suitable storage media are aqueous or H_2SO_4 solutions of CH_3OH or HCHO, which maintain the optimum activity even after prolonged immersion.

The modification of P-type catalysts results in materials of widely varying activities, depending upon the nature of the modification. However, the ordinary P-type catalyst continues to be equal to the best of the modified types prepared.

Phase 3 - Variable Studies Using P-Type Catalysts

The performance of the P-type catalyst improves with increasing temperature, the activation energy indicating an electron transfer limiting reaction mechanism. The catalyst is also sensitive to fuel concentration up to a certain amount, beyond which it is relatively independent of it. The value of this threshold decreases

with increasing temperature, amounting to about 0.4 M at 80°C.

The P-type electrode can, under certain conditions, be operated for extended periods of time with very stable performance. However, attempts at further stabilizing the P-type electrode were inconclusive and additional studies are necessary.

The presence of O_2 or HNO_3 reduces the performance of the P-type catalyst. The effect of O_2 is small, a saturated electrolyte reducing electrode output by about 10 mv. However, HNO_3 in sufficient amounts can reduce it by as much as 0.2 volts.

Phases 4 and 5- Performance Of Pt Electrodes In Rhenium Containing Electrolytes; Mechanism Of Pt-Re_2O_7 Catalysis

Improvements in performance with Pt or Pt + Au electrodes and CH_3OH fuel are obtained by adding small amounts of Re_2O_7 to the electrolyte. A similar effect is achieved by predipping the electrode in a Re_2O_7 solution.

The Pt-Re_2O_7 - fuel interaction appears to be a surface redox process, analogous to the Pt-MoO_3-fuel system. Adsorbed Re^{+7} is reduced by the fuel to the +6 state, the fuel being simultaneously oxidized to CO_2 and H^+. The +6 species is then electrochemically oxidized back to +7, completing the cycle.

5.2 Task B, Air Electrode

Phase 1 - HNO_3 Redox Performance Using C-Type Electrodes

Improved performance of the HNO_3 redox cathode can be obtained by using a new C-type electrode structure in place of the conventional Pt screen. Thus up to 70 mv benefit was observed with the new structure compared to an 80 mesh Pt screen.

Phase 2 - Direct O_2 Electrodes

Active direct O_2 electrodes can be made by application of a mixture of Pt and Teflon powders to a Pt screen support. Apparently the wetting properties of this system are important, as shown by the influence on performance of the amount of Teflon used. These electrodes are not, however, sensitive to the flow rate of O_2 after about twice the stoichiometric value has been exceeded. Although the direct O_2 system performs best in H_2SO_4 concentrations below the standard 3.7 M, total cell resistance considerations might rule out the use of a more dilute, less conductive electrolyte until less resistive cells are developed. Half-cell tests therefore will continue to be run in 3.7 M H_2SO_4.

The properties of Pt as a direct O_2 catalyst can be changed by incorporating other metals by means of simultaneous reduction with $NaBH_4$. As yet however, no significantly more active catalysts have been found.

5.3 Task C, The Total Cell

Phases 1, 2, and 3 - Cell Design Studies: CH_3OH-HNO_3 - Air Fuel Cell; Life Studies In The CH_3OH-HNO_3 - Air Fuel Cell; Performance Of New Electrode Structures In The CH_3OH-HNO_3 Fuel Cell

Further improvements have been made in the design of a compact CH_3OH cell. A long term test of over 1000 hours duration with a Pt fuel electrode demonstrated that performance could be maintained for extended periods with only a slight decrease in performance. Furthermore, this decrease is recoverable by the addition of fresh electrolyte. In addition, fuel chambers as small as 25 mils thick could be used without either impairing CO_2 release or decreasing electrode performance.

Testing of the same cell as a complete CH_3OH-HNO_3 - air fuel cell for 181 hours demonstrated that compatible operation (23 milliwatts/cm^2 at the terminals; 40 milliwatts/cm^2, neglecting IR) is obtainable. Furthermore, maintaining high CH_3OH conversion rates by using either low CH_3OH electrolyte circulation rates or operating at high current densities results in negligible CH3OH losses and improved HNO_3 regeneration efficiencies.

Additional tests using a C-type electrode structure at the cathode demonstrated that further increases in power out to 44 milliwatts/cm^2 are attainable in a CH_3OH-HNO_3-air fuel cell.

Phase 4 - Laboratory Studies Of The CH_3OH - Direct Oxygen Fuel Cell

Experiments in the compact glass cell have demonstrated that the P-type catalyzed fuel electrode can operate at its expected performance levels in a CH_3OH - direct O_2 fuel cell. The results show that power levels of 28 milliwatts/cm^2 are attainable at the terminals with good prospects of further increasing this value to 40 milliwatts/cm^2. In addition, the feasibility of operating two cells with a common air chamber has been demonstrated.

Phase 5 - The Water Balance

The mathematical analysis of heat and water transport has indicated that the water balance in a cell may be maintained by always removing in the air stream more water than is produced and then using the electrolyte liquid level to control the amount of water that is discarded. The analysis indicated that the temperature of a cell and the rate of water removed will be relatively insensitive to current density and would decrease linearly with increasing air rate and cell voltage.

Phase 6 - Methanol Analyzer And Controller

A reliable and electronically stable CH_3OH analyzer has been developed for use in the laboratory and for possible eventual use as a feed controller in a multicell system. The unit and its associated electronics equipment are appropriately compact and utilize relatively little power.

Phase 7 - Materials Of Construction

A variety of plastic materials have shown promise for use in the CH_3OH fuel cell. Of particular interest is polypropylene, which has been shown to maintain its physical properties in over 300 hours of testing and causes no harm to Pt catalysts.

SECTION 6

PROGRAM FOR NEXT INTERVAL

The work carried out in the first half of 1963 primarily concentrated on the development of a compact methanol fuel cell employing the HNO_3 redox air electrode, and on investigations aimed at improving fuel electrode catalyst performance with particular emphasis on translating these results into compatible electrode-electrolyte systems. Research during the remainder of the year will center on the development of improved fuel and direct air electrodes with some increased emphasis on the incorporation of these components into single and multicell systems.

The past and projected distribution of effort on each of these tasks are as follows. The exact division of emphasis, of course, will depend on the rates of progress in each area.

Task	Title	Effort Expended in 1963, % Actual Jan-June	Projected July-Dec
A	Fuel Electrode	35	20
B	Air Electrode	22	30
C	Total Cell	42	25
D	Multicell Systems	1	25

It is expected that these efforts will concentrate on the following aspects:

6.1 Task A, Fuel Electrode

Since significant progress has been made in developing an improved catalyst, compositing and testing of new catalyst systems will be carried out at a reduced rate of effort. Further studies will primarily center on establishing or extending the life of the presently developed catalysts. In addition, some work will be carried out on developing less expensive catalyst compositions.

6.2 Task B, Air Electrode

The air electrode is presently the area where the largest increase in cell efficiency can be made. Therefore the screening of new catalyst compositions will receive greater attention. In addition, efforts will be directed toward tailoring the air electrode structures to the requirements of the methanol fuel cell.

6.3 Task C, Total Cell

The newly developed compact cells have proven to be rugged and reliable. These will be used in evaluating the performance of cell components in sustained operation. Included will be studies of problems associated with feed introduction, product removal, startup, and transient operation. In addition the cells will be used to assess new materials and improve cell components.

6.4 Task D, Multicell Systems

Work has been initiated on the design and construction of multicell units. These units will be used to study the problems attendent to multicell operation, especially in terms of their effects on the individual cell components. Particular attention will be given to inventory control, temperature maintenance, and startup.

SECTION 7

IDENTIFICATION OF PERSONNEL AND DISTRIBUTION OF HOURS

7.1 Background of New Personnel

Kenneth Lewis (Ph.D., Physical Chemistry, New York University) joined Esso Research and the fuel cell section in 1962. His doctoral research consisted of an investigation of the effects of products produced by X-irradiation of electrolyte on the electrode behavior of bright platinum. His present work involves improvement of the air electrode catalyst.

Eugene H. Okrent (M.S., Chemical Engineering, Newark College of Engineering) has been at Esso Research since 1956 primarily engaged in long-range lubrication research. This study evolved six published papers on radio tracer research, lubrication of nuclear power surface vessels, bearing lubrication, rheology, and surface phenomena. Prior to employment at Esso, he served in the U.S. Army Chemical Corps and worked as a field engineer for the Committee on Fire Protection and Engineering Standards of the National Board of Fire Underwriters. His present assignment involves the solution of problems involving heat and mass transport within multi-cell systems.

7.2 Distribution of Hours

The following are the technical personnel who have contributed to the work during the reporting period 1 January 1963 - 30 June 1963 and the approximate number of hours of work performed by each:

Carl E. Heath	374
Barry L. Tarmy	941
I-Ming Feng	960
Eugene L. Holt	473
Kenneth Lewis	480
Duane G. Levine	781
Andreas W. Moerikofer	914
Eugene H. Okrent	670
Joseph A. Shropshire	899
James A. Wilson	901
Charles H. Worsham	864
Total	8257

SECTION 8

REFERENCES

(1) Heath, C. E., Tarmy, B. L., et al, Soluble Carbonaceous Fuel-Air Fuel Cell, Report No. 1, Contract DA 36-039 SC-89156, 1 Jan. 1962 - 30 June 1962.

(2) Tarmy, B. L., et al, Soluble Carbonaceous Fuel-Air Fuel Cell, Report No. 2, Contract DA 36-039 SC 89156, 1 Jan. 1962 - 31 Dec. 1962.

(3) Sidgwick, N. V., Chemical Elements and Their Compounds, Vol. II, Oxford University Press, London, 1950.

(4) Delahay, P., New Instrumental Methods in Electrochemistry, Interscience Publishers, Inc., New York, N. Y., 1954.

(5) Carslaw, H. S. and Jaeger, J. C., Conduction of Heat in Solids, 2nd ed., Oxford, Clarendon Press, 1959.

APPENDIX A-1

PREPARATION AND TESTING OF $NaBH_4$ REDUCED CATALYSYS

Electrode	Composition, Atom%	Preparative Solution, Moles/Liter Salt	$NaBH_4$	Polarization vs. Theor. CH_3OH @ Indicate ma/cm² 0	1	10	50	100	b	-Log i₀	Remarks *
Pd-Re 280		0.25 $PdCl_2$, 0.25 Re_2O_7	1.85	.41	.58	.69	.75	---	120	A 2	
Pt-Ag 283		0.25 Na_2PtCl_6, 0.25 $AgNO_3$	"	---	---	---	---	---	---	---	no activity
Pt-U 286		0.25 " , 0.25 $UO_2(NO_3)_2$	"	.37	.52	.58	.62	.64	.062	8.3	
Ru-Re 287		0.25 $RuCl_3$, 0.25 Re_2O_7	"	---	---	---	---	---	---	---	no activity
Sn-Re 288		0.25 $SnCl_2$, "	"	---	---	---	---	---	---	---	no activity
Zn-Re 289		0.25 $ZnCl_2$, "	"	---	---	---	---	---	---	---	no activity
Au-Pd 291		0.25 $HAuCl_4$, 0.25 $PdCl_2$	"	---	---	---	---	---	---	? 8	no activity, Pt dissolved
Pt-Ni 292		0.25 $PtCl_4$, 0.25 $NiCl_2$	"	.43	.55	.62	.66	.69	.070	---	
Au-Re 293		0.08 $HAuCl_4$, 0.42 Re_2O_7	"	---	---	---	---	---	---	---	no activity
Au-Re 295		0.20 " , 0.30 "	"	---	---	---	---	---	---	---	no activity
Au-Re 296		0.30 " , 0.20 "	"	---	---	---	---	---	---	---	no activity
Au-Re 297		0.25 " , 0.25 "	"	.46	.67	.77	.89	---	---	---	
Au-Re 299		0.25 " , 0.25 "	"	---	---	---	---	---	---	---	no activity
Pt-Cr 300		0.25 Na_2PtCl_6, 0.25 $Cr(Ac)_3$	"	.46	.53	.60	.64	.67	.069	" 7	
Pt-Zn 301		0.25 " , 0.25 $ZnCl_2$	"	.39	.47	.53	.57	.59	.058	8.7	
Au-Re 302		0.275 $HAuCl_4$, 0.225 Re_2O_7	"	---	---	---	---	---	---	---	no activity
Au-Re 303		0.225 " , 0.275 "	"	---	---	---	---	---	---	---	no activity
Pt-Sn 304		0.25 Na_2PtCl_6, 0.25 $SnCl_2$	"	.38	.49	.57	.61	.65	.064	5.8	
Pt-Au 310	Pt-86.8, Au-13.2	0.40 " , 0.10 $HAuCl_4$	"	.36	.45	.53	.58	.59	.060	7.0	
Pt-Cu 311	Pt-48.2, Cu-51.8	0.40 " , 0.10 $CuCl_2$	"	.40	.49	.55	.59	.62	.060	8.1	
Pt-Cu 312	Pt-36.6, Cu-63.4	0.30 " , 0.20 "	"	.40	.50	.57	.61	.63	.065	7.5	
Pt-Cu 313	Pt-38.6, Cu-61.4	0.20 " , 0.30 "	"	---	.45	.55	.62	.65	.100	4.1	
Pt-Cu 314	Pt-28.4, Cu-71.6	0.10 " , 0.40 "	"	.03	.09	.52	.62	...	...	...	no Tafel region observed
Pt-Au 318		0.30 " , 0.20 $HAuCl_4$	"	.35	.43	.51	.56	.58	.061	8.3	
Pt-Au 319		0.20 " , 0.30 "	"	.36	.47	.55	.60	.63	.072	6.6	
Pt-Au 320	Pt-21.2, Au-78.8	0.10 " , 0.40 "	"	.38	.52	.61	.67	.70	.087	6.0	
Pt-Ni 321		0.40 " , 0.10 $NiCl_2$	"	.38	.48	.56	.59	.62	.063	6.6	
Pt-Ni 322	Pt-53.6, Ni-46.4	0.30 " , 0.20 "	"	.29	.42	.49	.54	.59	.087	5.8	
Pt-Ni 323		0.20 " , 0.30 "	"	.22	.40	.47	.52	.58	.076	5.2	
Pt-Ni 324	Pt-71.1, 28.9	0.10 " , 0.40 "	"	.31	.41	.50	.55	.58	.073	5.9	
Pt-Ru 421		0.40 " , 0.10 $RuCl_3$	"	---	---	.51-.65	---	---	---	---	.45 volts polarization at 90°C
Pt-Ru 422		0.30 " , 0.20 "	"	---	---	.50	---	---	---	---	.41 volts polarization at 90°C
Pt-Ru 423		0.20 " , 0.30 "	"	---	---	.48-.61	---	---	---	---	
Pt-Ru 424		0.10 " , 0.40 "	"	---	---	.47	.49-.56	---	---	---	values at 50 ma/cm² taken at 90°C - .56 volts polarization after addition of 0.2 wt % HNO_3
Pt-Ru 425		0.10 " , 0.50 "	"	---	---	---	.48	---	---	---	Run in 1 M H_2SO_4 - 0.5 M CH_3OH - 90°C
Pt-Au 427	Pt-67, Ru-33			---	---	---	.49	---	---	---	1 M H_2SO_4 - 0.5 M CH_3OH - 90°C, thermal Mixture of Pt and Ru
Pt-Ru 428		0.05 " , 1.0 "	"	---	---	---	.41	---	---	---	1 M H_2SO_4 - 0.5 M CH_3OH - 90°C
Pt-Ru 429		0.025 " , 1.0 "	"	---	---	---	.43-.61	---	---	---	1 M H_2SO_4 - 0.5 M CH_3OH - 90°C, .61 volts polarization after addition of 0.2 wt % HNO_3
Pt-Ru 437		0.08 " , 0.80 "	"	---	.22	.31	.38-.63	.42	---	---	1 M H_2SO_4 - 0.5 M CH_3OH - 90°C, .64 volts polarization after addition of 0.2 wt % HNO_3
Pt 433		0.50 " , ---	"	---	.14	.44	.48	.49	.074	8.5	1 M H_2SO_4 - 0.5 M CH_3OH - 90°C, addition of 0.2 wt % HNO_3 caused no further polarization
Pt-Ru 436		0.125 " , 0.25 $RuCl_3$	"	---	---	.37	.41	---	---	---	1 M H_2SO_4 - 0.5 M CH_3OH - 90°C
Pt-Ru-Fe 439		0.07 " , 0.70 ", 0.07 $FeCl_3$	"	---	---	.46	.47	---	---	---	
Pt-Ru-Fe 441		0.07 " , 0.70 ", 0.07 "	"	---	---	---	.37-.97	---	---	---	1 M H_2SO_4 - 0.5 M CH_3OH - 90°C, .97 volts polarization after addition of 0.2 wt % HNO_3

*All runs in 3.7 M H_2SO_4 - 1 M CH_3OH at 60°C with pressed electrodes unless otherwise noted.

APPENDIX A-2

PREPARATION STUDIES OF BOROHYDRIDE REDUCED CATALYSTS

Electrode	Run No.	Composition, Atom %	Preparative Solution, moles/liter Salts		NaBH4	Polarization vs Theor CH_3OH @ Indicated ma/cm² 10	50	100	b	-Log i_o	Remarks on Catalyst Preparation*	Remarks on Electrode Testing**
Pt	1		0.055 H_2PtCl_6		0.50	0.52	0.56	0.61	0.05	9.3	reduced in absolute CH_3OH	
	10		0.110 $PtCl_4$ anhydr		0.50	0.52	0.56	0.58	0.06	7.6	reduced in heptane with L-type reducing agent	
	11		0.001 H_2PtCl_6,		0.01	0.52	0.56	0.61	0.06	7.6	reduced in absolute CH_3OH	
	12		0.002 "		0.01	0.50	0.55	0.57	0.07	6.8	reduced in abs CH_3OH	
	13A		0.005 "		0.05	0.51	0.54	0.55	0.04	12.7	reduced in abs CH_3OH, catalyst handled in argon atmosphere	
	13B		0.005 "		0.05	0.51	0.56		0.06	8.0	reduced in abs CH_3OH, pressed onto electrode at 5000 psi under argon	
	13C		0.005 "		0.05	0.46	0.52	0.54	0.08	5.6	reduced in abs CH_3OH, pressed onto electrode at -78°C	
	13E		0.005 "		0.05	0.53	0.58		0.07	7.0	reduced in abs CH_3OH, pressed onto electrode at 500 psi	
	13F		0.005 "		0.05	0.51	0.56		0.06	8.2	reduced in abs CH_3OH, pressed onto electrode at 5000 psi at -78°C	
	16A		0.066 "		1.0	0.51	0.56		0.04	14.3	reduced in abs CH_3OH, handled in argon	
	16B		0.066 "		1.0	0.53	0.57		0.05	10.2	reduced in abs CH_3OH, handled in pure O_2	
	16C		0.066 "		1.0	0.51	0.53		0.04	8.0	reduced in abs CH_3OH	
	16D		0.066 "		1.0	0.51	0.55		0.05	10.0	reduced in abs CH_3OH	
	16E		0.066 "		1.0	0.67	0.75		0.11	1.7	reduced in abs CH_3OH, 30 wt % Teflon powder (1 micron) added	
	18		0.01 "		0.2	0.50	0.56	0.59	0.05	9.1	reduced in abs CH_3OH, pressed onto electrode under argon at -78°C	
	19		0.025 "		1.0	0.50	0.55	0.57	0.05	9.1	reduced at 0°C	
	20		0.025 "		1.0	0.52	0.55	0.57	0.05	9.4	reduced at 90°C	
Pt-Au	33		0.015 "	0.015 $HAuCl_4$	2.4	0.61	0.67	0.72	0.09	6.3	reduced at 0°C	tested at 25°C
	33A		0.015 "	0.015 "	2.4	0.52	0.58	0.61	0.08	6.0		
	33B		0.015 "	0.015 "	2.4	0.58	0.66	0.72	0.08	6.0		electrode rinsed in H_2O, dried for 10 min in air at 100°C
	33C		0.015 "	0.015 "	2.4	0.52	0.58	0.62	0.08	6.0		
	34		0.015 "	0.015 "	2.4	0.50	0.55	0.58	0.08	5.6	reduced at 0°C	
	34A		0.015 "	0.015 "	2.4	0.50	0.56	0.59	0.08	5.6		electrode rinsed in H_2O, dried for 10 min in air at 150°C
	35		0.015 "	0.015 "	2.4	0.49	0.54	0.57	0.08	5.5	reduced at 0°C	
	35A		0.015 "	0.015 "	2.4	0.52	0.59	0.61	0.10	4.6		electrode rinsed in H_2O, dried for 10 min in air at 200°C
Pt-Fe	2		0.025 "	0.0025 $FeCl_3$	0.2	0.48	0.56	0.62	0.10	3.8	reduced in abs CH_3OH at 50°C	
	4		0.05 "	0.005 "	0.2	0.50	0.55	0.59	0.06	7.6	reduced in abs CH_3OH, at 50°C, 2 wt % methylene blue added	
	4A		0.05 "	0.005 "	0.2	0.44	0.51	0.55	0.10	3.4		tested at 80°C
	5		0.05 "	0.005 "	0.2	0.47	0.54	0.57	0.10	4.0	reduced in abs CH_3OH, at 50°C, 1 wt % lead acetate added	
	6		0.025 "	0.005 "	0.7	0.56	0.59	0.64	0.14	3.0	reduced with $NaPH_4$ suspension in ethyl ether	
	9		0.025 "	0.005 "	$LiBH_4$ 0.5	0.48	0.53	0.56	0.07	5.9	reduced with $LiBH_4$ in diglyme	

APPENDIX A-2 (CONT'D)

Electrode	Run No.	Composition, Atom%	Preparative Solution, moles/liter Salts				NaBH4	Polarization vs Theor CH_3OH @ Indicated ma/cm² 10	50	100	6	-Log I_o	Remarks on Catalyst Preparation*	Remarks on Electrode Testing**
Pt-Au-Fe	21		0.01125	H_2PtCl_6, 0.01125	$HAuCl_4$, 0.0025	$FeCl_3$	1.0	0.48	0.54	0.56	0.07	5.7	reduced at 0°C	
	22		0.01125	" , 0.01125	" , 0.0025	"	1.0	0.49	0.55	0.58	0.08	5.1	reduced at 30°C	
	22A		0.01125	" , 0.01125	" , 0.0025	"	1.0	0.45	0.51	0.45	0.08	4.6		
	23		0.01125	" , 0.01125	" , 0.0025	"	1.0	0.50	0.55	0.57	0.08	5.2	reduced at 60°C	electrode rinsed in H_2O, dried for 10 min in air at 160°C
	23A		0.00125	" , 0.01125	" , 0.0025	"	1.0	0.49	0.54	0.56	0.07	6.0		
	24		0.00125	" , 0.01125	" , 0.0025	"	1.0	0.49	0.56	0.58	0.09	4.4	reduced at 90°C	stored in H_2O for 2 weeks
	25	Pt 49.5, Au 49.5, Fe 1.0	0.0135	" , 0.0135	" , 0.00027	"	1.1	0.50	0.55	0.58	0.07	6.2		
	25A		0.0135	" , 0.0135	" , 0.00027	"	1.1	0.51	0.56	0.59	0.07	6.4		
	26		0.0139	" , 0.0139	" , 0.000027	"	1.1	0.52	0.57	0.60	0.07	5.0		electrode stored in 3.7 M H_2SO_4 for 24 hours at 60°C
	27	Pt 48.5, Au 48.5, Fe 3.1	0.0183	" , 0.0183	" , 0.0019	"	3.85	0.49	0.54	0.57	0.08	5.5	reduced at 0°C	
	27A		0.0183	" , 0.0183	" , 0.0019	"	3.85	0.51	0.57	0.59	0.08	5.5		
	28	Pt 47.4, Au 47.4, Fe 5.1	0.0173	" , 0.0173	" , 0.0038	"	3.85	0.46	0.52	0.55	0.08	4.8	reduced at 0°C	electrode run at 50 ma/cm² for 48 hours
	28A		0.0173	" , 0.0173	" , 0.0038	"	3.85	0.50	0.57	0.61	0.08	5.2		
	29	Pt 46.9, Au 46.9, Fe 6.3	0.0163	" , 0.0163	" , 0.0058	"	3.85	0.49	0.55	0.57	0.08	6.0	reduced at 0°C	electrode run at 50 ma/cm² for 48 hours
	29A		0.0163	" , 0.0163	" , 0.0058	"	3.85	0.50	0.55	0.59	0.08	6.0		electrode stored in H_2O for 1 week at room temperature
	29B		0.0163	" , 0.0163	" , 0.0058	"	3.85	0.49	0.56	0.58	0.08	6.0		electrode stored in 3.2 M H_2SO_4 for 16 hours at 60°C
	29C		0.0163	" , 0.0163	" , 0.0058	"	3.85	0.50	0.56	0.59	0.08	6.0		electrode cathodized at -0.2 V for 5 min
	29D		0.0163	" , 0.0163	" , 0.0058	"	3.85	0.52	0.63	0.68	0.14	3.0		electrode anodized at +1.2 V for 5 min
	30	Pt 46.3, Au 46.3, Fe 7.4	0.0144	" , 0.0144	" , 0.0096	"	3.85	0.49	0.54	0.57	0.07	6.0	reduced at 0°C	electrode run at various currents for 2 weeks
	30A		0.0144	" , 0.0144	" , 0.0096	"	3.85	0.50	0.57	0.60	0.09	4.9		
	31	Pt 47.6, Au 47.6, Fe 4.7	0.01156	" , 0.01156	" , 0.001875	"	2.5	0.48	0.53	0.56	0.07	6.2	reduced at 0°C	electrode rinsed in H_2O, dried for 10 min in air at 160°C
	31A		0.01156	" , 0.01156	" , 0.001875	"	2.5	0.46	0.54	0.56	0.09	4.2		
	31B		0.01156	" , 0.01156	" , 0.001875	"	2.5	0.47	0.53	0.55	0.09	4.2		run with decreasing current steps
	31C		0.01156	" , 0.01156	" , 0.001875	"	2.5	0.47	0.53	0.56	0.09	4.2		electrode stored in 3.7 M H_2SO_4 for 16 hours at 25°C
	46		0.0075	" , 0.0075	" , 0.00166	"	1.66	0.49	0.54	0.57	0.08	5.1	reduced at 0°C	electrode rinsed at H_2O, dried for 2 min in air at 160°C
	47	Pt 47.6, Au 47.6, Fe 4.7	0.0075	" , 0.0075	" , 0.00166	"	1.66	0.57	0.64	0.68	0.09	5.4	reduced in 0.33 M K-biphthalate buffer solution at 0°C	
	48	Pt 47.8, Au 47.8, Fe 4.4	0.0075	" , 0.0075	" , 0.00166	"	1.66	0.51	0.56	0.59	0.07	6.3	reduced at 0° in 1 wt % lead acetate	
	49		0.0075	" , 0.0075	" , 0.00166	"	1.66	0.52	0.57	0.59	0.07	6.7	reduced at 0°C	
	32	Pt 47.1, Au 47.1, Fe 5.8	0.0109	" , 0.0109	" , 0.003125	"	2.5	0.46	0.52	0.55	0.07	5.7	reduced at 0°C	
	32A		0.0109	" , 0.0109	" , 0.003125	"	2.5	0.45	0.52	0.55	0.13	2.5		
	32B		0.0109	" , 0.0109	" , 0.003125		2.5	0.46	0.52	0.55	0.09	4.2		run with decreasing current steps
														electrode rinsed in H_2O, dried for 20 min in air at 160°C

* All catalyst preparations in aqueous acetate ion buffer solution at room temperature with $NaBH_4$ unless otherwise noted (acetate buffer 1.0 to 2.33 M, equal amounts of CH_3COOH and CH_3COONa), catalyst pressed onto 2 cm x 2 cm Pt-screens backed with Pt-foil at 1000-2000 psi.

** All runs in 3.7 M H_2SO_4-1 M CH_3OH at 60°C unless otherwise noted.

APPENDIX A-3

PERFORMANCE OF P-TYPE CATALYSTS

Catalyst	Polarization vs Theor. CH_3OH at Indicated ma/cm^2 10	50	100	Remarks*
P 7	0.47	0.59	0.64	0.1 M HCHO added, 25°C
7	0.46	--	--	25°C
7	0.53	--	--	
7	0.40	0.47	0.50	
7	0.39	--	--	
7	0.27	0.35	0.38	1 M HCOOH
7	0.56	0.60	0.62	physical mixture of catalyst
7	0.44	0.50	0.54	electrodeposited
7	0.41	0.49	0.53	
7	0.47	0.53	0.56	Pt black added to catalyst
7	0.37	--	--	
7	0.38	--	--	stored in electrolyte 16 hours before running
7	0.30	0.38	--	stored in H_2O 16 hours
7	0.32	--	--	stored in 3.7 M H_2SO_4 16 hours
7	0.31	--	--	stored in 1 M CH_3OH in H_2O 21 hours
7	0.32	--	--	stored in electrolyte 23 hours
7	0.34	--	--	stored in H_2O 2 days
7	0.34	--	--	stored in 3.7 M H_2SO_4 2 days
7	0.39	--	--	stored in H_2O 4 days
7	0.47	--	--	stored in 3.7 M H_2SO_4 4 days
7	0.44	--	--	stored in H_2O 7 days
7	0.47	--	--	stored in 3.7 M H_2SO_4 7 days
7	0.38	0.44	--	operated 3 days
7	0.39	--	--	operated 1 day
7	0.37	--	--	stored in H_2O 16 hours
7	0.36	--	--	stored in electrolyte 16 hours
7	0.33	--	--	stored in H_2O 40 hours
7	0.39	--	--	stored in electrolyte 40 hours
7	1.40	--	--	stored in H_2O 6 days
7	0.40	--	--	stored in electrolyte 6 days
7	0.38	--	--	
7	0.46	--	--	
7	0.40	--	--	
7	0.34	--	--	
7	0.39	--	--	stored in H_2O 2 days
7	0.37	--	--	stored in 1 M CH_3OH in H_2O 2 days
7	0.39	--	--	stored in H_2O 4 days
7	0.35	--	--	stored in 1 M CH_3OH in H_2O 4 days
7	0.39	--	--	stored in H_2O 7 days
7	0.36	--	--	stored in 1 M CH_3OH in H_2O 7 days
7	0.39	--	--	
7	0.38	--	--	
18	0.33	--	--	
18	0.36	--	--	
18	0.35	--	--	
18	0.36	--	--	
18	0.36	--	--	
18	0.35	--	--	
18	0.34	--	--	
18	0.36	--	--	
18	0.34	--	--	
18	0.37	0.43	--	
18	0.35	--	--	
18	0.47	--	--	stored in H_2O 2 days
18	0.41	--	--	stored in H_2O 6 days
18	0.34	--	0.44	stored in H_2O 10 days
18	0.32	--	--	stored in 1 M HCHO in H_2O 1 hour
18	0.32	0.40	0.44	stored in 1 M HCHO in H_2O 2 days
18	0.32	--	--	stored in 1 M HCHO in H_2O 6 days
18	0.34	--	--	stored in 1 M HCHO in H_2O 10 days
18	0.33	--	--	0.9 M CH_3OH + 0.1 M HCHO
18	0.28	0.37	0.43	0.5 M H_2SO_4, stored in 1 M HCHO in H_2O 2 days
18	0.37	--	--	reduced with 0.5 wt % $NaBH_4$, non-steady state value
18	0.37	--	--	1.0 wt % $NaBH_4$, non-steady state value
18	0.30	--	--	5.0 wt % $NaBH_4$, non-steady state value
18	0.39	--	--	10.0 wt % $NaBH_4$
18	--	0.29	--	2 M CH_3OH, 90°C
18	--	0.31	--	6 M H_2SO_4-2 M CH_3OH, 100°C
18	--	0.34	--	6 M H_2SO_4-2 M CH_3OH, 90°C
18	--	0.44	--	9 M H_2SO_4- 2 M CH_3OH, 80°C
18	0.40	--	--	1.0 wt % $NaBH_4$
18	0.38	--	--	2.5 wt % $NaBH_4$
18	0.32	--	--	5.0 wt % $NaBH_4$

* All runs in 3.7M H_2SO_4 - 1 M CH_3OH at 60°C with pressed electrodes unless otherwise noted.

APPENOIX A-3 (CONT'D)

PERFORMANCE OF P-TYPE CATALYSTS

Catalyst	Polarization vs Theor. CH_3OH at indicated ma/cm^2 10	50	100	Remarks*
P 18	0.35	--	--	7.5 wt % $NaBH_4$
18	0.37	0.43	--	3.5 wt % $NaBH_4$
18	0.37	0.43	--	4.5 wt % $NaBH_4$
18	0.36	0.42	--	5.5 wt % $NaBH_4$
18	0.36	0.43	--	6.5 wt % $NaBH_4$
18	0.25	0.36	--	7.5 wt % $NaBH_4$, 90°C
18	0.36	--	--	5.0 wt % $NaBH_4$
18	0.30	0.35	--	5.0 wt % $NaBH_4$, 1 M H_2SO_4 - 0.5 M CH_3OH, 90°C
18	0.37	--	--	5.0 wt % $NaBH_4$, 1 M H_2SO_4 - 0.5 M CH_3OH, 90°C
18	0.22	0.29	.32-.41	5.0 wt % $NaBH_4$, 1 M H_2SO_4 - 0.5 M CH_3OH, 90°C .41 vslue with 0.2 wt.% HNO_3 added
18	0.35	--	--	5.0 wt % $NaBH_4$, unpressed
18	0.37	0.43	--	5.0 wt % $NaBH_4$, washed twice in H_2O
18	0.32	0.40	--	5.0 wt % $NaBH_4$, washed twice in 3.7 M H_2SO_4
18	0.34	0.42	--	5.0 wt % $NaBH_4$, waahed once in H_2O, once in 3.7 M H_2SO_4
18	0.29	0.36	--	5.0 wt % $NaBH_4$, waahed twice in H_2O, twice in 3.7 M H_2SO_4, once in H_2O
18	0.38	0.45	--	5.0 wt % $NaBH_4$, washed once in 3.7 M H_2SO_4 once in H_2O
18	0.37	0.43	--	5.0 wt % $NaBH_4$, waahed once in H_2O
18	0.39	0.46	--	5.0 wt % $NaBH_4$, washed once in 3.7 M H_2SO_4
18	0.36	0.43	--	5.0 wt % $NaBH_4$
18	0.39	0.45	--	5.0 wt % $NaBH_4$, reduced at 2°C
18	0.35	0.41	--	5.0 wt % $NaBH_4$, reduced at 25°C
18	0.36	0.44	--	5.0 wt % $NaBH_4$
18	0.33	0.41	--	5.0 wt % $NaBH_4$, $NaBH_4$ solution added to salt solution
18	0.38	--	--	5.0 wt % $NaBH_4$
18	0.36	--	--	5.0 wt % $NaBH_4$, washed twice in H_2O, twice in 3.7 M H_2SO_4, once in H_2O
18	0.51	--	--	5.0 wt % $NaBH_4$, reduced in acetate buffer
18	0.35	--	--	5.0 wt % $NaBH_4$, $NaBH_4$ solution added to salt solution
7	0.30	0.49	0.60	1 M HCHO, 82°C
7	0.20	0.30	0.40	1 M HCHO, 82°C
7	0.30	0.44	0.52	82°C
7	0.32	0.45	0.52	82°C, corrected for IR
7	0.38	0.44	0.51	82°C
7	0.45	0.53	0.56	82°C
7	0.44	0.64	--	82°C, catalyst stored one week prior to use
7	0.26	0.36	0.41	82°C
7	0.26	0.36	0.41	82°C, Na_2WO_4 added to electrolyte
7	0.40	0.46	0.50	82°C
69	0.47	0.54	0.57	82°C
70	0.44	0.50	0.55	82°C
7	0.40	0.49	0.56	40°C
7	0.32	0.40	0.45	
7	0.26	0.34	0.38	80°C
7	0.25	0.34	0.39	82°C
7	0.21	0.34	0.40	82°C
7	0.38	0.46	0.50	82°C, 0.5 M CH_3OH
7	0.44	0.52	0.56	anodized at +1.5 V vs H_2 approx 10 seconds in 3.7 M H_2SO_4 82°C, 0.5 M CH_3OH
7	0.26	0.37	0.44	increasing loads, 82°C, 0.5 M CH_3OH
7	0.28	0.38	0.45	decreasing loads, same electrode as above 82°C, 0.5 M CH_3OH
7	0.30	0.38	0.45	with O_2 sparge during run, O_2 flow started 10 minutes previous to run, 82°C, 0.5 M CH_3OH
7	0.27	0.37	0.42	82°C, 0.5 M CH_3OH
7	0.30	0.40	0.46	82°C,
7	0.31	0.39	0.45	
7	0.30	0.38	0.45	H_2SO_4 pre-electrolyzed for 1 hour
7	0.30	0.38	0.45	H_2SO_4 not cleaned
7	0.24	0.34	0.39	
7	0.27	0.34	0.39	
7	0.27	0.35	0.39	
7	0.27	0.35	0.38	

* All runs in 3.7 M H_2SO_4 - 1 M CH_3OH at 60°C with pressed electrodes unless otherwise noted.

APPENDIX A-4

PREPARATION STUDIES OF P-TYPE AND MODIFIED P-TYPE CATALYSTS

Catalyst	Run Number	Polarization vs Theor CH_3OH @ Indicated ma/cm^2 10	50	100	b	-log I_o	Remarks*
P-Type							
P 7	7	0.46	0.53	0.59	0.09	4.1	reduced with $NaBH_4$ in absolute CH_3OH at 25°C
	8	0.48	0.53	0.56	0.07	5.9	reduced with KBH_4 instead of $NaBH_4$ in absolute CH_3OH at 25°C, stored in H_2O for 2 days before pressing
P 72	14	0.49	0.54	0.57	0.075	6.0	reduced with L-type reagent in dimethoxyethane at 25°C, electrode pressed at 3000 psi
P 3	15A	0.44	0.51	0.54	0.11	3.4	reduced with L-type reagent in dimethoxyethane at 25°C,
	15B	0.55	0.64	0.68	0.13	3.5	reduced with L-type reagent in dimethoxyethane at 25°C,
P 73	17	0.57	0.62		0.06	11.0	reduced with L-type reagent in dimethoxyethane at 25°C,
P 6	42	0.41	0.50	0.56	0.115	2.7	reduced in aqueous acetate ion buffer (1.5 M) at 0°C
	42A	0.44	0.53	0.59	0.115	2.7	
	43	0.46	0.54		0.11	3.2	reduced in H_2O at 0°C
	44	0.36	0.45	0.50	0.14	1.6	reduced in H_2O at 50°C
Modified P-Type							
P 77	36	0.46	0.55	0.60	0.105	3.4	reduced in aqueous acetate buffer (1.5 M) at 0°C
	37	0.46	0.53	0.58	0.10	3.6	reduced in aqueous acetate buffer (1.5 M) at 0°C
	38	0.46	0.54		0.09	4.3	reduced in H_2O at 0°C
	38A	0.46	0.54		0.09	4.3	electrode rinsed in water, dried for 10 min in air at 45°C
	39	0.46	0.54		0.11	3.2	reduced in H_2O at 0°C
	39A	0.48	0.57		0.11	3.2	electrode rinsed in water, dried for 5 min in air at 145°C, catalyst flaked partly off electrode
P 75	40	0.39	0.47	0.51	0.10	2.9	reduced in aqueous acetate buffer solution (1.5 M) at 0°C
	40A	0.33	0.42	0.46	0.11	2.0	performance tested at 80°C
P 74	41	0.39	0.47	0.51	0.10	2.8	reduced in aqueous acetate buffer solution (1.5 M) at 0°C
	41A	0.34	0.41	0.45	0.11	2.1	performance tested at 80°C
P 76	45	0.46	0.55		0.125	2.6	reduced in H_2O at 0°C, catalyst flaked partly off electrode

* All electrodes pressed at 1000-2000 psi and tested in 3.7 M H_2SO_4 and 1 M CH_3OH at 60°C unless otherwise noted.

APPENOIX A-5

PERFORMANCE OF MOOIFIEO P-TYPE CATALYSTS

Catalyst	Polarization vs Theor. CH_3OH at Indicated ma/cm^2 10	50	100	Remarks*
P 61	0.40	0.50	0.53	
29	0.50	0.58	0.61	22.5°C
	0.34	0.42	0.45	
	0.31	0.40	0.43	80°C
32	0.25	0.33	0.41	
	0.18	0.29	0.36	80°C
45	0.51	0.58	0.61	
54	0.46	0.53	0.56	
58	0.38	0.49	--	
63	0.54	0.61	--	
63	0.41	0.51	--	
64	0.53	0.62	--	
34	0.36	0.46	--	
31	0.40	0.48	--	
30	0.35	0.44	--	
28	0.43	0.51	--	
33	0.45	--	--	
27	0.42	0.52	--	
56	0.35	0.44	--	
57	0.41	--	--	
53	0.33	--	--	
55	0.42	0.50	--	
59	0.43	0.50	0.53	
60	0.36	0.47	0.50	
65	--	--	--	no activity
66	0.43	0.50	0.53	
61	0.36	--	--	
29	0.43	--	--	
32	0.31	--	--	
54	0.46	0.52	0.56	
52	0.44	0.49	0.58	
29	0.43	--	0.56	
36	0.42	--	--	
33	0.42	--	--	
32	0.41	--	--	
39	0.38	--	--	
38	0.41	--	--	
34	0.35	--	--	
42	0.36	--	--	stored in electrolyte 3 days
40	0.37	--	--	stored in electrolyte 3 days
39	0.53	--	--	stored in electrolyte, lost catalyst
44	0.38	--	--	stored in electrolyte 16 hours
43	0.41	--	--	stored in electrolyte 16 hours
42	0.47	--	--	stored in electrolyte 16 hours
39	0.40	--	--	stored in electrolyte 16 hours
40	0.38	--	--	stored in electrolyte 16 hours
41	0.40	--	--	stored in electrolyte 16 hours
43	0.34	--	--	stored in H_2O 16 hours
43	0.36	--	--	stored in H_2O 16 hours
46	0.37	--	--	stored in electrolyte 16 hours
48	0.34	--	--	
51	0.40	--	--	
47	0.38	--	--	stored in 2 M CH_3OH in 3.7 M H_2SO_4 1 day
49	0.38	--	--	
50	0.38	--	--	
35	0.37	--	--	
35	0.40	--	--	
23a	0.42	0.50	--	reduced with 5.0 wt % $NaBH_4$
23	0.40	--	--	reduced with 5.0 wt % $NaBH_4$
23	0.35	--	--	
67	0.40	0.48	--	
68	0.44	0.52	--	
67	--	0.36-0.72	--	0.72 value after addition of 0.2 wt % HNO_3
32	0.38	0.47	0.53	1 M H_2SO_4 - 0.5 M CH_3OH, 90°C
32	0.23	0.34	0.44	82° C, potentiostatted
32	0.24	0.44	--	82° C, 1 M HCHO
				82° C,potentiostatted, 1 M HCHO

* All runs in 3.7 M H_2SO_4 - 1 M CH_3OH at 60° C with pressed electrodes unless otherwise noted.

APPENDIX A-6

TEMPERATURE DEPENDENCE OF CH_3OH REACTION ON P-TYPE CATALYST

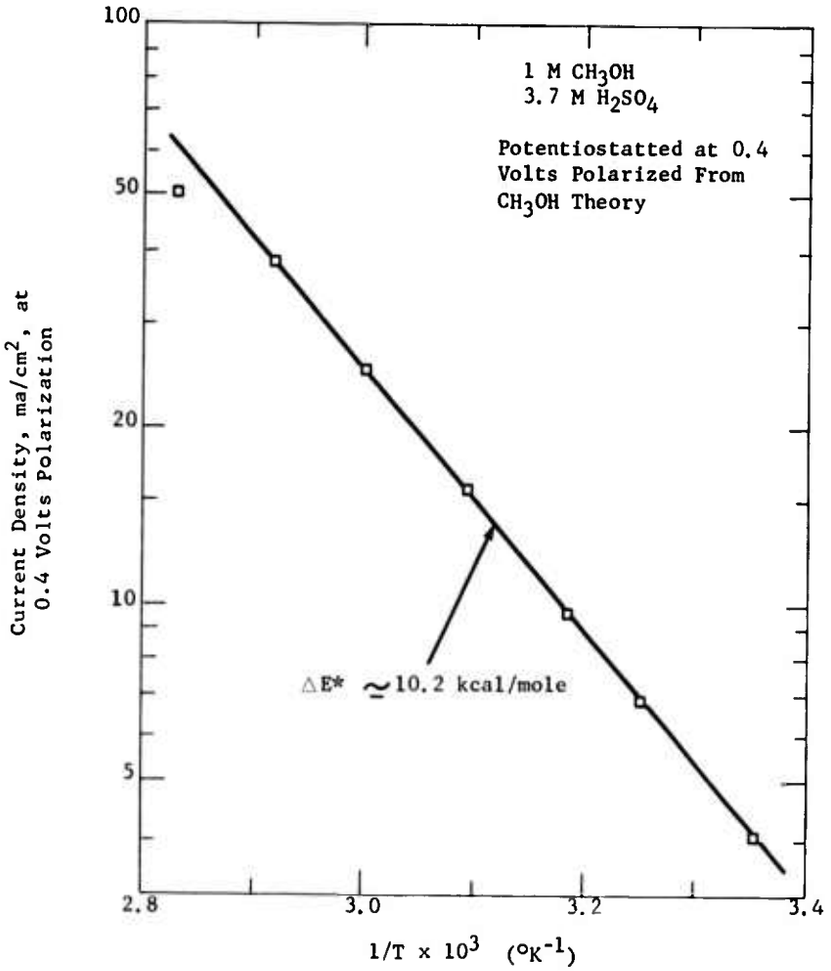

APPENDIX A-7

EFFECT OF CH_3OH CONCENTRATION ON PERFORMANCE OF P-TYPE CATALYST

CH_3OH Conc, moles/liter	Current Density, ma/cm^2 at 0.40 Volts Polarization From Theoretical CH_3OH					
	40°C		60°C		80°C	
	O_2	No O_2	O_2	No O_2	O_2	No O_2
0.14	3.2	4.2	13.2	12.7	30.5	31.5
0.27	4.5	5.2	17.5	16.7	39.5	45.0
0.41	6.5	7.5	21.5	20.5	46.2	52.5
0.54	7.0	9.0	24.0	22.7	52.5	57.5
0.68	8.5	10.7	25.7	24.0	55.0	58.0
0.81	--	11.5	28.0	26.7	57.5	--
0.94	--	12.5	29.5	30.0	61.2	67.5
1.06	--	12.7	31.0	31.5	62.5	--
1.19	--	14.0	31.7	32.5	63.7	--
1.32	9.7	12.5	32.2	34.0	63.7	72.0

APPENDIX A-8

LIFE TESTS - P-TYPE CATALYSTS

Catalyst	Current Density, ma/cm^2	Polarization After Indicated Hours						Time of Failure	Remarks
		1	25	50	100	500	1000		
P 7	38	0.30	0.33	0.34	0.41	--	--	288 hours	
P 7	50	0.34	0.40	0.39	--	--	--	<100	
P 7	50	0.36	0.40	0.39	0.39	--	--	216 hours	
P 7	38	0.47	0.53	--	--	--	--	--	Mechanical failure
P 7	38	0.32	0.35	--	--	--	--	45 hours	
P 7	38	0.38	0.41	0.42	0.44	0.45	0.45	Shut down 1020 hours	Open circuited for 30 sec once a day.
P 7	48-50	0.34	0.37	0.36	0.37	0.39	0.40	Shut down	Electrolyte sat'd with H_2WO_4 - open circuited for 30 sec once a day.
P 7	50	0.33	0.40	--	--	--	--	< 100	Electrolyte sat'd with H_2WO_4 - open circuited for 30 sec once a day.
P 7	50	0.37	0.40	0.41	0.41	0.44	--	700 hours	
P 7	50	0.31	0.36	0.36	0.38	0.40	--	Still operating	Electrolyte sat'd with H_2WO_4 - open circuited for 30 sec once a day.
P 7	50	0.35	0.36	0.37	0.38	0.39	--	576 hours	Open circuited once a day - CH_3OH loss possible cause of failure.
P18	50	0.41	0.41	0.41	0.41	--	--	Shut down	Open circuited once a day - run for 310 hours 60°C
P18	50	0.44	0.44	0.44	0.44	--	--	Shut down	Open circuited once a day - run for 380 hours 60°C

All runs at 82°C, 1 M CH_3OH and 3.7 M H_2SO_4 unless otherwise indicated.
Runs of less than 25 hours duration are omitted.

APPENDIX A-9

PERFORMANCE TESTS - SOLUBLE RHENIUM SYSTEMS

Catalyst	Fuel - Conc.	Re_2O_7 moles/liter	Polarization vs Theor. CH_3OH at Indicated ma/cm² 0	1	10	50	100	h	Comments
Pt(*)	1 M HCHO	2 x 10^{-2}	0.20	0.21	0.28	0.40	0.47	--	
Pt(*)	1 M CH_3OH	2 x 10^{-2}	0.38	0.39	0.45	0.55	0.62	--	Re_2O_7 conc
Pt(*)	1 M CH_3OH	2 x 10^{-3}	0.27	0.30	0.39	0.45	0.48	0.09	study - same
Pt(*)	1 M CH_3OH	2 x 10^{-4}	0.19	0.27	0.39	0.46	0.50	0.11	electrode
Pt(*)	1 M CH_3OH	2 x 10^{-5}	0.32	0.40	0.48	0.55	0.59	0.10	
Pt(*)	1 M HCHO	2 x 10^{-2}	0.29	0.29	0.40	0.48	0.58		
Pt(*)	1 M CH_3OH	2 x 10^{-3}	0.34	0.38	0.44	0.51	--	0.08	
Pt(*)	1 M HCHO	2 x 10^{-3}	0.23	0.26	0.31	0.40	0.46		
Pt(*)	1 M CH_3OH	2 x 10^{-4}	0.25	0.33	0.42	0.51	0.54	0.12	
Pt(*)	1 M CH_3OH	2 x 10^{-3}	0.28	0.35	0.42	0.49	0.54	0.08	
comm'l Pt black	1 M CH_3OH	2 x 10^{-4}	0.23	0.32	0.42	0.48	0.52	0.09	
Pt(*)	1 M CH_3OH	2 x 10^{-4}	0.34	0.38	0.45	0.52	0.55		Also 4 x 10^{-3} M Na_2MoO_4
Pt(*)	1 M CH_3OH	2 x 10^{-3}	0.28	0.32	0.41	0.47	0.50	0.09	
Pt(*)	1 M CH_3OH	2 x 10^{-3}	0.28	0.34	0.42	0.49	0.53	0.09	CH_3OH conc
Pt(*)	2 M CH_3OH	2 x 10^{-3}	0.28	0.31	0.40	0.48	0.52	0.10	variation
Pt(*)	1 M CH_3OH	2 x 10^{-3}	0.17	0.20	0.27	0.33	0.36	--	
Pt-Au (**)	1 M CH_3OH	2 x 10^{-3}	0.26	0.31	0.40	0.46	0.48	0.09	Physical 50/50 mix
Pt-Au (**)	1 M CH_3OH	2 x 10^{-4}	0.27	0.33	0.40	0.46	0.51	0.08	
Pt-Au (**)	1 M CH_3OH	2 x 10^{-3}	0.23	0.26	0.35	0.42	0.45	0.09	0.5 M H_2SO_4
Pt-Au (**)	0.25 M CH_3OH	2 x 10^{-3}	0.32	0.35	0.43	0.50	0.54	0.08	0.25 M CH_3OH
Pt (*)	1 M CH_3OH	2 x 10^{-3}	0.12	0.32	0.42	0.60	--	0.12	Re_2O_7 reduced overnight @ +0.15 vs N.H.E.
Pt(*)	1 M CH_3OH	2 x 10^{-3}	0.22	0.33	0.43	0.58	0.73		Purple sol'n of partially oxidized ReO_2
Pt	1 M HCHO	2 x 10^{-3}	0.19	0.24	0.32	0.40	0.48		8.9 gms/ft² Pt
Pt-Au (**)	1 M CH_3OH	2 x 10^{-3}	0.29	0.35	0.41	0.49	0.56		
Pt-Au (**)	1 M CH_3OH	DIP	0.20	0.28	0.39	0.53	0.60	0.12	5 min dip in Re_2O_7 - CH_3OH - H_2SO_4
Platinized Pt	1 M HCHO	DIP	0.16	0.28	0.34	0.41	0.47	0.07	Irreversible 10 min dip in Re_2O_7 - CH_3OH - H_2SO_4
Platinized Pt	1 M CH_3OH	DIP	0.42	0.46	0.53	0.57	0.63	0.06	10 min dip in Re_2O_7 - CH_3OH - H_2SO_4

(*) Precipitated from H_2PtCl_6 solution with excess $NaBH_4$.
(**) Metals precipitated separately from H_2PtCl_6 and $HAuCl_4$ solutions respectively with excess $NaBH_4$.

All runs in 3.7 M H_2SO_4 at 82°C.

APPENDIX B-1

HNO_3 HALF-CELL

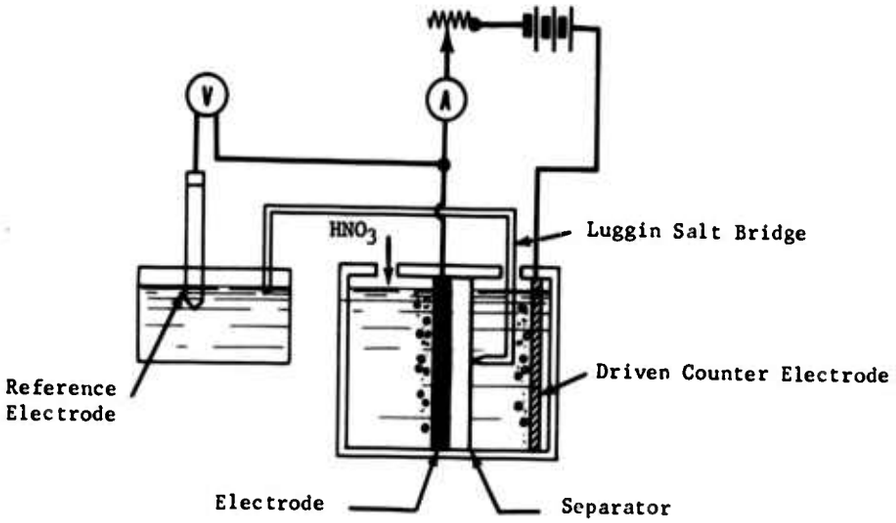

APPENDIX B-2

PERFORMANCE STUDIES OF THE NITRIC ACID CATHODE*

Electrolyte: 3.7 M H_2SO_4

Temperature: 82°C

Pressure: 1 atm

Electrode Structure: C-type

Catalyst: 8 mg/cm^2 electrodeposited Pt black

Current Density, ma/cm^2		0	15	30	45	60	75	90	135	180	225	265
Polarization, Volts, From Theoretical O_2	1 wt % HNO_3	0.07	0.15	0.17	0.18	0.18	0.19	0.20	0.23	0.29	failed	--
	2 wt % HNO_3	0.07	0.15	--	--	--	--	0.18	--	--	0.19	failed

*This data represents the best performances obtained from a series of tests on various electrodes.

APPENDIX B-3

HALF-CELL ASSEMBLY FOR EVALUATION OF DIRECT O_2 ELECTRODE PERFORMANCES

A four inch diameter glass cell was used for performance tests. The O_2 electrodes, described in Phase 2, were in direct contact with a membrane separator on one side and a gold current collector on the other. An end plate, held away from the current collector by a 1.5 mm spacer, completed the cathode compartment. The O_2 feed entered through a hole in the end plate and exited through a slot in the spacer. On the anode side, a Pt screen served as the driven counter electrode. This assembly is illustrated in Figure B-1.

Figure B-1

Half-Cell Assembly For Evaluating Direct Oxygen Electrodes

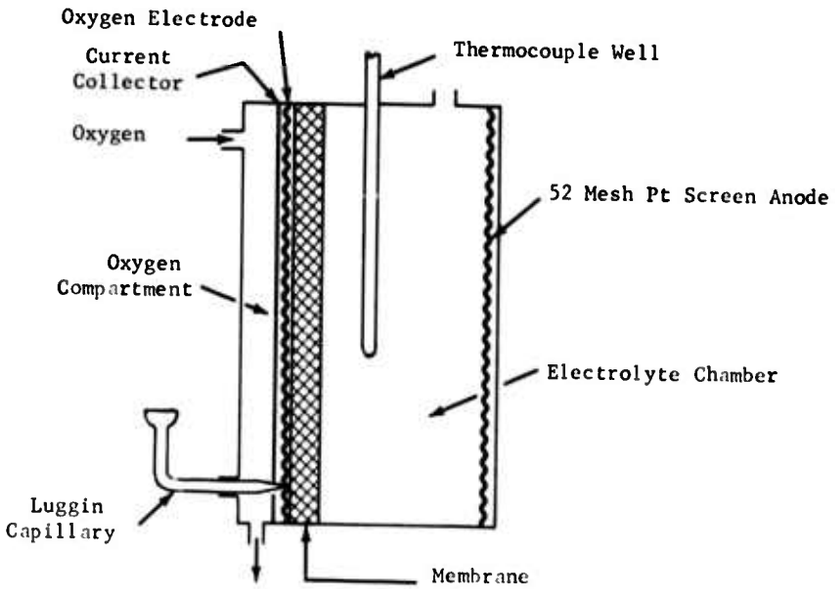

APPENDIX B-4

EFFECT OF PT-TEFLON COMPOSITION ON ELECTRODE PERFORMANCE

Electrolyte = 3.7 M H_2SO_4
Oxidant = Oxygen
Membrane = A-type

Test No.	Cathode	Temp. °C	Polarization from Theoretical O_2 at Indicated ma/cm^2					
			1.2	5	10	20	50	100
1059-16	85-15 Pt-Teflon*	Ambient	0.22	0.30	0.35	0.42	0.54	0.66
1059-17	85-15 Pt-Teflon	Ambient	0.21	0.28	0.33	0.40	0.57	0.76
1059-32a	80-20 Pt-Teflon	38	0.22	0.26	0.29	0.32	0.40	0.50
1059-32a	80-20 Pt-Teflon	60	0.20	0.23	0.25	0.29	0.35	0.44
1059-33II	75-25 Pt-Teflon	38	0.18	0.21	0.23	0.26	0.33	0.43
1059-35I	75-25 Pt-Teflon	60	0.15	0.18	0.20	0.23	0.29	0.37
1059-36	70-30 Pt-Teflon	38	0.19	0.21	0.24	0.27	0.33	0.41
1059-36	70-30 Pt-Teflon	60	0.16	0.19	0.21	0.24	0.29	0.37
1048-6	50-50 Pt-Teflon	60	0.18	-	0.23	0.25	0.31	0.39

* Borohydride reduced Pt black.

APPENDIX B-5

EFFECT OF PT-CARBON-TEFLON COMPOSITION ON ELECTRODE PERFORMANCE

Electrolyte = 3.7 M H_2SO_4
Oxidant = Oxygen
Membrane = A-type

Test No.	Cathode	Temp. °C	Polarization from Theoretical O_2 at Indicated ma/cm^2					
			1.2	5	10	20	50	100
1059-31a	70-10-20 Pt-C-Teflon	32	0.25	0.29	0.33	0.38	0.49	0.63
1059-31a	70-10-20 Pt-C-Teflon	60	0.21	0.25	0.28	0.32	0.41	0.55
1059-29	60-20-20 Pt-C-Teflon	38	0.22	0.27	0.30	0.35	0.45	0.57
1059-29	60-20-20 Pt-C-Teflon	62	0.21	0.25	0.28	0.31	0.39	0.51
1059-31b	50-30-20 Pt-C-Teflon	60	0.24	0.29	0.34	0.42	0.61	-
1059-30	33-33-33 Pt-C-Teflon	28	0.19	0.27	0.33	0.44	0.67	-
1059-30	33-33-33 Pt-C-Teflon	62	0.17	0.23	0.27	0.33	0.48	0.69

APPENDIX B- 6

EFFECT OF OXYGEN FLOW RATE ON PERFORMANCE

Cathode = 90-10 Pt-Teflon
Oxidant = Oxygen
Electrolyte = 3.7 M H_2SO_4
Membrane = A-type

Test No.	Current Density ma/cm^2	Temp, °C	Polarization from Theoretical O_2 at Indicated Ratio of Actual to Stoichiometric Oxygen Flow Rate						
			1.1	1.6	2.0	4.0	8.0	12	20
1059-26	20	30	0.61	-	0.44	0.43	0.43	0.43	0.43
1059-26	20	60	0.47	-	0.36	0.35	0.35	0.35	0.35
1059-26	20	82	0.41	-	0.33	0.33	0.33	0.33	0.33
1059-26	50	39	Sharp Increase	0.57	0.55	0.55	0.55	-	-
1059-26	50	60	Sharp Increase	0.50	0.49	0.49	0.49	-	-
1059-26	50	82	Sharp Increase	0.48	0.47	0.47	0.47	-	-

APPENDIX B-7

EFFECT OF IDLING TIME ON PERFORMANCE

Cathode = 75-25 Pt-Teflon
Oxidant = Oxygen
Electrolyte = 3.7 M H_2SO_4
Membrane = A-type

Test No.	Idling Time	Temp. °C	Polarization from Theoretical O_2 at Indicated ma/cm^2						
			0	1.2	5	10	20	50	100
1059-33II	None	38	0.13	0.18	0.21	0.23	0.26	0.33	0.43
1059-34I	16 hours	38	0.11	0.17	0.20	0.23	0.27	0.34	0.44
1059-34I	22 hours	38	-	0.17	0.21	0.24	0.27	0.33	0.43
1059-35I	86 hours	38	0.11	0.17	0.21	0.24	0.27	0.34	0.44
1059-33II	None	60	0.13	0.18	0.21	0.23	0.25	0.31	0.38
1059-34I	16 hours	60	0.12	0.15	0.18	0.20	0.23	0.29	0.37
1059-34I	22 hours	60	-	0.15	0.18	0.20	0.23	0.29	0.38
1059-35I	86 hours	60	-	0.15	0.18	0.20	0.23	0.29	0.37
Cathode = 70-30 Pt-Teflon									
1059-35III	None	38	-	0.22	-	0.27	0.30	0.36	0.46
1059-36	22 hours	38	0.10	0.19	0.23	0.26	0.29	0.35	0.42
1059-36	38 hours	38	0.11	0.19	0.21	0.24	0.27	0.33	0.41
1059-35III	None	60	-	0.19	0.22	0.24	0.26	0.31	0.38
1059-36	22 hours	60	0.10	0.17	0.20	0.22	0.25	0.30	0.37
1059-36	38 hours	60	0.11	0.16	0.19	0.21	0.24	0.29	0.37

APPENDIX B-8

EFFECT OF ACID CONCENTRATION ON PERFORMANCE

Cathode = 75-25 Pt-Teflon
Oxidant = Oxygen
Electrolyte = H_2SO_4

Test No.	H_2SO_4 Concentration	Temp, °C	Polarization from Theoretical O_2 at Indicated ma/cm^2* 1.2	5	10	20	50	100
1059-33II	0.75 M	38	0.12	0.16	0.20	0.24	0.31	0.42
1059-34I	1.5 M	38	0.14	0.17	0.19	0.22	0.28	0.37
1059-34I	3.7 M	38	0.17	0.21	0.24	0.27	0.33	0.47
1059-34I	1.5 M	60	0.13	0.16	0.18	0.20	0.26	0.33
1059-35I	3.7 M	60	0.15	0.18	0.20	0.23	0.29	0.37
Cathode = 80-20 Pt-Teflon								
1059-34II	0.5 M	50	0.16	0.20	0.22	0.26	0.34	0.46
1059-34II	0.75 M	50	0.19	0.22	0.25	0.29	0.36	0.46
1059-34II	1.5 M	50	0.21	0.24	0.27	0.30	0.36	0.45
1059-32a	3.7 M	50	0.24	0.28	0.31	0.35	0.43	0.53
1059-34II	0.5 M	60	0.15	0.18	0.21	0.24	0.31	0.41
1059-34II	0.75 M	60	0.17	0.21	0.23	0.27	0.34	0.43
1059-34II	1.5 M	60	0.18	0.21	0.24	0.27	0.33	0.41
1059-32a	3.7 M	60	0.22	0.25	0.28	0.31	0.39	0.50

*Corrected for changes in pH.

APPENDIX B-9

OXYGEN CATALYST PREPARATION AND TESTING

Temperature - 60° C
H_2SO_4 Concentration - 3.7 M

Catalyst	Preparative Solution, moles/liter		Polarization vs Theoretical O_2 at Indicated ma/cm^2				
	Salt	$NaBH_4$	0	1	10	50	100
Pt-Ni	0.25 Na_2PtCl_6, 0.25 $NiCl_2$	1.97	0.19	0.22	0.28	0.37	0.45
Pt-Pb	0.25 Na_2PtCl_6, 0.25 $Pb(Ac)_2$	1.97	0.20	0.25	0.40	--	--
Pt-Cr	0.25 Na_2PtCl_6, 0.25 $K_2Cr_2O_7$	1.97	0.14	0.17	0.25	0.33	0.40
Pt-Mo	0.25 Na_2PtCl_6, 0.25$(NH_4)_4Mo_7O_{24}$	1.97	0.25	0.32	0.41	0.57	0.67

APPENDIX C-1

TOTAL CELL EQUIPMENT DETAILS

1. The new compact cell used in these tests was described in an earlier report(1).

2. The coulometric timer was modified to provide addition of fuel or HNO_3 when the voltage drops from a preset level. The modification, shown in Appendix C-2, consists of a 1 ohm resistor in series with the timer operating circuit from a 100 mv shunt in the fuel cell current circuit. A voltage drop is imposed across this resistor by means of external direct current, so that the coulometric timer is on about 1% of the time at 100% of the shunt reading and 40% of the time at zero shunt reading.

3. An air feed rate controller was built to maintain the air rate proportional to the fuel cell current. The controller operates off of the 100 mv Esterline Angus shunt as shown schematically in Appendix C-3. A small current of 0.05 to 0.5 ma from the operating shunt, proportional to the fuel cell current, operates an amplifier which controls a 0.5 to 5 ma pneumatic relay. The relay regulates its output air pressure proportional to the cell current. Capillary tubes between the pneumatic relay and cell are calibrated to control the ratio of air to current.

APPENDIX C-2

MODIFICATION OF COULOMETRIC TIMER

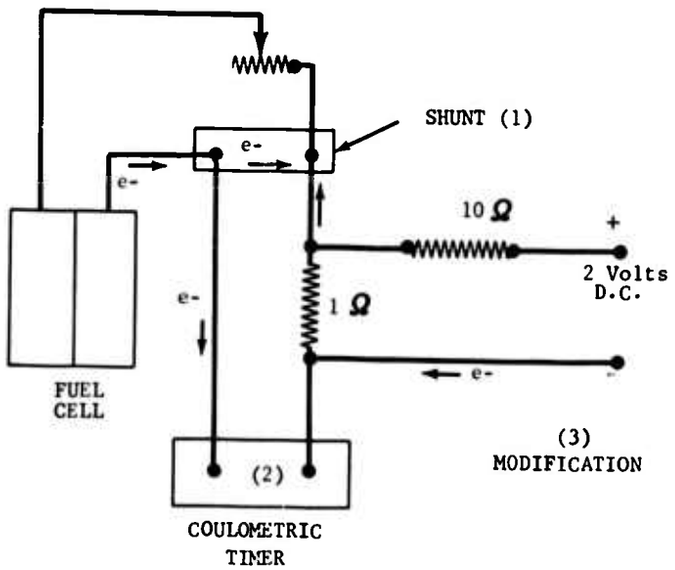

(1) 100 mv shunt, Esterline-Angus Co., Indianapolis, Ind., for use with model AW recording DC ammeter.

(2) Coulometric timer described in earlier report (1).

(3) The modification, made in the external circuit, consisted of adding a 1 ohm resistor in series with the signal circuit. A voltage drop is imposed across this resistor by means of a DC source.

APPENDIX C-3

AIR CONTROL SCHEMATIC

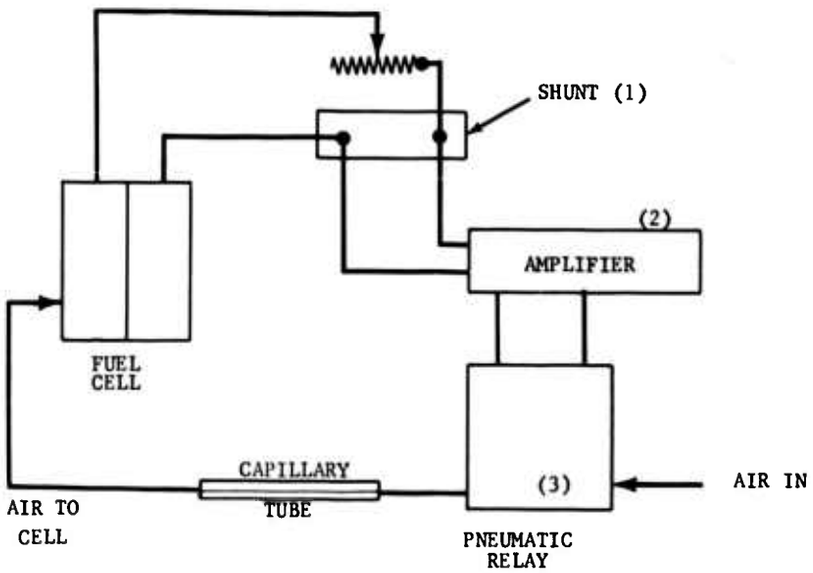

(1) 100 mv shunt, Esterline-Angus Co., Indianapolis, Ind., for use with model AW recording DC ammeter.

(2) DC amplifier, model A-12, Electro Instruments, Inc., San Diego, Cal.

(3) Pneumatic relay, Type 138R, 0.5-5.0 MADC input, air supply 20 psig, air output 3-15 psig, Manning Maxwell and Moore, Inc., Stratford, Conn.

APPENDIX C-4

METHANOL ELECTRODE LIFE STUDY

Run Condition, Electrical Performance, Feed and Product Rates

Run Number	3618-55 (Continued)											
Run Hours	693	744	813	837	861	909	981	1009	1029 (**)	1080 (***)	1130	1149
Cell Temp, °C	82	80	82	83	80	80	80	80	80	82	83	83
Current Collectors	0.001" thick x 3/16" wide Pt sheet around periphery plus center electrode contacts											
Cathode	52 mesh Pt screen plus 8 mg Pt black/cm^2 (8 mils thick)											
Anode	80 mesh Pt screen plus 8 mg Pt black/cm^2 (6 mils thick)											
Membrane	Ionics CR-61 cationic (21.3 mils thick), tight between electrodes											
Electrolyte between Electrodes	None											
Current Density, ma/cm^2	50	50	50	49	50	50	49	49	30	49	107	105 (****)
Volts Polarization at Constant Current	0.64	0.65	0.67	0.67	0.65	0.66	0.66	0.62	--	--	--	--
Volts Polarization with Open Circuiting	0.62	0.63	0.62	0.63	0.62	0.61	0.62	0.60 (*)	0.61 (*)	0.59	0.71	0.69
Feed Solution During Period:												
Methanol, ml	31.2	70.2	98.8	34.9	37.7	67.9	104.6	36.4	33.9	78.5	133	51
Water, ml	64.8	148.8	210.2	74.1	80.3	144.1	222.4	77.6	72.1	145.5	230	86
Total, ml	96.0	219.0	309.0	109.0	118.0	212.0	327.0	114.0	106.0	224.0	363	137
Feed Solution For Run:												
Methanol, ml	1117.9	1188.1	1286.9	1321.8	1359.5	1427.4	1532.0	1568.4	1602.3	1680.8	133	184
Water, ml	1939.1	2087.9	2298.1	2372.2	2452.5	2596.6	2819.0	2896.6	2968.7	3114.2	230	316
Total, ml	3057.0	3276.0	3585.0	3694.0	3812.0	4024.0	4351.0	4465.0	4571.0	4795.0	363	500
Methanol, ml/hr	1.61	1.59	1.58	1.58	1.58	1.57	1.56	1.56	1.56	1.55	2.66	2.66
Make up 30% H_2SO_4 Soln., ml	55	--	--	47	67	--	--	--	--	--	--	--
Condensate from CO_2 Anode at 26°C.												
For Period, ml	15	26	38	13	12	25	35	13	12	20	46	20
Total for Run, ml	434	460	498	511	523	548	583	596	608	628	46	66
Total Methanol, ml (calc.)	74.7	76.3	79.0	79.7	80.6	84.6	88.1	90.0	91.4	--	3.6	4.7
Total Methanol, ml/hr	0.108	0.102	0.097	0.095	0.093	0.093	0.090	0.090	0.089	--	0.072	0.068
Condensate from H_2 Cathode at 26°C.												
For Period, ml	50	133	153	114	40	120	158	39	38	55	143	59
Total for Run, ml	1836	1969	2122	2236	2276	2396	2554	2593	2631	2686	143	202
Total Methanol, ml (calc.)	96.3	97.6	97.6	98.7	99.7	117.1	147.1	152.1	155.5	--	1.0	1.4
Total Methanol, ml/hr	0.139	0.131	0.120	0.118	0.116	0.129	0.150	0.152	0.151	--	0.020	0.020
Total CO_2, CF @ 26°C.	19.00	20.41	22.39	23.05	23.70	25.00	27.00	27.67	28.29	29193	2.78	3.45
Total H_2, CF @ 26°C.	56.41	60.76	66.77	68.85	70.90	75.12	81.20	83.27	85.20	89.39	8.61	11.81

(*) Started open circuiting 15 seconds every 3 hours.

(**) Removed electrolyte from system and replaced with fresh 1 vol % CH_3OH in 30 wt % H_2SO_4 and recycled for 51 hours.

(***) Current increased to 105 ma/cm^2, less than 6 mv oscillations observed.

(****) 147 ma/cm^2 gave 0.73 volts polarization, 30 ma/cm^2 gave 0.57 volts polarization.

APPENDIX C-4 (CONT'D)

METHANOL ELECTRODE LIFE STUDY-SOLUTION ANALYSES AT 26°C.

Run Number	3618-55 (Continued)										
Run Hours	693	744	813	837	861	909	981	1009	1029	1130	1149
Anolyte Electrolyte Recycle											
Density, gms/ml	1.19	1.20	1.20	1.18	1.18	1.19	1.18	1.17	1.16	1.226	1.225
H_2SO_4, normality	7.20	7.25	7.0	6.8	6.6	6.7	6.6	6.6	6.2	8.0	8.1
H_2SO_4, wt %	29.1	29.3	28.2	27.7	26.1	26.9	26.1	26.1	25.0	31.7	32.0
Methanol, vol %	--	--	--	0.93	--	--	--	--	--	--	--
Methanol, vol % calc.	2.4	0.82	0.90	0.80	1.0	2.4	1.3	2.0	1.5	1.0	0.7
Catholyte Electrolyte:											
Density, gms/ml	--	--	--	1.16	--	--	--	--	--	--	1.152
H_2SO_4, normality	--	--	--	6.33	--	--	--	--	--	--	5.65
H_2SO_4, wt %	--	--	--	25.4	--	--	--	--	--	--	23.2
Methanol, vol %	--	--	--	0.55	--	--	--	--	--	--	--
Methanol, vol % calc.	2.5	0.25	0.0	0.25	0.30	2.0	2.7	1.8	1.0	0.1	0.1
Condensate from CO_2 Anode:											
Density, gms/ml	0.974	0.988	0.987	0.989	0.986	0.974	0.983	0.977	0.981	0.986	0.989
H_2SO_4, normality	0.05	0.03	0.02	0.04	0.02	0.03	0.03	0.03	0.02	0.05	0.02
H_2SO_4, wt %	0.23	0.14	0.09	0.16	0.09	0.14	0.14	0.14	0.09	0.23	0.09
Methanol, vol %	--	--	--	4.5	--	--	--	--	--	--	--
Methanol, vol % calc.	17.0	6.3	7.0	5.6	7.8	17.0	10.0	14.7	11.5	7.8	5.6
Condensate from H_2 Cathode:											
Density, gms/ml	1.017	1.072	1.058	1.119	1.028	1.053	1.034	1.003	1.016	0.998	0.998
H_2SO_4, normality	1.52	2.58	1.98	4.21	1.20	2.60	2.15	0.95	1.09	0.07	0.08
H_2SO_4, wt %	7.2	11.5	9.1	17.5	5.6	11.8	9.9	4.5	5.1	0.32	0.40
Methanol, vol %	--	--	--	1.10	--	--	--	--	--	--	--
Methanol, vol % calc.	18.0	1.0	0.0	1.0	2.5	14.5	19.0	13.0	9.0	0.7	0.7
Fuel Fed:											
Methanol, vol %	32	32	32	32	32	32	32	32	32	37	37
Water, vol %	68	68	68	68	68	68	68	68	68	63	63
H_2SO_4, normality	0.79	0.90	0.90	0.90	0.90	0.90	0.90	0.90	0.90	0.8	0.8
Electrolyte Sample from Cell:											
Anolyte, total ml	62.4	64.1	66.1	73.1	75.3	77.5	79.4	86.3	Completely Removed from Cell	2.9	6.9
Catholyte, total ml	16.1	16.1	16.1	22.9	22.9	22.9	22.9	28.9		--	5.0

APPENDIX C-5

OVER-ALL MATERIAL AND ELECTROCHEMICAL BALANCES

For 1029 Hour Run 3618-55

Reactions:

Anode $CH_3OH + H_2O \longrightarrow CO_2 + 6H^+ + 6e^-$

Cathode $6H^+ + 6e^- \longrightarrow 3H_2$

Coulombs for run, 1029 hours @ 5.0 amps..... 18.52×10^6

Coulombic equivalent CH_3OH reacted..... 32.0 gm moles

Carbon Balance

CH_3OH Fed.....	39.6 gm moles
CO_2 Produced.....	31.8 gm moles
CH_3OH in Gas Condensates.....	6.2 gm moles
CH_3OH in Exit Gases.....	0.6 gm moles
Total Out.....	38.6 gm moles

% Carbon Balance (out/in)..... 97.5

Mole Ratio Methanol Reacted/CO_2 Produced..... 1.02

Water Balance

H_2O Fed.....	181.3 gm moles
H_2O Equiv. of H_2 Produced.....	32.0 gm moles
H_2O in Exhaust Gases.....	151.5 gm moles
Total Out.....	184.8 gm moles

% Water Balance (out/in)..... 101.9

% Coulombs Equivalent to H_2..... 100.0

% Coulombs Equivalent to CO_2..... 99.4

Mole Ratio H_2/CO_2 Produced..... 3.02

Over-all Weight Balance:

CH_3OH Fed.....	1266 gms
H_2O Fed.....	3264 gms
Total Input.....	4530 gms
CH_3OH Unreacted.....	216 gms
H_2O Unreacted.....	2735 gms
H_2 Produced.....	192 gms
CO_2 Produced.....	1390 gms
Total Output.....	4533 gms

% Weight Balance (out/in)..... 100.1

APPENDIX C-6

FEED AND GAS RATES-RUN 3618-55

Figure C-1
Log Of Feed

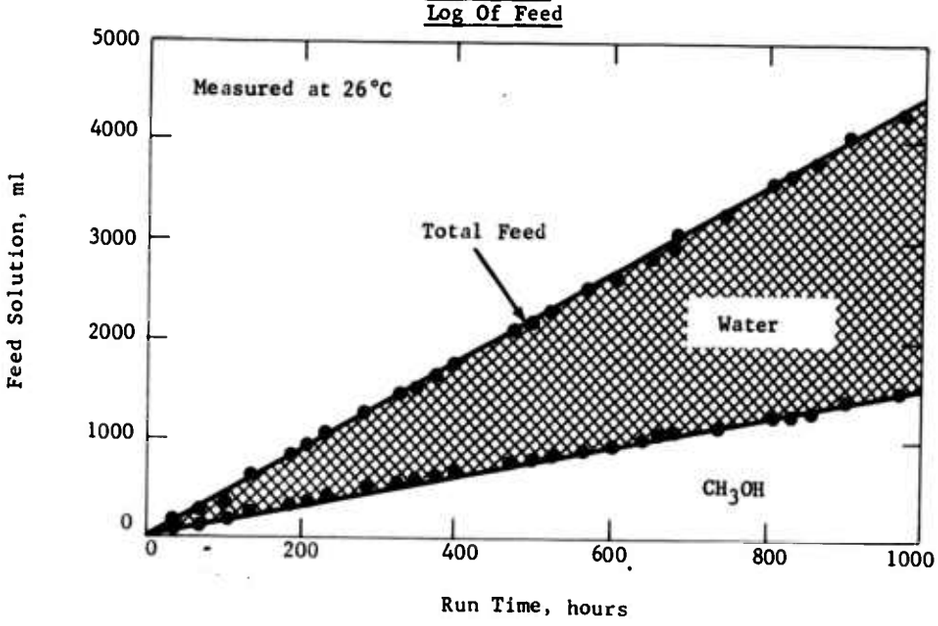

Figure C-2
Log Of Gas Production

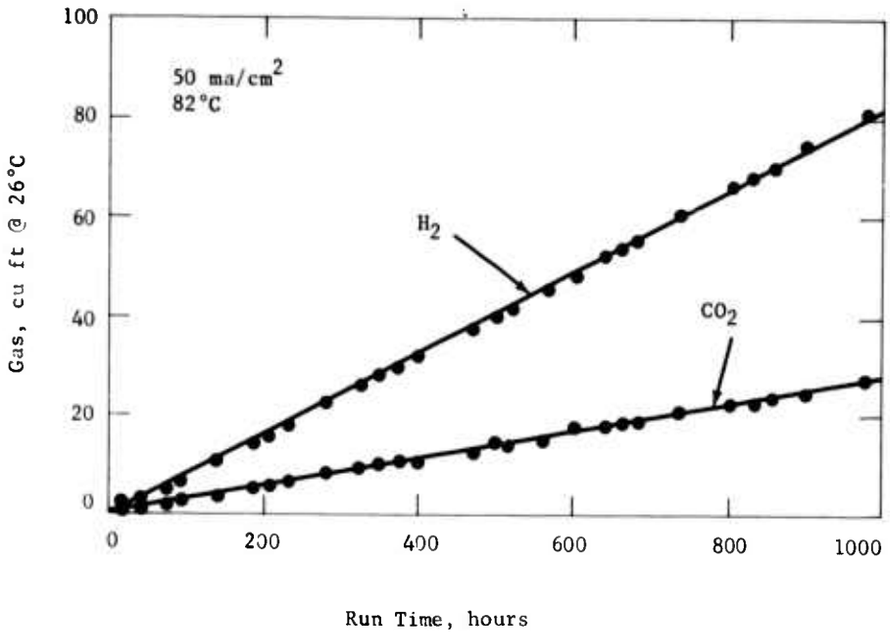

APPENDIX C-7

METHANOL ELECTROLYTE CHAMBER SIZE STUDIES OF THE METHANOL ELECTRODE

Electrolyte: 1 vol % methanol in 30 wt % H_2SO_4 (initial concentration)
Temp: 85°C
Electrode: 80 mesh platinum rhodium screen plus 8 mg platinum black per cm^2

Electrolyte Chamber Thicknesa, mils	Current ma/cm^2	Current from Cell, amps	Test Period, hours	Exhaust Gas	Total Exhaust Gaa, cu ft at 24°C	Condensate From Gaa, ml collected at 20°C	Gas Condensate Analysea			Gm Molea of Exhaust per Hour	Water Condensed, molea/mole of exhauat***	Liquid Entrainment, vol % on water**	Voltage Oscillation at Anode During Test, mv
							gms/cc at 24°C	vol % CH_3OH*	H_2SO_4 normality				
225	50	5.0	285	CO_2	7.88	148	0.983	10.2	0.025	0.032	0.80	0.05	5
225	50	5.0	285	H_2	24.44	698	1.055	8.7	2.36	0.099	0.78	3.8	--
225	105	10.5	69	CO_2	3.45	66	0.988	7.0	0.03	0.065	0.77	0.06	6
225	105	10.5	69	H_2	11.81	202	0.998	0.5	0.08	0.199	0.81	0.16	--
100	94	9.4	24	CO_2	0.84	15	0.977	15.0	0.06	0.041	0.73	0.12	30
50	45	4.5	18	CO_2	--	4	--	--	--	--	0.41	--	20-30
25	50	5.0	24	CO_2	0.49	4	0.993	3.0	0.038	0.022	0.41	0.08	20-40
25	100	10.0	18	CO_2	0.64	7.4	0.990	5.0	0.025	0.041	0.52	0.05	60
25	25	2.5	25	CO_2	0.28	2.0	0.977	14.5	0.025	0.013	0.29	0.05	10-20
25	25	2.5	70	CO_2	0.82	5.0	0.984	9.2	0.003	0.014	0.27	0.01	10-20

* Calculated from density and acidity. No screen was in exit port, therefore methanol contents are high. Methanol in electrolyte unknown.
** Calculated from acidity assuming entrainment as 30 wt % H_2SO_4.
*** Equilibrium = 0.80 moles H_2O/mole of exhaust

APPENDIX C-8

LOG OF PROCEDURES

Run 3618-80

Startup

Cell was assembled, filled with 30 wt % H_2SO_4, and heated to 70° C overnight. Next morning the cell temperature was raised to 82° C and started by pumping 1 wt % HNO_3 in 30 wt % H_2SO_4 through the catholyte side and 2 vol % CH_3OH in 30 wt % H_2SO_4 through the anolyte side. After about 20 minutes a voltage response was observed permitting the cell to be put into current operation.

Operation During Hours 0-1.5

With once through pumping of anolyte and catholyte streams the current was varied to determine performance.

1.5 Hours

Recycle of anolyte at 320 ml/hour and catholyte at 620 ml/hour started with methanol and HNO_3 addition respectively. The methanol was added in a water solution containing 69 vol % methanol or one to one mole ratio of methanol to water. The nitric acid solution consisted of 66 vol % of concentrated nitric acid (70 wt %) made up to 100 vol % with 30 wt% H_2SO_4 solution. Addition was controlled with the coulometric timer.

22 Hours

Current had dropped from 50 to 22 ma/cm^2 due to methanol deficiency. Performance was restored by adding methanol to the recycle electrolyte equivalent to about 0.6 vol %. Current interrupter was put in service opening circuit 1 minute every hour.

40 Hours

Performance deteriorated because of HNO_3 deficiency.

50 Hours

Performance restored by addition of HNO_3 to recycle followed by opening and closing circuit at about 2 minute intervals for about 40 minutes.

62-75 Hours

Performance was lost to about 8 ma/cm^2 due to deficiency of methanol. Performance was again restored by methanol addition.

100 Hours

Performance was lost to about 20 ma/cm^2 due to low methanol concentration. To assure steady feed addition the coulometric timer was removed from the circuit. The feed pumps were controlled at a constant rate by a conventional timer.

124 Hours

Catholyte removed and fresh 2 wt % HNO_3 in 30 wt% H_2SO_4 added. Performance deteriorated after 5 hours from about 35 to 6 ma/cm^2.

149 Hours

Washed fresh 1 vol % methanol in 30 wt % H_2SO_4 through anolyte section until performance recovered. Anode polarization increased sharply after 3 hours and continued so for 178 hours. The poor level of operation was apparently caused by build up of HNO_3 in the anolyte recycle.

179-181 Hours

The anode electrode was rejuvenated by washing with fresh 1 vol % methanol in 30 % H_2SO_4 at 82° C for several hours followed by evolution of hydrogen at the cathode for 1 hour at 3 amperes.

APPENDIX C-9

ELECTRICAL PERFORMANCE DATA
TOTAL FUEL CELL STUDIES WITH CH_3OH AND AIR-HNO_3 REDOX SYSTEMS

Run Number	-3618-80-												
Pressure, atm abs	-1.0-												
Cell Temp, °C	76	76	71	76	76	76	76	76	77	82	-	-	81
HNO_3 Regen. Temp., °C	-28-												
Electrolyte	-30 wt % H_2SO_4 (nominal)												
CH_3OH in Anolyte, vol %	-2.0-												
HNO_3 in Catholyte, wt %	-1.0-												
Run Hours	-0-1.5-									2	10	18	22
Current Density, ma/cm^2	29.5	38.5	50.5	60.0	68.5	78.0	88.0	112	11.5	50	50	43	22
Volts Polarization at:													
CH_3OH Anode	0.56	0.57	0.58	0.58	0.59	0.60	0.59	0.60	0.52	0.56	0.60	0.65	0.83
Air-HNO_3 Cathode	0.18	0.18	0.21	0.22	0.23	0.24	0.24	0.24	0.17	0.21	0.17	0.17	0.16
IR Drop, volts	0.11	0.14	0.16	0.15	0.17	0.20	0.19	0.26	0.04	0.08	0.09	0.09	0.07
Observed Cell Voltage	0.36	0.32	0.26	0.26	0.22	0.17	0.19	0.11	0.48	0.35	0.35	0.30	0.15
Efficiency, %	28.6	25.4	20.6	20.6	17.5	13.5	15.1	8.7	38.1	27.8	27.8	23.8	11.9
Cell Resistance, ohms	0.037	0.036	0.032	0.025	0.025	0.026	0.021	0.023	0.035	0.016	0.018	0.021	0.032
Power, m watts/cm^2:													
Ex IR	13.6	17.6	21.2	24.6	26.7	29.0	33.9	41.4	5.9	21.5	22.0	16.8	4.8
Observed	10.5	12.1	13.1	15.3	15.1	13.7	16.3	12.4	5.5	17.5	17.5	12.9	3.3
CH_3OH Conversion per Pass through Cell, %(calc.)	11.6	15.2	19.9	23.5	26.8	30.6	34.5	44.0	4.5	19.4	19.4	16.7	8.5
HNO_3 Conversion per Pass through Cell, %(calc.)	30.9	40.4	52.9	62.8	71.7	81.8	92.2	117	12.0	50.2	50.2	45.0	23.0

APPENDIX C-9 (CONT'D)

ELECTRICAL PERFORMANCE DATA

TOTAL FUEL CELL STUDIES WITH CH_3OH AND AIR-HNO_3 REDOX SYSTEMS

Run Number	- 3618-80 -													
Pressure, atm abs	- 1.0 -													
Cell Temp, °C	82	--	--	85	83	--	84	84	--	84	--	83	83	
HNO_3 Regen. Temp, °C	27	--	--	28	28	--	25	25	--	26	29	29	--	
Electrolyte	- 30 wt % H_2SO_4, nominal -													
CH_3OH in Anolyte, vol %	- - - - -2.0 (nominal at start of run)- - - - - - - - - - - - - - - - - - - -(27 wt % H_2SO_4)- - - - - - - - - - -													
HNO_3 in Catholyte, wt %	- - - - -1.0 (nominal at start of run)- - - - - - - - - - - - - - - - - - - -(23 wt % H_2SO_4)- - - - - - - - - - -													
Run Hours	23	30	40	50	51	56	75	76	84	102	118	142	149	
Current Density, ma/cm^2	50	40	25	49	50	38	4	39	33	38	30	6	47	
Volts Polarization at:														
CH_3OH Anode	0.59	0.64	0.66	0.61	0.61	0.67	0.97	0.60	0.65	0.61	0.61	1.03	0.54	
Air-HNO_3 Cathode	0.17	0.17	0.29	0.16	0.16	0.19	0.16	0.18	0.19	0.19	0.23	0.11	0.17	
IR Drop, volts	0.10	0.12	0.06	0.11	0.10	0.08	0.03	0.09	0.08	0.12	0.14	0.03	0.10	
Observed Cell Voltage	0.35	0.28	0.20	0.33	0.34	0.27	0.05	0.34	0.29	0.29	0.23	0.04	0.40	
Efficiency, %	27.8	22.2	15.9	26.2	27.0	21.4	4.0	27.0	23.0	23.0	18.2	3.2	31.7	
Cell Resistance, ohms	0.020	0.030	0.024	0.022	0.020	0.021	--	0.023	0.024	0.032	0.046	--	0.021	
Power, m watts/cm^2:														
Ex IR	22.5	16.0	6.5	21.6	22.0	13.3	0.03	16.8	12.2	15.6	11.1	0.04	23.5	
Observed	17.5	11.2	5.0	16.2	17.0	10.2	0.02	13.6	9.6	11.0	6.9	0.02	18.8	
CH_3OH Conversion per Pass through Cell, % (calc.)	19.4	15.5	9.7	19.0	19.4	14.8	1.6	15.1	12.8	14.8	11.7	2.3	18.3	
HNO_3 Conversion per Pass through Cell, % (calc.)	52.3	41.8	26.2	51.2	52.3	39.8	4.2	40.8	34.6	39.8	31.4	3.1	24.6	

APPENDIX C-9 (CONT'D)

ELECTRICAL PERFORMANCE DATA

TOTAL FUEL CELL STUDIES WITH CH_3OH AND AIR-HNO_3 REDOX SYSTEMS

Run Number	3618-80								
Pressure, atm abs	1.0								
Cell Temp, °C	--	80	83	82	84	83	80	80	82
HNO_3 Regen. Temp, °C	--	30	--	--	--	--	--	--	--
Electrolyte	30 wt % H_2SO_4 nominal								
CH_3OH in Anolyte, vol %	2.0 (nominal)		1.0						
HNO_3 in Catholyte, wt %	2.0 (nominal)		1.0						
Run Hours	154	166	178	179-181					
Current Density, ma/cm^2	2	2	44	40	41	32-42 oscillating	40	40	40
Volts Polarization at:									
CH_3OH Anode	1.08	1.10	0.58	0.57	0.57	0.77	0.60	0.58	0.62
Air- HNO_3 Cathode	0.12	0.08	0.17	0.27	0.33	0.18	0.33	0.32	0.33
IR Drop, volts	0.00	0.00	0.09	0.11	0.06	0.17	0.12	0.16	0.09
Observed Cell Voltage	0.01	0.03	0.37	0.26	0.25	0.09	0.16	0.15	0.17
Efficiency, %	0.8	2.4	29.3	20.6	19.8	7.1	12.7	11.9	13.5
Cell Resistance, ohms	--	--	0.020	0.028	0.015	0.047	0.030	0.040	0.022
Power, mwatts/cm^2:									
Ex IR	--	--	20.2	14.8	12.7	9.3	11.2	12.4	10.4
Observed	--	--	16.3	10.4	10.2	3.2	6.4	6.0	6.8
CH_3OH Conversion per Pass through Cell, % (calc.)	0.8	0.8	34.2	62.2	79.8	93.0	38.8	77.8	89
HNO_3 Conversion per Pass through Cell, % (calc.)	1.0	1.0	46.1	83.6	107	125	52.4	105	120

APPENDIX C-9 (CONT'D)

MATERIAL BALANCE DATA

TOTAL FUEL CELL STUDIES WITH CH_3OH AND AIR-HNO_3 REDOX SYSTEMS

Run Number	3618-80		
Test Period, hours	0-121	24-25	180.4-181
Average Current, amps	3.15	4.8	4.1
Total Coulombs	1,374,000	17,300	9,100
Coulombic Equivalent of:			
CH_3OH Reacted, gm moles	2.37	0.0299	0.0157
HNO_3 Reacted, gm moles	4.74	0.0598	0.0314
O_2 Reacted, gm moles	3.55	0.0448	0.0236
Feed Rates, stoichiometric ratio to current:			
CH_3OH	3.38	2.66	1.56
HNO_3	0.96	1.99	1.17
O_2 in Air	1.76	1.60	1.90
Oxygen Used, gm moles	3.55(*)	0.0500	0.0174
Oxygen Used, % of stoichiometric	100(*)	110	74
Equiv. HNO_3 regen. by O_2 used, gm moles	4.74(*)	0.0667	0.0232
% Conversion per Pass through Cell:			
CH_3OH (coulombic)	29.6	37.5	64.0
HNO_3 (coulombic)	104	50.2	85.3
O_2 in Air	56.8(*)	69.5	38.8
CH_3OH (coulombic + chem)	58.0	58.9	93.5
HNO_3 Regeneration Efficiency, coulombs/coulomb equiv. of HNO_3 consumed	1.04(*)	1.73	2.16
CH_3OH Loss, lbs/100 lbs reacted coulombically	96(*)	57	46

(*) Calculated assuming 100% stoichiometric use of O_2.

APPENDIX C-10

LOG OF ELECTRICAL PERFORMANCE RUN 3618-80
WITH CH_3OH AND AIR-HNO_3 SYSTEMS

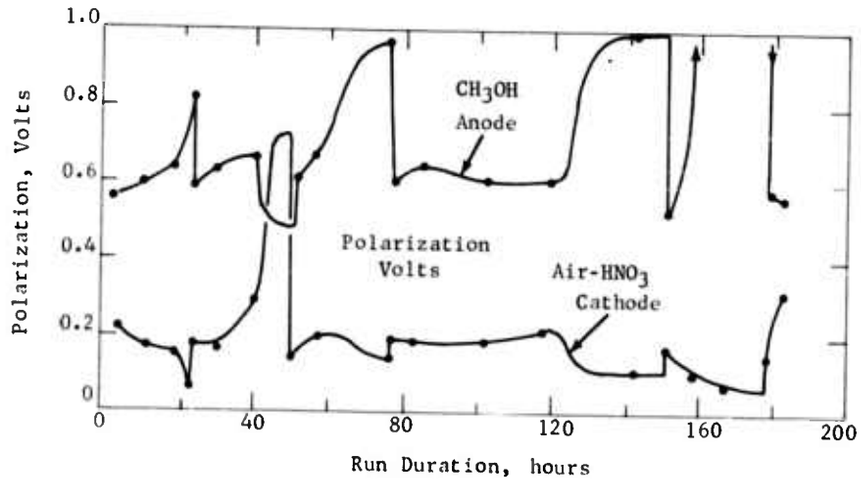

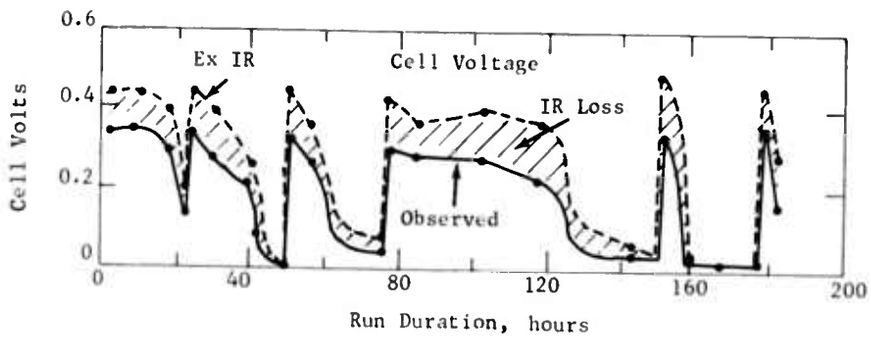

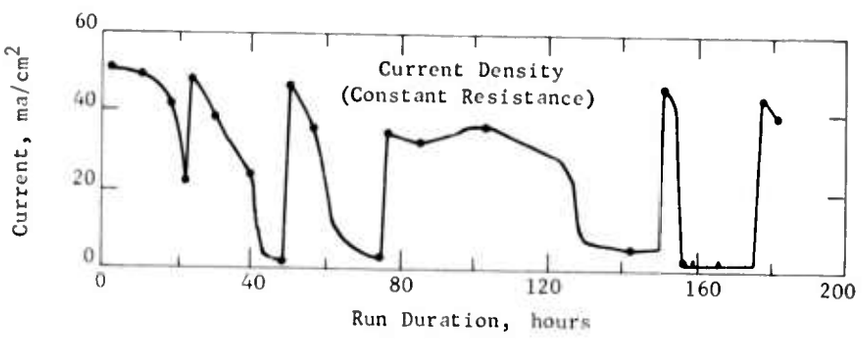

See Appendix C-10 for descriptive details

APPENDIX C-11

SUMMARY OF CELL ASSEMBLY COMPONENTS AND DIMENSIONS

Run Number	3618-80	3618-92	3618-96	3618-100	3618-105	3618-114	3618-120
Anolyte Chamber, mils	225	225	225	225	225	225	225
Anode Gold Current Collector, mils	6	6	6	6	18	18	18
Anode							
Number of Screens	3	3	3	3	1	1	1
Mesh (Pt-Rh)	80	80	80	80	80	80	80
Pt Black, mgs/cm^2	8	8	8	8	8	8	8
Thickness, mils	18	18	18	18	6	6	6
Membrane Between Electrodes							
Type	CR-61*	A-type**	C-313***	C-313***	C-313***	C-313***	C-313***
Thickness, mils	21	4	5.6	5.6	5.6	5.6	5.6
Cathode							
Number of Screens	3	2	2	1	1	1	1
Mesh (Pt-Rh)	80	150	150	80	80	80	80
Pt Black, mgs/cm^2	8	8	8	8	8	8	8
Thickness, mils	18	8	8	6	6	6	6
Cathode Gold Current Collector, mils	6	18	18	18	18	18	18
Catholyte Chamber, mils	225	225	225	225	225	225	225
Cell Electrode Dimensions, inches	4x4	4x4	4x4	4x4	4x4	4x4	4x4

* Ionics CR-61 sulfonated polystyrene reinforced with dynel fabric.
** A-Type membrane.
*** AMFion C-313 cation membrane.

APPENDIX C-12

FUEL CELL ASSEMBLY DATA

STUDIES WITH CH_3OH AND AIR-HNO_3 REDOX SYSTEMS

Run Number	3618-124	3618-126
Anolyte Chamber, mils	225	225
Teflon Filler Back of Current Collector, mils	2	5
Anode Gold Current Collector, mils	18	18
Anode		
Number of Screens	1	1
Mesh (Pt-Rh)	80	80
Pt Black, mgs/cm^2	8	8
Thickness, mils	6	6
Teflon Spacer for Gas Release, mils	None	20
Membrane Between Electrodes		
Type	C-313*	C-313*
Thickness, mils	5.6	5.6
Teflon Spacer for Gas Release, mils	None	20
Cathode		
Number of Screens	1	1
Mesh (Pt-Rh)	80	80
Pt Black, mgs/cm^2	8	8
Thickness, mils	6	6
Cathode Gold Current Collector, mils	18	18
Teflon Filler Back of Current Collector, mils	2	5
Catholyte Chamber, mils	225	225
Cell Electrode Dimensions, inches	4 x 4	4 x 4

* AMFion C-313 cation membrane.

APPENDIX C-13

ELECTRICAL PERFORMANCE DATA

TOTAL FUEL CELL STUDIES WITH CH_3OH AND AIR-HNO_3 REDOX SYSTEMS

Run Number	3618-92						3618-96				
Run Part	A				B	C	A	B	C	D	E
Pressure, atm abs	1.0						1.0				
Cell Temp, °C	84	84	84	84	85	84	83	82	83	82	83
HNO_3 Regen. Temp, °C	23	23	23	23	23	23	28	27	28	28	28
Electrolyte	30 wt % H_2SO_4						30 wt % H_2SO_4				
CH_3OH in Anolyte, vol %	1.0						1.0				
HNO_3 in Catholyte, wt %	1.0						1.0				
Run Test Period, minutes	83				50	48	22	133	66	50	45
Current Density, ma/cm^2	34	22	30	11	30	30	20	20	29	20	38
Volts Polarization at:											
CH_3OH Anode	0.69	0.61	0.68	0.55	0.71	0.65	0.63	0.61	0.69	0.61	0.69
Air-HNO_3 Cathode	0.36	0.29	0.34	0.24	0.28	0.32	0.24	0.23	0.27	0.22	0.22
IR Drop, volts	0.05	0.045	0.06	0.01	0.06	0.07	0.10	0.08	0.14	0.08	0.22
Observed Cell Voltage	0.11	0.265	0.13	0.41	0.15	0.17	0.24	0.29	0.11	0.30	0.08
Efficiency, %	8.8	21.0	10.3	32.5	11.9	13.5	19.0	23.0	8.8	23.8	6.3
Cell Resistance, ohms	0.015	0.020	0.020	0.009	0.020	0.023	0.050	0.040	0.048	0.040	0.058
Power, $mwatts/cm^2$											
Ex IR	5.5	6.8	5.7	4.6	6.3	7.2	6.8	7.4	7.2	7.6	11.4
Observed	3.7	5.8	3.9	4.5	4.5	5.1	4.8	5.8	3.2	6.0	3.0
CH_3OH Conversion per Pass through Cell, % (calc)	46.4	30.0	40.9	15.0	75.0	50.0	45.2	45.2	48.1	44.2	45.0
HNO_3 Conversion per Pass through Cell, % (calc)	71.5	46.1	63.0	23.1	101.3	101.3	12.8	12.8	27.8	13.0	24.4

APPENDIX C-14

MATERIAL BALANCE DATA

TOTAL FUEL CELL STUDIES WITH CH_3OH AND AIR-HNO_3 REDOX SYSTEMS

Run Number	3618-92----		---------- 3618-96 ----------				
Run Part	B	C	A	B	C	D	E
Test Period, minutes	50	48	22	133	66	50	45
Average Current, amps	3.0	3.0	2.0	2.0	2.9	2.0	3.8
Total Coulombs	9,000	8,640	2,640	15,950	11,480	6,000	10,250
Coulombic Equivalent of:							
CH_3OH Reacted, gm moles	0.0155	0.0149	0.0046	0.0276	0.0198	0.0104	0.0177
HNO_3 Reacted, gm moles	0.0310	0.0298	0.0091	0.0552	0.0396	0.0208	0.0354
O_2 Reacted, gm moles	0.0233	0.0224	0.0068	0.0414	0.0298	0.0156	0.0265
Feed Rates, Stoichiometric Ratio to Current:							
CH_3OH	1.34	2.00	2.21	2.21	2.08	0.26	2.22
HNO_3	0.98	0.09	7.8	7.8	5.4	7.7	4.1
O_2 in Air	1.68	1.77	1.52	1.46	1.73	1.91	2.23
Oxygen Used, gm moles	0.0144	0.0151	0.0048	0.0309	0.0259	0.0124	0.0249
Oxygen Used, % of stoichiometric	62.0	67.7	70.6	74.6	87.0	79.5	93.8
Equiv. HNO_3 Regen. by O_2 Used, gm moles	0.0192	0.0201	0.0064	0.0412	0.0345	0.0165	0.0332
% Conversion Per Pass Through Cell:							
CH_3OH (coulombic)	75.0	50.0	45.2	45.2	48.1	44.2	45.0
HNO_3 (coulombic)	101.3	101.3	12.8	12.8	27.8	13.0	24.4
O_2 in Air	36.7	38.0	46.4	51.0	50.2	41.6	41.8
CH_3OH (coulombic + chem)	75.5	67.2	46.6	45.2	48.1	44.2	56.8
HNO_3 Regeneration Efficiency, coulombs/coulomb equiv. of HNO_3 consumed	2.58	1.49	3.04	8.50	9.90	8.10	3.08
CH_3OH Loss, lb/100 lbs reacted coulombically	0.65	34.5	3.1	0.00	0.00	0.00	26.3

APPENDIX C-15

ELECTRICAL PERFORMANCE DATA

TOTAL FUEL CELL STUDIES WITH CH_3OH AND AIR-HNO_3 REDOX SYSTEMS

Run Number	3618-100											
Run Part	A	B	C	D	E	F	G					
Pressure, atm abs	1.0											
Cell Temp, °C	82	82	80	80	81	81	82					
HNO_3 Regen. Temp, °C	27	27	23	27	23	23	27					
Electrolyte	30 wt % H_2SO_4											
CH_3OH in Anolyte, vol %	1.0											
HNO_3 in Catholyte, wt %	2.0	2.0	1.0	2.0	2.0	2.0	2.0					
Run Test Period, minutes	88	21	60	62	60	30	45					
Current Density, ma/cm^2	27.3	66	14	30	40	39	8.0	23.0	38.5	41.0	66.0	85.0
Volts Polarization at:												
CH_3OH Anode	0.65	0.64	0.56	0.63-0.79	0.63	0.63	0.52	0.57	0.59	0.57	0.61	0.60
Air-HNO_3 Cathode	0.22	0.25	0.24	0.21	0.25	0.26	0.20	0.21	0.24	0.23	0.24	0.22
IR Drop, volts	0.12	0.23	0.06	0.16-0.15	0.20	0.16	0.03	0.07	0.12	0.13	0.24	0.27
Observed Cell voltage	0.22	0.09	0.35	0.21-0.06	0.13	0.16	0.46	0.36	0.26	0.28	0.12	0.12
Efficiency, %	17.5	7.1	27.8	16.6-4.8	10.3	12.7	36.5	28.6	20.6	22.2	9.5	9.5
Cell Resistance, ohms	0.044	0.035	0.043	0.052	0.050	0.041	0.038	0.030	0.031	0.032	0.036	0.032
Power, mwatts/cm^2												
Ex IR	9.3	21.1	5.8	11.1-6.3	13.2	12.5	3.9	9.9	14.6	16.8	23.8	33.1
Observed	6.0	5.9	4.9	6.3-1.8	5.2	6.2	3.7	8.3	10.0	11.5	7.9	10.2
CH_3OH Conversion per Pass through Cell, % (calc)	25.3	54.9	69.5	63.6	56.8	46.4	4.7	13.4	23.4	23.8	38.4	49.5
HNO_3 Conversion per Pass through Cell, % (calc)	26.1	106	6.7	7.2	9.6	9.4	12.8	36.9	61.9	65.8	106	136

APPENDIX C-16

MATERIAL BALANCE DATA

TOTAL FUEL CELL STUDIES WITH CH_3OH AND AIR-HNO_3 REDOX SYSTEMS

Run Number	3618-100					
Run Part	A	B	C	D	E	F
Test Period, minutes	88	21	60	62	60	30
Average Current, amps	2.7	6.6	1.4	3.0	4.0	3.9
Total Coulombs	14,250	8,310	5,040	11,160	14,400	7,010
Coulombic Equivalent of:						
CH_3OH Reacted, gm moles	0.0246	0.0144	0.0087	0.0193	0.0248	0.01213
HNO_3 Reacted, gm moles	0.0492	0.0287	0.0174	0.0386	0.0496	0.0242
O_2 Reacted, gm moles	0.0369	0.0215	0.0130	0.0270	0.0372	0.0182
Feed Rates, Stoichiometric Ratio to Current:						
CH_3OH	3.94	1.82	1.44	1.57	1.76	2.16
HNO_3	3.84	0.94	14.9	13.8	10.4	10.7
O_2 in Air	2.09	2.07	1.92	1.79	1.90	1.75
Oxygen used, gm moles	0.0394	0.0238	0.0065	0.0212	0.0344	0.0154
Oxygen used, % of stoichiometric	106.5	110.5	48.2	78.5	92.2	84.6
Equiv. HNO_3 Regen. by O_2 Used, gm moles	0.0525	0.0317	0.0086	0.0282	0.0458	0.0205
% Conversion Per Pass Through Cell:						
CH_3OH (coulombic)	25.3	54.9	69.5	63.6	56.8	46.4
HNO_3 (coulombic)	26.1	106	6.7	7.2	9.6	9.4
O_2 in Air	51.2	53.3	25.1	44.0	48.8	48.4
CH_3OH (coulombic & chem.)	36.8	84.5	69.5	63.6	76.8	62.2
HNO_3 Regeneration Efficiency, coulombs/ coulomb equivalent of HNO_3 consumed	2.57	2.30	4.34	4.88	2.32	3.10
CH_3OH Loss, lbs/100 lbs reacted coulombically	45.7	53.9	0.0	0.0	35.2	33.8

APPENDIX C-17

ELECTRICAL PERFORMANCE DATA

TOTAL FUEL CELL STUDIES WITH CH_3OH AND AIR-HNO_3 REDOX SYSTEMS

Run Number	3618-105												
Run Part	A						B	C	D	E	F	G	H
Pressure, atm abs	1.0												
Cell Temp, °C	81						84	84	80	84	70	83	80
HNO_3 Regen Temp, °C	24						22	22					
Electrolyte	30 wt % H_2SO_4												
CH_3OH in Anolyte, vol %	1.0												
HNO_3 in Catholyte, wt %	2.0												
Run Test Period, minutes	32						60	55	25	35	23	41	48
Current Density, ma/cm^2	42	67	28	10	75	85	36	35	37	26	52	64	30
Volts Polarization at:													
CH_3OH Anode	0.61	0.64	0.58	0.55	0.66	0.67	0.66	0.59	0.66	0.95	0.69	0.63	0.63
Air-HNO_3 Cathode	0.23	0.24	0.21	0.19	0.25	0.28	0.31	0.39	0.24	0.18	0.32	0.33	0.24
IR Drop, volts	0.11	0.18	0.08	0.02	0.18	0.20	0.08	0.08	0.12	0.02	0.12	0.15	0.08
Observed Cell Voltage	0.26	0.15	0.34	0.45	0.11	0.06	0.16	0.15	0.19	0.06	0.08	0.10	0.26
Efficiency, %	20.6	11.9	27.0	35.8	13.8	4.8	12.7	11.9	15.1	4.8	6.3	7.9	20.6
Cell Resistance, ohms	0.026	0.027	0.028	0.020	0.024	0.024	0.022	0.022	0.032	0.008	0.023	0.023	0.026
Power, mwatts/cm^2													
Ex IR	15.5	22.1	11.8	4.7	21.7	22.1	8.6	8.0	11.5	2.1	10.4	16.0	10.2
Observed	10.9	10.0	9.5	4.5	8.2	5.1	5.8	5.3	7.0	1.6	4.2	6.4	7.8
CH_3OH Conversion per Pass through Cell, % (calc)	50.0	79.6	33.3	11.9	89.0	101	42.8	34.7	26.3	21.5	43.2	87.5	15.6
HNO_3 Conversion per Pass through Cell, % (calc)	27.0	43.1	18.0	6.4	48.2	54.6	64.8	71.3	66.7	58.5	46.8	43.1	54.1

APPENDIX C-18

MATERIAL BALANCE DATA

TOTAL FUEL CELL STUDIES WITH CH_3OH AND AIR-HNO_3 REDOX SYSTEM

Run Number	3618-105						
Run Part	B	C	D	E	F	G	H
Test Period, minutes	60	55	25	35	23	41	48
Average Current, amps	3.6	3.5	3.7	2.6	5.2	6.4	3.0
Total Coulombs	12,960	11,550	5,550	5,460	7,180	15,750	8,640
Coulombic Equivalent of:							
CH_3OH Reacted, gm moles	0.0224	0.0199	0.0096	0.0094	0.0124	0.0272	0.0150
HNO_3 Reacted, gm moles	0.0448	0.0398	0.0192	0.0188	0.0248	0.0544	0.0300
O_2 Reacted, gm moles	0.0336	0.0298	0.0144	0.0141	0.0186	0.0408	0.0225
Feed Rates, Stoichiometric Ratio to Current:							
CH_3OH	2.34	2.88	3.80	4.66	2.31	1.13	6.40
HNO_3	1.54	1.40	1.50	1.71	2.14	2.32	1.85
O_2 in Air	2.10	2.17	2.40	2.07	2.09	2.07	2.08
Oxygen Used, gm moles	0.0345	0.0283	0.0070	0.0106	0.0171	0.0327	0.0217
Oxygen Used, % of stoichiometric	103	94.8	48.6	75.2	92.0	54.8	96.3
Equiv. HNO_3 Regen. by O_2 Used, gm moles	0.0459	0.0376	0.0093	0.0141	0.0227	0.0435	0.0288
% Conversion per Pass through Cell:							
CH_3OH (coulombic)	42.8	34.7	26.3	21.5	43.2	87.5	15.6
HNO_3 (coulombic)	64.8	71.3	66.7	58.5	46.7	43.1	54.1
O_2 in Air	48.7	43.7	20.1	36.3	43.9	38.7	46.2
CH_3OH (coulombic + chem.)	65.9	51.2	26.3	25.6	61.5	87.5	22.2
HNO_3 Regeneration Efficiency coulombs/coulomb equiv. of HNO_3 consumed	1.94	1.45	2.59	2.19	1.92	2.92	2.12
CH_3OH Loss, lbs/100 lbs reacted coulombically	53.9	46.2	0.0	19.1	42.3	0.0	42.0

APPENDIX C-19

ELECTRICAL PERFORMANCE DATA

TOTAL FUEL CELL STUDIES WITH CH_3OH AND AIR-HNO_3 REDOX SYSTEMS

Run Number	3618-114								
Run Part	A	B	C	D	E	F	G	H	I
Pressure, atm abs	1.0								
Cell Temp, °C.	80	80	82	82	83	82	82	82	82
HNO_3 Regen. Temp, °C	20	20	20	20	30	28	31	30	27
Electrolyte	30 wt % H_2SO_4								
CH_3OH in Anolyte, vol %	1.0								
HNO_3 in Catholyte, wt %	2.0								
Run Test Period, minutes	70			60	123	95	109	52	89
Current Density, ma/cm^2	27	52	65	46	10	20	20	20	20
Volts Polarization at:									
CH_3OH Anode	0.54	0.55	0.64	0.57	0.53	0.56	0.57	0.60-0.83	0.59
Air-HNO_3 Cathode	0.28	0.27	0.23	0.30	0.17	0.22	0.22	0.22-0.22	0.29
IR Drop, volts	0.07	0.17	0.19	0.14	0.02	0.05	0.05	0.07-0.06	0.04
Observed Cell Voltage	0.32	0.22	0.15	0.20	0.49	0.38	0.37	0.32-0.10	0.29
Efficiency, %	25.4	17.4	11.9	15.9	38.9	30.1	29.3	27-8	23.0
Cell Resistance, ohms	0.026	0.033	0.029	0.030	0.015	0.025	0.025	0.032	0.020
Power, m watts/cm^2									
Ex IR	10.5	20.3	12.3	15.6	5.1	8.6	8.4	8.2-3.2	6.6
Observed	8.6	11.4	9.8	9.2	4.9	7.6	7.4	6.4-2.0	5.8
CH_3OH Conversion per Pass through Cell, % (calc)	32.8	63.1	78.4	55.8	50.0	50.0	62.0	80.0	69.4
HNO_3 Conversion per Pass through Cell, % (calc)	38.2	73.6	72.3	51.7	9.0	18.0	18.0	18.0	18.0

APPENDIX C-20

MATERIAL BALANCE DATA

TOTAL FUEL CELL STUDIES WITH CH_3OH AND AIR - HNO_3 REDOX SYSTEMS

Run Number	3618-114					
Run Part	D	E	F	G	H	I
Test Period, minutes	60	123	95	109	53	89
Average Current, amps	4.6	1.0	2.0	2.0	2.0	2.0
Total Coulombs	16,550	7,380	11,400	13,080	6,360	10,680
Coulombic Equivalent of:						
CH_3OH Reacted, gm moles	0.0286	0.0128	0.0197	0.0226	0.0110	0.0184
HNO_3 Reacted, gm moles	0.0572	0.0256	0.0394	0.0452	0.0220	0.0368
O_2 Reacted, gm moles	0.0427	0.0192	0.0296	0.0339	0.0165	0.0276
Feed Rates, Stoichiometric Ratio to Current:						
CH_3OH	1.79	2.00	2.00	1.61	1.25	1.44
HNO_3	1.93	11.05	5.55	5.55	5.55	5.55
O_2 in Air	1.99	2.42	2.22	1.95	1.99	1.99
Oxygen Used, gm moles	0.0350	0.0188	0.0289	0.0354	0.0132	0.0283
Oxygen Used, % of stoichiometric	81.9	97.8	97.6	104.2	92.0	102.5
Equivalent HNO_3 Regen. by O_2 Used, gm moles	0.0465	0.0250	0.0385	0.0471	0.0176	0.0376
% Conversion per Pass through Cell:						
CH_3OH (coulombic)	55.8	50.0	50.0	62.0	80.0	69.4
HNO_3 (coulombic)	51.7	9.0	18.0	18.0	18.0	18.0
O_2 in Air	50.2	41.2	43.8	53.5	40.2	51.6
CH_3OH (coulombic + chem.)	66.0	59.8	65.9	92.5	86.0	103.8
HNO_3 Regeneration Efficiency, coulombs/ coulomb equiv. of HNO_3 consumed	2.72	3.87	2.94	2.22	2.86	2.11
CH_3OH Loss, lbs/100 lbs reacted coulombically	18.2	19.6	31.7	49.1	7.5	49.4

APPENDIX C-21

MATERIAL BALANCE DATA

TOTAL FUEL CELL STUDIES WITH CH_3OH AND AIR-HNO_3 REDOX SYSTEMS

Run Number	3618-120		
Run Length, hours	2.5	6.5	26.5
Run Part	A	B	C
Test Period, minutes	135	76	137
Average Current, amps	1.9	1.9	1.95
Total Coulombs	15,370	8,650	16,000
Coulombic Equivalent of:			
CH_3OH Reacted, gm moles	0.0266	0.0149	0.0277
HNO_3 Reacted, gm moles	0.0532	0.0298	0.0554
O_2 Reacted, gm moles	0.0399	0.0224	0.0415
Feed Rates, Stoichiometric Ratio to Current:			
CH_3OH	1.69	1.70	1.30
HNO_3	5.84	5.84	5.72
O_2 in Air	3.98	2.04	2.04
Oxygen Used, gm moles	0.0410	0.0251	0.0432
Oxygen Used, % of stoichiometric	102.5	109.5	104.3
Equiv. HNO_3 Regen. by O_2 Used, gm moles	0.0545	0.0333	0.0570
% Conversion per Pass through Cell:			
CH_3OH (coulombic)	59.2	58.8	76.9
HNO_3 (coulombic)	17.1	17.1	17.5
O_2 in Air	25.8	55.0	51.0
CH_3OH (coulombic + chem)	96.8	98.2	93.3
HNO_3 Regeneration Efficiency, coulombs/coulomb equiv. of HNO_3 consumed	2.84	3.77	7.38
CH_3OH Loss, lbs/100 lbs reacted coulombically	37.6	39.4	16.4

APPENDIX C-22

ELECTRICAL PERFORMANCE DATA

TOTAL FUEL CELL STUDIES WITH CH_3OH AND AIR-HNO_3 REDOX SYSTEMS

Run Number	3618-120			3618-124			3618-126										
Run Hours	2.5	6.5	26.5		2.0						1.0						
Run Part	A	B	C	A	B	C	A	B	C	D	E	F	G	H	I	J	K
Pressure, atm abs	1.0						1.0										
Cell Temp , °C	60.5	62.5	62.5	75	75	75	75	75	75	75	75	75	75	75	75	75	75
HNO_3 Regen. Temp, °C	27	26	28	27	27	27	25	25	25	25	25	25	25	25	25	25	25
Electrolyte	30 wt % H_2SO_4						30 wt % H_2SO_4										
CH_3OH in Anolyte, vol %	1.0						1.0										
HNO_3 in Catholyte, wt %	2.0						2.0										
Run Test Period, minutes	135	76	137	--	--	--	60										
Current Density, ma/cm^2	19.0	19.0	19.5	10.0	22.0	32.0	17.0	22.0	33.0	40.0	50.0	61.5	70.0	81.0	98.0	124	135
Volts Polarization at:																	
CH_3OH Anode	0.61	0.61	0.58	0.60	0.63	0.59	0.53	0.56	0.57	0.58	0.59	0.61	0.61	0.62	0.63	0.67	0.68
Air-HNO_3 Cathode	0.23	0.23	0.22	0.20	0.21	0.18	0.17	0.17	0.18	0.18	0.18	0.19	0.20	0.21	0.21	0.22	0.26
IR Drop, volts	0.07	0.07	0.07	0.06	0.16	0.28	0.04	0.03	0.05	0.06	0.07	0.08	0.10	0.11	0.13	0.16	0.18
Observed Cell Voltage	0.30	0.30	0.34	0.35	0.21	0.16	0.47	0.45	0.41	0.39	0.37	0.33	0.30	0.27	0.24	0.16	0.09
Efficiency, %	23.8	23.8	27.0	27.8	16.7	12.7	37.3	35.7	32.5	30.9	29.3	26.2	23.8	21.4	19.0	12.7	7.1
Cell Resistance, ohms	0.037	0.037	0.036	0.060	0.072	0.087	0.023	0.014	0.015	0.015	0.014	0.013	0.014	0.014	0.013	0.013	0.013
Power, mwatts/cm^2																	
Ex IR	7.0	7.0	7.8	4.1	8.1	14.1	8.5	10.5	15.0	18.0	21.5	25.2	28.0	30.4	35.8	39.6	36.5
Observed	5.7	5.7	6.4	3.5	4.6	5.1	7.9	9.8	13.4	15.6	18.2	20.3	21.0	21.9	23.1	19.9	12.1
CH_3OH Conversion per Pass through Cell, % (calc)	59.2	58.8	76.9	28.5	62.5	91.4	7.0	9.1	13.7	16.9	20.6	25.4	29.0	33.4	40.6	51.3	56.0

Figure C-3

CH_3OH- HNO_3 Cell

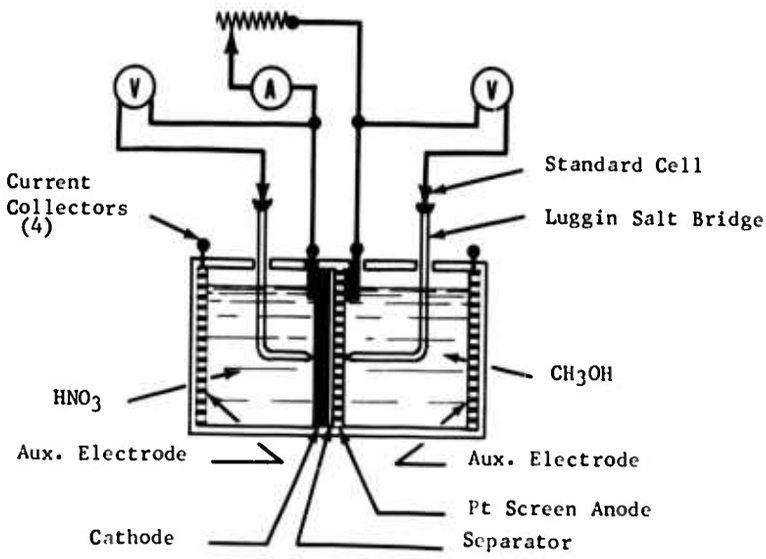

APPENDIX C-23

LABORATORY STUDIES OF THE METHANOL-NITRIC ACID FUEL CELL

Electrolyte: 30 wt % H_2SO_4
Temperature: 82°C
Pressure: 1 atm
Catalyst: 8 mg/cm² electrodeposited Pt black

Electrodes	Current Density, ma/cm²	Cell Potential at Terminals, volts	Reactant Concentrations CH_3OH vol %	Reactant Concentrations HNO_3 wt %	Polarization, volts from theoretical CH_3OH	Polarization, volts from theoretical HNO_3 (•)	Power mwatts/cm²	Electrolytic IR Loss, volts	Comments
Anode: C-type	0	0.54	1.0	1.0	0.52	0.15	0	0	Gas accumulation between electrodes. CH_3OH adsorbed on anode surface and in separator before startup.
Cathode: C-type	3.0	0.51			0.52	0.18	1.5	0	
	6.0	0.46			0.52	0.23	2.8	0	
	7.5	0.44			0.52	0.25	3.3	0	
	12.0	0.40			0.52	0.29	4.8	0	
	15.0	0.38			0.52	0.31	5.7	0	
	33.0	0.20			0.52	0.49	6.6	0	
Anode: C-type	0	0.54	1.0	1.0	0.52	0.15	0	0	Gas accumulation between electrodes. Cathode electrochemically unstable.
Cathode: C-type	13.5	0.17			0.66	0.38	2.3	0	
Anode: 80 mesh	0	0.60	1.0	1.0	0.42	0.19	0	0	CH_3OH adsorbed on anode surface and in separator before startup.
Pt screen	45.0	0.46			0.53	0.22	20.1	0	
Cathode: C-type	48.0	0.45			0.53	0.23	21.6	0	
	55.0	0.40			--	--	22.0	-	
	75.0	0.39			--	--	29.2	-	
	- - - - - - - - - - - - - - - -	After 3 hours of continuous operation							
	45.0	0.41			0.54	0.26	18.4	0	
Anode: 80 mesh	0	0.62	4.0	2.0	0.50	0.09	0	0	HNO_3 adsorbed on cathode surface and in separator before startup.
Pt screen	18.0	0.41			0.62	0.18	7.4	0	
Cathode: C-type	30.0	0.34			0.68	0.19	10.2	0	
Anode: 80 mesh	0	0.65	4.0	2.0	0.47	0.09	0	0	HNO_3 adsorbed on cathode surface and in separator before startup. Short-circuit and open circuit pulses applied to maintain performance.
Pt screen	46.5	0.43			0.57	0.21	20.0	0	
Cathode: C-type	61.5	0.40			--	--	24.6	-	
	75.0	0.38			--	--	28.5	-	
	93.0	0.36			--	--	33.4	-	
	108.0	0.34			--	--	36.7	-	
Anode: 80 mesh	0	0.80	1.0	1.0	0.32	0.09	0	0	HNO_3 adsorbed on cathode surface. CH_3OH adsorbed on anode surface. Short circuit - open circuit pulses applied to maintain performance.
Pt screen	45.0	0.42			0.56	0.23	18.9	0	
Cathode: C-type	60.0	0.38			0.58	0.25	22.8	0	
Auxiliary Current	75.0	0.35			0.59	0.27	26.2	0	
Collectors	90.0	0.33			0.60	0.28	29.7	0	
	112.5	0.30			0.62	0.29	33.8	0	
Anode: 80 mesh	0	0.80	3.0	2.0	0.32	0.09	0	0	HNO_3 adsorbed on cathode surface. CH_3OH adsorbed on anode surface. Short circuit - open circuit pulses applied to maintain performance.
Pt screen	45.0	0.44			0.57	0.20	19.8	0	
Cathode: C-type	60.0	0.41			0.58	0.22	24.6	0	
	90.0	0.38			0.60	0.23	34.2	0	
Auxiliary Current Collectors	129.0	0.34			0.61	0.26	44.0	0	
Anode: 80 mesh	0	0.67	1.0	2.0	0.44	0.10	0	0	
Pt screen	45.0	0.41			0.57	0.23	18.4	0	
Cathode: C-type	60.0	0.36			0.59	0.26	21.6	0	
	90.0	0.32			0.60	0.29	28.8	0	
	105.0	0.30			0.61	0.30	31.5	0	

APPENDIX C-23 (CON'T.)

Anode: 80 mesh	0	0.67	1.0	2.0	0.44	0.10	0	0	
Pt screen	84.0	0.30			0.61	0.30	25.2	0	
Cathode: C-type									
Anode: 80 mesh	0	0.67	4.0	1.0	0.44	0.10	0	0	
Pt screen	45.0	0.44			0.56	0.21	19.8	0	
Cathode: C-type	110.0	0.32			0.61	--	35.2	--	
Anode: 150 mesh	0	0	1.0	0.5	0.42	0.79	0	0	CH_3OH adsorbed on anode surface and in separator before startup. Both electrodes anodized and washed.
Pt screen	- Start up impossible -								
Cathode: C-type									
Anode: 150 mesh	0	0.75	1.0	1.0	0.32	0.14	0	0	CH_3OH adsorbed on anode surface and in separator before startup. Both electrodes anodized and washed. Startup: 5 ma/cm^2 for 20 min and apply open circuit pulse.
Pt screen	48.0	0.37			0.55	0.25	17.8	0.041	
Cathode: C-type									
Anode: 150 mesh	0	0.75	1.0	2.0	0.32	0.14	0	0	CH_3OH adsorbed on anode surface and in separator before startup. Both electrodes anodized and washed. Startup: 5 ma/cm^2 for 20 min and apply open circuit pulse.
Pt screen	38.5	0.38			0.55	0.23	14.6	0.05(*)	
Cathode: C-type	50.5	0.33			0.57	0.27	16.7	0.04	
	62.5	0.26			0.58	0.33	16.3	0.04	
	74.5	0.19			0.60	0.38	14.2	0.04	
	79.5	0.13			0.62	0.43	10.3	0.03	
Anode: 150 mesh	0	0.80	1.0	1.0	0.32	0.09	0	0	HNO_3 adsorbed on cathode surface and in separator before startup. Anode cathodized to H_2 in presence of 1 vol % CH_3OH:1.0 wt % HNO_3 added to catholyte. Immediate startup.
Pt screen	39.6	0.42			0.58	0.21	16.6	0	
Cathode: C-type	49.2	0.39			0.59	0.23	19.2	0	
	60.0	0.36			0.60	0.25	21.6	0	
	72.0	0.31			0.62	0.28	22.3	0	
	84.0	0.29			0.62	0.30	24.4	0	
Anode: 150 mesh	0	0.80	1.0	2.0	0.32	0.09	0	0	HNO_3 adsorbed on cathode surface and in separator before startup. Anode cathodized to H_2 in presence of 1 vol % CH_3OH: 2.0 wt % HNO_3 added to catholyte. Immediate startup.
Pt screen	42.0	0.43			0.58	0.20	18.1	0	
Cathode: C-type	70.0	0.36			0.61	0.24	25.2	0	
	89.0	0.31			0.62	0.28	27.6	0	
	92.0	0.27			0.64	0.30	24.8(+)	0	
	103.0	0.25			0.64	0.32	25.8(+)	0	
	144.0	0.22			0.65	0.34	31.6	0	
Anode: 150 mesh	0	0.66	1.0	2.0	0.42	0.13	0	0	CH_3OH adsorbed on anode surface and in separator before startup. Cathode anodized in presence of HNO_3 and anode cathodized in presence of CH_3OH. Immediate startup.
Pt screen	18.0	0.53			0.50	0.18	9.5	0	
Cathode: C-type	30.6	0.49			0.52	0.20	15.0	0	
	43.2	0.45			0.54	0.22	19.6	0	
	57.5	0.40			0.57	0.24	23.0	0	
	81.0	0.24			0.65	0.32	19.4	0	
	- - - - - - - - - - - - Increasing (HNO_3) to 2.5 wt % did not improve performance - - - - - - - - - - - -								
	- - - - - - - - - - - - Increasing (HNO_3) to 3.0 wt % did not improve performance - - - - - - - - - - - -								

(•) HNO_3 polarization is measured from theoretical O_2.
(*) Electrolytic IR loss actually decreased with time and therefore appears to be decreasing at higher currents.
(+) Decrease in power due to decrease in reactant concentrations.

APPENDIX C-24

DIRECT METHANOL-OXYGEN TOTAL CELL ASSEMBLY

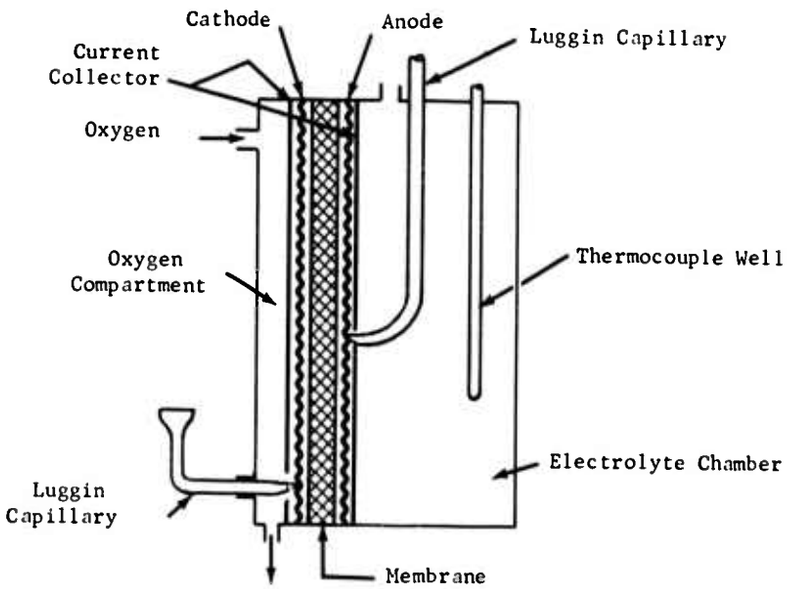

APPENDIX C-25

METHANOL TOTAL CELL PERFORMANCE

Test No.	Anode	Cathode	Membrane	Anolyte	Oxidant	Temp., °C	Current Density, ma/cm^2	Cell Voltage at Terminals, volts	Anode Polarization, volts	Cathode Polarization, volts	IR Loss, volts	Cell Voltage Ex IR, volts	Power at Terminals, mwatts/cm^2	Power Ex IR, mwatts/cm^2
1059-40-1	P-5	72-28 Pt-Teflon	Ionics CR-61	0.5 M CH_3OH in 30% H_2SO_4	O_2	28	31	0.12	0.57	0.33	0.18	0.30	3.7	9.3
1059-40-1	P-5	72-28 Pt-Teflon	Ionics CR-61	0.5 M CH_3OH in 30% H_2SO_4	O_2	43	43	0.17	0.53	0.33	0.17	0.34	7.3	14.6
1059-40-I	P-5	72-28 Pt-Teflon	Ionics CR-61	0.5 M CH_3OH in 30% H_2SO_4	O_2	52	50	0.20	0.50	0.34	0.17	0.37	10	17.1
1059-40-I	P-5	72-28 Pt-Teflon	Ionics CR-61	0.5 M CH_3OH in 30% H_2SO_4	O_2	60	55	0.22	0.50	0.34	0.15	0.37	12	20
1059-40-1	P-5	72-28 Pt-Teflon	Ionics CR-61	0.5 M CH_3OH in 30% H_2SO_4	O_2	82	60	0.24	0.46	0.36	0.15	0.39	14.4	23.4
1059-40-1V	P-5	72-28 Pt-Teflon	2 Nalfilm 0-30	0.5 M CH_3OH in 30% H_2SO_4	O_2	43	27	0.15	0.74	0.26	0.05	0.20	4	5.4
1059-41-I	P-5	72-28 Pt-Teflon	Ionics CR-61	0.5 M CH_3OH in 30% H_2SO_4	O_2	43	54	0.26	0.54	0.34	0.06	0.32	14	17.3
1059-41-I	P-5	72-28 Pt-Teflon	Ionics CR-61	0.5 M CH_3OH in 30% H_2SO_4	O_2	52	59	0.28	0.53	0.32	0.07	0.35	16.5	20.6
1059-41-I	P-5	72-28 Pt-Teflon	Ionics CR-61	0.5 M CH_3OH in 30% H_2SO_4	O_2	60	58	0.28	0.50	0.32	0.11	0.39	16.2	22.6
1059-41-1	P-5	72-28 Pt-Teflon	Ionics CR-61	0.5 M CH_3OH in 30% H_2SO_4	O_2	82	57	0.27	0.47	0.34	0.13	0.40	15.4	22.8
1059-44	P-5	72-28 Pt-Teflon	Ionics CR-61	1.5 M CH_3OH in 30% H_2SO_4	O_2	28	55	0.26	0.53	0.38	0.03	0.29	14.3	16
1059-44	P-5	72-28 Pt-Teflon	Ionics CR-61	1.5 M CH_3OH in 30% H_2SO_4	O_2	43	64	0.30	0.51	0.37	0.03	0.33	19.2	21.1
1059-44	P-5	72-28 Pt-Teflon	Ionics CR-61	1.5 M CH_3OH in 30% H_2SO_4	O_2	60	70	0.31	0.49	0.37	0.04	0.35	21.6	24.5

APPENDIX C-25 (CONT'D)

METHANOL TOTAL CELL PERFORMANCE

Test No.	Anode	Cathode	Membrane	Anolyte	Oxidant	Temp., °C	Current Density, ma/cm²	Cell Voltage at Terminals, volts	Power at Terminals, mwatts/cm²	Anode Polarization, volts
1059-12	P-71	C-Type	No additional membrane	1 M CH_3OH in 30% H_2SO_4	Air	Ambient	1	0.30	0.30	0.49
1059-12	P-71	C-Type	No additional membrane	1 M CH_3OH in 30% H_2SO_4	Air	57	20	0.16	3.2	0.54
1059-12	P-71	C-Type	No additional membrane	1 M CH_3OH in 30% H_2SO_4	Air	82	26	0.18	4.7	0.47
1059-22	P-71	Pt	Ionic CR-61 + A-Type	0.25 M CH_3OH in 30% H_2SO_4	O_2	Ambient	6	0.17	1.0	0.61
1059-22	P-71	Pt	Ionic CR-61 + A-Type	0.25 M CH_3OH in 30% H_2SO_4	O_2	60	9	0.24	2.2	0.52
1059-22	P-71	Pt	Ionic CR-61 + A-Type	0.25 M CH_3OH in 30% H_2SO_4	O_2	85	9.5	0.25	2.4	0.47
1059-24	P-71	90-10 Pt-Teflon Pressed	Ionic CR-61 + A-Type	0.25 M CH_3OH in 30% H_2SO_4	O_2	Ambient	18	0.14	2.5	0.58
1059-24	P-71	90-10 Pt-Teflon Pressed	Ionic CR-61 + A-Type	0.25 M CH_3OH in 30% H_2SO_4	O_2	60	30	0.21	6.3	0.52
1059-24	P-71	90-10 Pt-Teflon Pressed	Ionic CR-61 + A-Type	0.50 M CH_3OH in 30% H_2SO_4	O_2	83	50	0.28	14	0.44
1059-24	P-71	90-10 Pt-Teflon Pressed	Ionic CR-61 + A-Type	0.50 M CH_3OH in 30% H_2SO_4	O_2	82	20	0.46	9.2	0.36
1059-24	P-71	90-10 Pt-Teflon Pressed	Ionic CR-61 + A-Type	0.50 M CH_3OH in 30% H_2SO_4	O_2	82	9.6	0.54	5.2	0.35
1059-24	P-71	90-10 Pt-Teflon Pressed	Ionic CR-61 + A-Type	0.50 M CH_3OH in 30% H_2SO_4	O_2	82	1.2	0.70	0.8	0.27
1059-37	P-5	72-28 Pt-Teflon Without Pressing	Ionic CR-61 + A-Type	0.75 M CH_3OH in 30% H_2SO_4	O_2	Ambient	50	0.23	11.5	0.60
1059-37	P-5	72-28 Pt-Teflon Without Pressing	Ionic CR-61 + A-Type	0.75 M CH_3OH in 30% H_2SO_4	O_2	51	59	0.26	15.3	0.59
1059-38-II	P-5	72-28 Pt-Teflon Without Pressing	A-Type	0.5 M CH_3OH in 30% H_2SO_4	O_2	Ambient	8.6	0.19	1.6	0.69
1059-38-II	P-5	72-28 Pt-Teflon Without Pressing	A-Type	0.5 M CH_3OH in 30% H_2SO_4	O_2	51	15	0.21	3.2	0.68
1059-38-II	P-5	72-28 Pt-Teflon Without Pressing	A-Type	0.5 M CH_3OH in 30% H_2SO_4	O_2	71	20	0.27	5.4	0.54

APPENDIX C-25 (CONT'D)

METHANOL TOTAL CELL PERFORMANCE

Test No.	Anode	Cathode	Membrane	Anolyte	Oxidant	Temp, °C	Current Density, ma/cm²	Cell Voltage at Terminals, volts	Anode Polarization, volts	Cathode Polarization, volts	IR Loss, volts	Cell Voltage Ex IR, volts	Power at Terminals, mwatts/cm²	Power Ex IR, mwatts/cm²
1059-42-1	72-28 Pt-Teflon	75-25 Pt-Teflon	Ionics CR-61	1.5 M CH_3OH in 30% H_2SO_4	O_2	28	27	0.14	0.42	0.30	0.24	0.38	3.8	10.2
1059-42-I	72-28 Pt-Teflon	75-25 Pt-Teflon	Ionics CR-61	1.5 M CH_3OH in 30% H_2SO_4	O_2	52	51	0.28	0.56	0.31	0.06	0.34	14.3	17.3
1059-42-I	72-28 Pt-Teflon	75-25 Pt-Teflon	Ionics CR-61	1.5 M CH_3OH in 30% H_2SO_4	O_2	52	22	0.44	0.50	0.24	0.03	0.47	9.7	10.3
1059-42-I	72-28 Pt-Teflon	75-25 Pt-Teflon	Ionics CR-61	1.5 M CH_3OH in 30% H_2SO_4	O_2	52	10	0.49	0.48	0.22	0.02	0.51	4.9	5.1
1059-42-I	72-28 Pt-Teflon	75-25 Pt-Teflon	Ionics CR-61	1.5 M CH_3OH in 30% H_2SO_4	O_2	52	1.2	0.66	0.36	0.19	-	0.66	0.8	0.8
1059-43-I	P-5 + 30% Teflon	72-28 Pt-Teflon	Ionics CR-61	1.5 M CH_3OH in 30% H_2SO_4	O_2	28	48	0.20	0.63	0.33	0.04	0.24	9.6	11.5
1059-43-I	P-5 + 30% Teflon	72-28 Pt-Teflon	Ionics CR-61	1.5 M CH_3OH in 30% H_2SO_4	O_2	52	60	0.25	0.61	0.31	0.04	0.29	15	17.4

APPENDIX C-26

METHANOL TOTAL CELL PERFORMANCE

No. 1059-45I
Anode = P-5
Anolyte = 1.83 M CH_3OH in 30% H_2SO_4
Membrane = Ionics CR-61
Temperature = 51°C
Cathode = 72-28 Pt-Teflon

		Power and Voltage at Indicated ma/cm^2				
	Oxidant	1	5	10	20	72
Cell Voltage at Terminals, volts	O_2	0.68	0.62	0.57	0.52	0.33
Anode Polarization, volts	O_2	0.34	0.38	0.41	0.44	0.52
Cathode Polarization, volts	O_2	0.19	0.21	0.22	0.24	0.32
IR Loss, volts	O_2	-	-	0.01	0.01	0.04
Cell Voltage Ex IR, volts	O_2	0.68	0.62	0.58	0.53	0.37
Power at Terminals, mwatts/cm^2	O_2	0.68	3.1	5.7	10.4	23.8
Power Ex IR, mwatts/cm^2	O_2	0.68	3.1	5.8	10.6	26.6
Cell Voltage at Terminals, volts	Air	0.62	0.53	0.45	0.37	--
Anode Polarization, volts	Air	0.34	0.38	0.41	0.45	--
Cathode Polarization, volts	Air	0.25	0.30	0.34	0.38	--
IR Loss, volts	Air	-	-	0.01	0.01	--
Cell Voltage Ex IR, volts	Air	0.62	0.53	0.46	0.38	--
Power at Terminals, mwatts/cm^2	Air	0.62	2.6	4.5	7.4	--
Power Ex IR, mwatts/cm^2	Air	0.62	2.6	4.6	7.6	--

APPENDIX C-26 (CONT'D)

METHANOL TOTAL CELL PERFORMANCE

No. 1059-46III
Anode = P-5
Anolyte = 1.5 M CH_3OH in 30% H_2SO_4
Membrane = Ionics CR-61
Temperature = 61°C
Cathode = 72-28 Pt-Teflon

		Power and Voltage at Indicated ma/cm^2			
	Oxidant	10	50	72	100
Cell Voltage at Terminals, volts	O_2	0.62	0.41	0.34	0.26
Anode Polarization, volts	O_2	0.34	0.43	0.46	0.48
Cathode Polarization, volts	O_2	0.23	0.32	0.34	0.38
IR Loss, volts	O_2	0.02	0.05	0.07	0.09
Cell Voltage Ex IR, volts	O_2	0.64	0.46	0.41	0.35
Power at Terminals, $mwatts/cm^2$	O_2	6.2	20.5	24.5	26
Power Ex IR, $mwatts/cm^2$	O_2	6.4	23	29.5	35

APPENDIX C-26 (CONT'D)

METHANOL TOTAL CELL PERFORMANCE

No. 1059-47
Anode = P-5 + 30% Teflon
Anolyte = 1.5 M CH_3OH in 30% H_2SO_4
Membrane = Ionics CR-61
Temperature = 57°C
Cathode = 72-28 Pt-Teflon

		Power and Voltage at Indicated ma/cm^2					
	Oxidant	5	10	20	50	72	100
Cell Voltage at Terminals, volts	O_2	0.58	0.52	0.44	0.31	0.23	0.18
Anode Polarization, volts	O_2	0.40	0.44	0.48	0.51	0.52	0.54
Cathode Polarization, volts	O_2	0.23	0.24	0.27	0.33	0.36	0.39
IR Loss, volts	O_2	-	0.01	0.02	0.06	0.10	0.10
Cell Voltage Ex IR, volts	O_2	0.58	0.53	0.46	0.37	0.33	0.28
Power at Terminals, mwatts/cm^2	O_2	2.9	5.2	8.8	15.5	16.5	18
Power Ex IR, mwatts/cm^2	O_2	2.9	5.3	9.2	18.5	23.8	28

APPENDIX C-26 (CONT'D)

METHANOL TOTAL CELL PERFORMANCE

No. 1059-48
Anode = P-5
Anolyte = 1.83 M CH_3OH in 30% H_2SO_4
Membrane = Ionics CR-61 + A-Type Membrane
Temperature = 82°C
Cathode = 72-28 Pt-Teflon

		Power and Voltage at Indicated ma/cm^2				
	Oxidant	10	20	50	72	100
Cell Voltage at Terminals, volts	O_2	0.65	0.57	0.41	0.31	0.20
Anode Polarization, volts	O_2	0.29	0.33	0.38	0.40	0.42
Cathode Polarization, volts	O_2	0.26	0.29	0.36	0.42	0.49
IR Loss, volts	O_2	0.01	0.02	0.06	0.08	0.10
Cell Voltage Ex IR, volts	O_2	0.66	0.59	0.47	0.39	0.30
Power at Terminals, mwatts/cm^2	O_2	6.5	11.4	20.5	22.3	20
Power Ex IR, mwatts/cm^2	O_2	6.6	11.8	23.5	28	30
After 16 hr idling with electrolyte in the cell.						
Cell Voltage at Terminals, volts	O_2	0.66	0.58	0.44	0.33	0.23
Anode Polarization, volts	O_2	0.28	0.32	0.37	0.40	0.42
Cathode Polarization, volts	O_2	0.26	0.29	0.35	0.40	0.45
IR Loss, volts	O_2	0.01	0.02	0.05	0.08	0.11
Cell Voltage Ex IR, volts	O_2	0.67	0.60	0.49	0.41	0.33
Power at Terminals, mwatts/cm^2	O_2	6.6	11.6	22	23.8	23
Power Ex IR, mwatts/cm^2	O_2	6.7	12.0	24.5	29.5	33

APPENDIX C-26 (CONT'D)

METHANOL TOTAL CELL PERFORMANCE

No. 1059-49
Anode = P-5
Anolyte = 1.83 M CH_3OH in 30% H_2SO_4
Membrane = Ionics CR-61 + A-Type Membrane
Temperature = 82°C
Cathode = 72-28 Pt-Teflon

		Power and Voltage at Indicated ma/cm^2				
	Oxidant	10	20	50	72	100
Cell Voltage at Terminals, volts	O_2	0.65	0.58	0.44	0.37	0.28
Anode Polarization, volts	O_2	0.30	0.34	0.38	0.39	0.40
Cathode Polarization, volts	O_2	0.25	0.27	0.33	0.37	0.42
IR Loss, volts	O_2	0.01	0.02	0.06	0.08	0.11
Cell Voltage Ex IR, volts	O_2	0.66	0.60	0.50	0.45	0.39
Power at Terminals, $mwatts/cm^2$	O_2	6.5	11.6	22	26.6	28
Power Ex IR, $mwatts/cm^2$	O_2	6.6	12	25	32.4	39

APPENDIX C-26 (CONT'D)

METHANOL TOTAL CELL PERFORMANCE

No. 1348-4A
Anode = P-5
Anolyte = 1.83 M CH_3OH in 30% H_2SO_4
Membrane = AMF C-313
Temperature = 60°C
Cathode = 72-28 Pt-Teflon

		Power and Voltage at Indicated ma/cm^2				
	Oxidant	10	20	50	72	100
Cell Voltage at Terminals, volts	O_2	0.53	0.48	0.28	0.19	0.05
Anode Polarization, volts	O_2	0.36	0.38	0.45	0.48	0.50
Cathode Polarization, volts	O_2	0.28	0.29	0.35	0.36	0.41
IR Loss, volts	O_2	0.04	0.06	0.13	0.18	0.25
Cell Voltage Ex IR, volts	O_2	0.57	0.54	0.41	0.37	0.30
Power at Terminals, mwatts/cm^2	O_2	5.3	9.6	14	13.7	5
Power Ex IR, mwatts/cm^2	O_2	5.7	10.8	20.5	38.6	30

APPENDIX C-26 (CONT'D)

METHANOL TOTAL CELL PERFORMANCE

No. 1348-5B
Anode = P-5
Anolyte = 0.25 M CH_3OH in 30% H_2SO_4
Membrane = Two Nalfilm D-30 Separated by 70 mil 30% H_2SO_4
Temperature = 60°C
Cathode = 56-44 Pt-Teflon

		Power and Voltage at Indicated ma/cm^2				
	Oxidant	10	20	50	72	100
Cell Voltage at Terminals, volts	O_2	0.50	0.40	0.29	0.23	0.16
Anode Polarization, volts	O_2	0.44	0.50	0.55	0.57	0.60
Cathode Polarization, volts	O_2	0.27	0.31	0.35	0.38	0.42
IR Loss, volts	O_2	0.00	0.00	0.02	0.03	0.03
Cell Voltage Ex IR, volts	O_2	0.50	0.40	0.31	0.26	0.19
Power at Terminals, mwatts/cm^2	O_2	5	8	14.5	16.5	16
Power Ex IR, mwatts/cm^2	O_2	5	8	15.5	18.7	19
Cell Voltage at Terminals, volts	Air	0.37	0.25	0.06	--	--
Anode Polarization, volts	Air	0.45	0.51	0.56	--	--
Cathode Polarization, volts	Air	0.39	0.44	0.58	--	--
IR Loss, volts	Air	0	0.01	0.01	--	--
Cell Voltage Ex IR, volts	Air	0.37	0.26	0.07	--	--
Power at Terminal, mwatts/cm^2	Air	3.7	5.0	3.0	--	--
Power Ex IR, mwatts/cm^2	Air	3.7	5.2	3.5	--	--

APPENDIX C-27

BI-CELL PERFORMANCE

Anode = P-5
Anolyte = 1.83 M CH_3OH in 30% H_2SO_4
Membrane = Ionics CR-61
Cathode = 72-28 Pt-Teflon

No.	Description	Oxidant	Temp, °C	Power and Bi-Cell Voltage at Indicated ma/cm^2 1	10	20	50	85	100	115
1348-3	Bi-Cell Voltage at Terminals, volts	O_2	50	1.50	1.15	--	0.80	0.60	0.50	0.43
1348-3	Average Net Power Density, mwatts/cm^2	O_2	50	0.75	5.75	--	20	25.5	25	24.8
1348-4B	Bi-Cell Voltage at Terminals, volts	Air	54	1.28	0.89	0.69	0.37	--	--	--
1348-4B	Average Net Power Density, mwatts/cm^2	Air	54	0.64	4.45	6.9	9.25	--	--	--

APPENDIX C-28

MECHANISM OF WATER REMOVAL FROM THE AIR ELECTRODE SURFACE

The rates of water and heat removal are two closely interconnected variables since water removal is a primary mode of heat loss from the fuel cell system. Thus, the water evaporated at the air electrode determines the mean air electrode temperature and consequently the cell efficiency.

Water arrives at the air electrode surface in a number of ways - seepage, diffusion, electrochemical oxidation, water of hydration, etc. Consequently, it was assumed in this analysis that the net water flux through the electrode-membrane system is sufficient to produce a wet electrode surface. That is, the diffusion of water through the barrier membrane is not controlling. The proposed model for this forced convection mass transfer problem is illustrated below.

FORCED CONVECTION MASS TRANSPORT MODEL

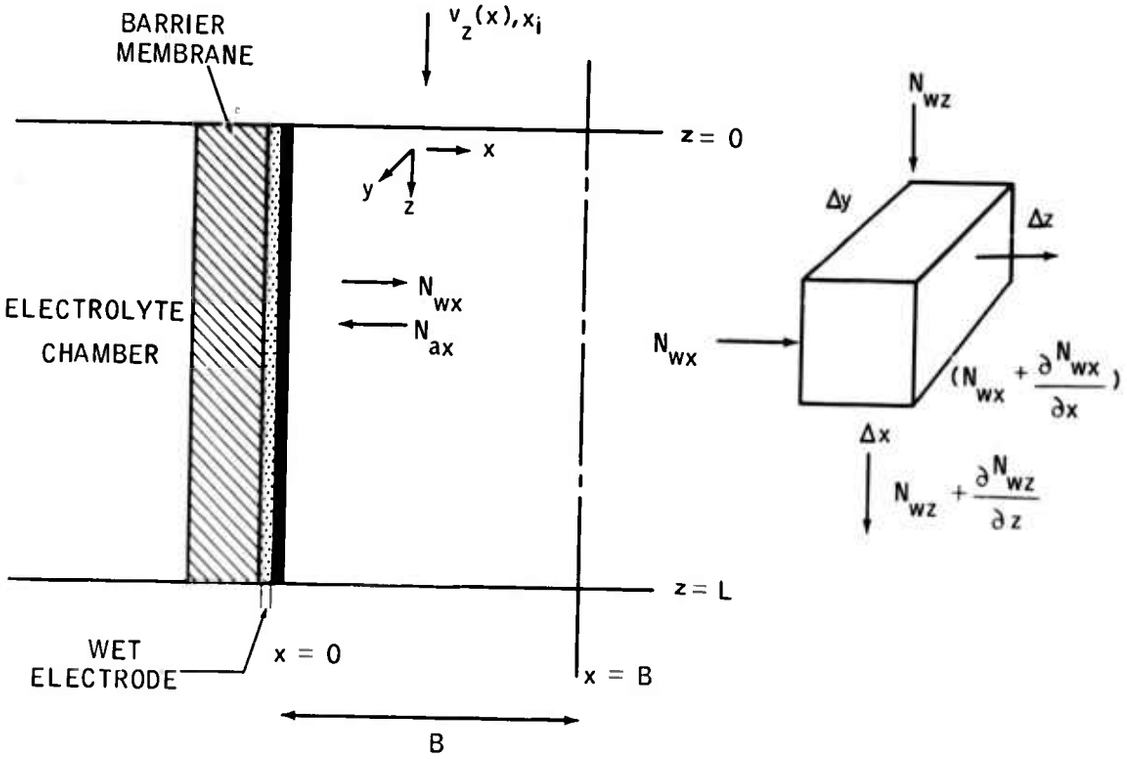

N_{iq} = MOLAR FLUX OF WATER WITH RESPECT TO A FIXED AXIS MOLE/CM^2 SEC.

w = WATER a = AIR

In this model, air (containing X_i moles of water/mole of gas) enters at z=o with a velocity $V_z(x)$ and diffuses towards the electrode; water diffuses from the wet electrode surface into the air stream. As a consequence of the previous assumption, the equilibrium moisture content of the electrode is high enough so that molecular forces do not come into play. Furthermore, it is assumed that the diffusion of water into the gas stream does not change the velocity profile in either the x or z directions. This is not strictly true since the molar flux of water in the positive x direction is greater than the molar flux of oxygen towards the electrode. The effect of this increased velocity has not been included in the calculation directly. However, a mean value of the velocity has been used in the final calculations. The error introduced by using this mean velocity is less than 5% at air rates above six times stoichiometric, increasing to about 25% at the stoichiometric air rate.

The first step in attaining this solution is to obtain the velocity profile $V_z(x)$. This of course can be obtained from the Reynolds equation if one assumes the gas density $\rho(z)$ is close to $\bar{\rho}$, the gas density at the mean temperature. However, when the resultant equation

$$V_z(x) = \frac{B^2 \Delta P}{2\mu L}\left[1 - \left(\frac{x}{B}\right)^2\right]$$

is introduced into the mass transfer equations, the resultant differential equations are not readily solved. Therefore, it was assumed that the air stream behaves as an inviscid fluid, that is we have a plug flow velocity distribution

$$\frac{\partial V_z}{\partial x} = 0 \quad .$$

This assumption is valid to the same degree of approximation as the assumption of a z mean velocity discussed previously.

A water balance over the volume element

$$\Delta x, \Delta z, \Delta y, \quad \text{yields}$$

$$\frac{\partial N_{wx}}{\partial x} + \frac{\partial N_{wz}}{\partial z} + \frac{\partial N_{wy}}{\partial y} = 0 \tag{1}$$

but $N_{wy}=0$ so that the equation of conservation of mass is simply

$$\frac{\partial N_{wx}}{\partial x} + \frac{\partial N_{wz}}{\partial z} = 0 \tag{1a}$$

The molar fluxes (N_{wx} and N_{wy}) with respect to a space fixed coordinate system are

For x

$$N_{wx} = -CD\frac{\partial X_w}{\partial x} + X_w(N_{wx} + N_{ax}) \tag{2}$$

For z

$$N_{wz} = - CD \frac{\partial X_w}{\partial z} + X_w (N_{wz} + N_{az}) \tag{3}$$

where

N_w = Molar flux of water $\frac{\text{moles}}{\text{cm}^2 \text{ sec}}$

N_a = Molar flux of dry gas $\frac{\text{moles}}{\text{cm}^2 \text{ sec}}$

X_w = Mole fraction of water

D = Mean diffusivity of water through air $\frac{\text{cm}^2}{\text{sec}}$

C = Molar density $\frac{\text{moles}}{\text{cm}^3}$

Next it was assumed that all transport in the z direction is due to flow $\frac{\partial X_w}{\partial z} = 0$ while transport in the x direction is solely due to diffusion, that is $V_x = 0$. However, this approximation does not assume equimolar counter diffusion. Rather, any increase in the total number of moles in a volume element $\Delta x \, \Delta z \, \Delta y$ results in an increase V_z since the pressure is assumed to remain constant. In any event, the net flux in the x direction is small compared to the total flux in the z direction.

Applying these assumptions,

$$N_{wx} = - CD \frac{\partial X_w}{\partial x} \tag{4}$$

$$N_{wz} = C_w V_z \tag{5}$$

Substituting equations (4) and (5) in (1a) and recalling that $X_w = C_w/C$ we obtain

$$V_z \frac{\partial X_w}{\partial z} = D \frac{\partial^2 X_w}{\partial x^2} \tag{6}$$

Equation (6) is a classical differential equation occurring frequently in heat, mass, and momentum transport problems. The solution being of the form

$$\Phi(\eta) = \frac{X_w}{X_{wi}} \text{ , where} \tag{7}$$

$$\eta = X_w / \sqrt{4D/V_z z}$$

X_{wi} = Inlet Molar Humidity

Assuming this solution we obtain

$$\Phi(\eta) = \frac{X_w}{X_{wi}} = C_1 \int_0^{\eta} e^{-\eta^2} d\eta + C_2; \tag{8}$$

Inserting the boundary conditions

$$z \leq o \quad o < x < B \quad X_w = X_i \quad \eta = \infty \quad \phi(\eta) = 1$$

$$z = L \quad x = o \quad X_w = X^* \quad \eta = o \quad \phi(\eta) = \frac{X^*}{X_i}$$

we obtain

$$\frac{X_w - X^*}{X_i - X^*} = \text{erf}\left[\frac{x}{\sqrt{4D/V_z z}}\right], \tag{9}$$

where erf denotes the probability integral and X_w^* is the molar humidity at the air-electrode interface. The value of X_w^* is determined from the vapor pressure of water over the sulfuric acid water solution existent at the interface at Z = L. For this calculation this was assumed to be 30% sulfuric acid.

Next the mean molar humidity of the air leaving the air electrode chamber (X_L) was determined by applying the mean value theorem, remembering that the error function can be expanded as a series. For small values of the argument, this yields

$$\frac{X_L - X^*}{X_i - X^*} = \sqrt{\frac{B^2 \bar{V}_z}{4\pi D L}} \tag{10}$$

in terms of percent saturation

$$\frac{X_L}{X_w^*} \times 100\% = \left[1 - \left(1 - \frac{X_i}{X^*}\right)\sqrt{\frac{B^2 \bar{V}_z}{4\pi D L}}\right] \times 100\% \tag{10a}$$

In most cases, the nature of $\frac{X_i}{X^*}$ may be neglected.

Equation (10a) can now be used to estimate the exit gas humidity as a function of air rate and cell geometry. This equation indicates that the percent saturation (for a given air rate, A_R) decreases as the square root of the cell thickness (B). Since the water evaporated is a prime source of heat loss, some compromise between cell thickness (B) and regenerative heat exchanger volume may be necessary.

TABLE C-1

HUMIDITY AIR RATE CURVES FOR VARIOUS CURRENT DENSITIES
(Air Chamber Size 0.068 inches)

Air Rate $A_R = \frac{\text{Actual Air}}{\text{Stoich. Air}}$	Fraction Accomplished Humidity Change = $\frac{X_L}{X_x^*}$		
	18.5 ma/cm^2	37 ma/cm^2	55 ma/cm^2
1	0.990	0.985	0.982
2	0.980	0.970	0.963
4	0.969	0.955	0.945
6	0.958	0.940	0.927
10	0.943	0.920	0.895
20	0.922	0.890	0.865

APPENDIX C-29

HEAT LOSSES FROM A PLANAR ELECTRODE-MATHEMATICAL ANALYSIS

The heat generated in the electrodes is dissipated by evaporation of water and conduction to the air and electrolyte streams. As indicated earlier, by far the largest heat loss is due to evaporation of water from the air electrode surface.

To solve this problem mathematically, it was necessary to select conditions at the electrode surface. It was assumed that the electrode temperature cannot vary markedly in the z direction because it is a good conductor. At the same time the gas stream is entering at a low temperature and leaving at a much higher one. Since the electrolyte temperature generally controls the temperature of the electrode, it was also assumed that the z dependence of electrode temperature is small enough so that the electrode is releasing heat at a constant rate per unit area $\left(q = \frac{Q}{A}\right)$.

Using a model similar to the mass transport model (Appendix C-28) and remembering that both air and electrolyte are in laminar flow, it is seen that under steady state conditions,

$$\rho\, C_p\, V_z \frac{\partial T}{\partial z} = k \frac{\partial^2 T}{\partial x^2} \qquad (1)$$

(convective) (conductive)

where ρ = density, C_p is the specific heat, and k is the thermal conductivity. Equation (1) assumes (as in the mass transport case) that heat is transported in the x direction only through conduction, while in the z direction heat is transferred solely by convection. A solution for this differential equation with the electrode at x = L and the boundary conditions

$$0 < x < B \qquad z = 0 \qquad T = T_0$$

$$x = 0 \qquad 0 < z < L \qquad \left.\frac{\partial T}{\partial z}\right|_{x=0} = \frac{q}{k}$$

can be found in Carslaw & Jaeger(5)

$$T - T_0 = \frac{2q}{k}\sqrt{\alpha t}\left[\sum_{n=0}^{\infty} i\,\mathrm{erfc}\left[\frac{(2n+1)(L-x)}{2\sqrt{\alpha t}}\right] + i\,\mathrm{erfc}\left[\frac{(2n+1)(L+x)}{2\sqrt{\alpha t}}\right]\right] \qquad (2)$$

where

$$i\,\mathrm{erfc}\,x = \frac{1}{\sqrt{\pi}} e^{-x^2} - x\,[1 - \mathrm{erf}\,x], \text{ and}$$

$t = \frac{L}{V}$. A solution similar to equation 10 can also be found for this case with the axis(x= 0) at the electrode.

$$T - T_o = \frac{q}{k}(\pi \alpha t)^{1/2} \left[\operatorname{erfc} \frac{x}{2(\alpha t)^{1/2}}\right] \qquad (3)$$

Although this writer's equation (3) is simpler to evaluate, equation (2) was used in the analysis since (T-To) values have already been tabulated by Carslaw and Jaeger. To arrive at the air electrode solution one more assumption is required concerning the value which should be assigned to the q transmitted to the air stream via conduction. It was assumed that the heat transfer to the "vaporizing film" of water on the electrode is high and hence not controlling. Therefore the net q_c available for conduction to the air is given by

$$q_c = q_t - (q_{vap} + q_{electrolyte}).$$

Some typical air temperature profiles are shown in Appendix Figures $\bar{C}$-4 and $\bar{C}$-5. The calculations illustrate the temperature profiles for a cell operating at 40.3% efficiency and 37 ma/cm^2 having the geometry comparable to the proposed fuel cell. Appendix Figure $\bar{C}$-4 indicates that the vertical temperature profile at the air electrode is almost linearly dependent on z/L. Thus, the mean air electrode temperature can be evaluated as the arithmetic average at the inlet and outlet conditions. Furthermore, an examination of the x dependence of temperature (Appendix Figure $\bar{C}$- 5) indicated that the profile is rather shallow (dropping only 2°C. across the entire cross section). This fact allows us to substitute a simple material balance for this rather complex heat exchange problem.

Figure $\bar{C}$-4

"z" Temperature Profile

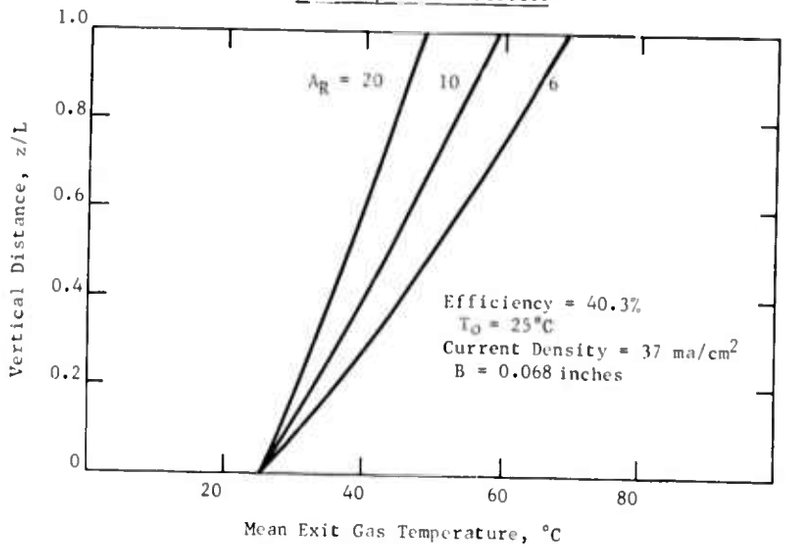

Figure C-5

"x" Temperature Profile

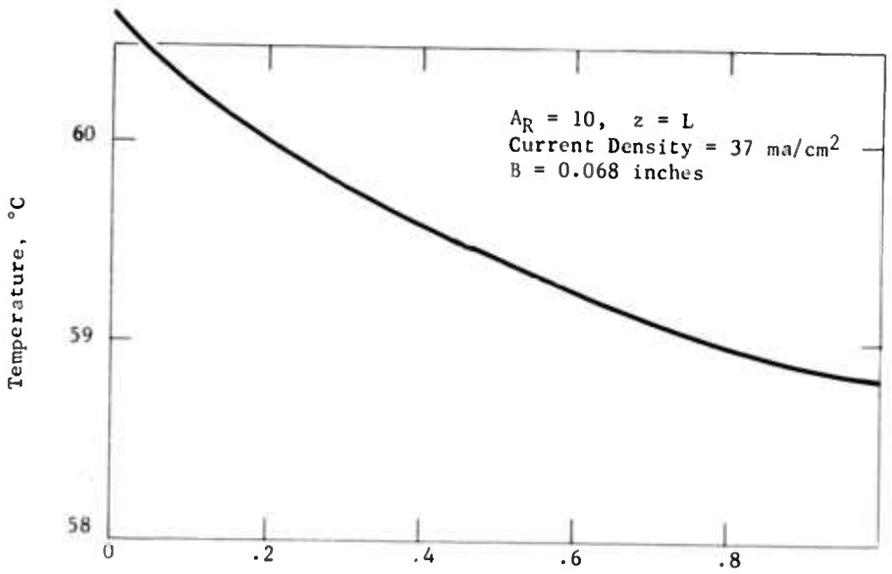

Figure C-6

Effect Of Ambient Temperature On Water Removal And Recovery

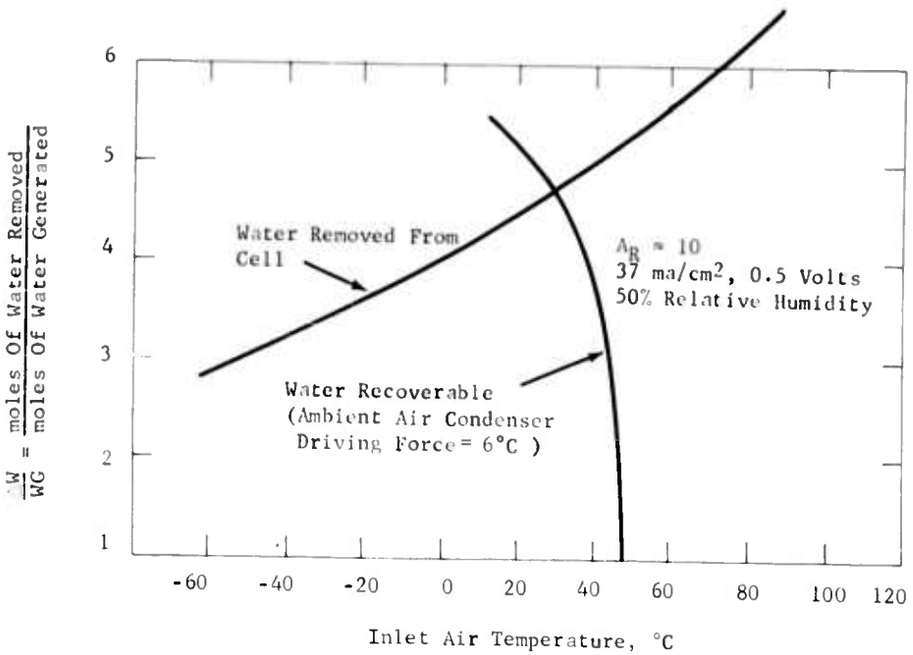

Earlier in this analysis the assumption was made that the electrode produces heat at a constant rate per unit area, that is the electrode temperature does not vary greatly in the z direction. Since the electrode temperature is primarily controlled by the electrolyte, we are now in a position to check the validity of this assumption. This can be accomplished by applying equation (2) to the fuel electrode chamber. The results of this analysis are tabulated in Tables $\bar{C}$-2 and $\bar{C}$-3, for a number of cases in which the reservoir heat loss varied from 0-15% of the total heat generated.

TABLE $\bar{C}$-2

EFFECT OF HEAT LOSS IN RESERVOIR ON ELECTROLYTE TEMPERATURE

(% of Heat Generated)	Inlet Temp, °C	Outlet Temp, °C	Electrolyte Temperature Rise °C As Calculated By	
			Heat Transfer To Electrolyle	Energy Balance On Reservoir
0	80.7	83.3	2.55	2.60
1	80.5	83.6	3.04	3.10
5	80.0	84.0	3.95	4.00
10	79.3	84.7	5.37	5.50
15	78.5	85.5	6.95	7.00

TABLE $\bar{C}$-3

EFFECT OF HEAT LOSS ON EXIT GAS TEMPERATURE AND WATER REMOVAL

(A_R = 10, 37 ma/cm^2, 0.5 Volts)

% Heat Loss	Water Removal Ratio $\frac{\Delta W}{WG}$	Exit Gas Temperature, °C
0	4.6	58
5	4.5	57
10	4.1	56
15	3.5	54

APPENDIX C-30

METHANOL ANALYZER - ELECTRODE PERFORMANCE

ELECTRICAL MEASURING CONDITIONS:
- Esso Analyzer
- Analysis conditions - "A"-mild, "B"-severe, "C"-intermediate
- Readout - peak current on Varian recorder

ANALYZER CELL:
- 100 cc volume
- Platinum wire electrodes with platinum black catalyst
- Magnetic stirring with chip

TEMP:
- 24°C to 27°C

ORIGINAL PERFORMANCE - CONDITION "A" - 5 GMS/FT^2 CATALYST

DATE

4-26		4-27		4-27		4-27		4-29		4-30		5-1	
CH_3OH Vol %	Peak Current ma/cm^2	CH_3OH Vol %	Peak Current ma/cm^2	CH_3OH Vol %	Peak Current ma/cm^2	CH_3OH Vol %	Peak Current ma/cm^2	CH_3OH Vol %	Peak Current ma/cm^2	CH_3OH Vol %	Peak Current ma/cm^2	CH_3OH Vol %	Peak Current ma/cm^2
0.1	32	0.2	69	0.2	67	1.2	191	0.21	39	0.2	32	0.24	41
0.2	52.5	0.6	105	0.39	77			0.61	81	0.61	66	0.84	103
0.29	66	1.0	153	0.79	129			1.21	133	1.22	120	1.84	210
0.50	96	1.8	264	1.39	210			1.81	172	1.80	153		
0.70	118	2.6	337	1.99	277			2.81	240	2.80	213		
1.22	172			2.59	333								
1.72	236												
2.72	315												

PERFORMANCE WITH CONDITION "B" - 5 GMS/FT^2 CATALYST

DATE

4-27		5-1		5-1		5-2		5-2		5-2		
CH_3OH Vol %	Peak Current ma/cm^2	CH_3OH Vol %	Peak Current ma/cm^2	CH_3OH Vol %	Peak Current ma/cm^2	CH_3OH Vol %	Peak Current ma/cm^2	CH_3OH Vol %	Peak Current ma/cm^2	CH_3OH Vol %	Peak Current ma/cm^2	Peak Current ma/cm^2(R)
0.21	62	0.2	84	.19	92	0.2(R)	83	0.19	94	0.2	57	83
0.62	135	0.6	137	.61	129	0.61(R)	107	0.60	122	0.6	71	105
0.93	206	1.12	210	1.25	191	1.21(R)	206	1.20	216	1.2	109	204
1.33	268	1.93	308	2.02	268	1.71	252	2.00	270	2.21	163	450
2.33	365	1.93(R)	150	3.01	312	1.81	253					
		2.51	338	5.01(R)	156	2.61	294					
						3.61	333					

R-REVERSED ELECTRODES

PERFORMANCE WITH CONDITION "B" - NEW ANODE - 5 GM $/FT^2 CATALYST

DATE

5-3		5-3		5-3		5-3		5-3		5-6		
CH_3OH Vol %	Peak Current ma/cm^2	CH_3OH Vol %	Peak Current ma/cm^2	CH_3OH Vol %	Peak Current ma/cm^2	CH_3OH Vol %	Peak Current ma/cm^2	CH_3OH Vol %	Peak Current ma/cm^2	CH_3OH Vol %	Peak Current ma/cm^2	Peak Current ma/cm^2(R)
UNKNOWN		UNKNOWN		.05	27	UNKNOWN		.015	12	0.19	71	44
UNIT II	58	UNIT III	58	.12	51	UNIT IV	120	.03	20	0.59	165	109
+0.11	84	+ .06	90	.19	72	+0.5	196	.045	26	1.19	278	202
0.22	136	.16	138	.26	91			.06	32	1.59	306	240
				.32	107			.27	68	1.99	401	316
								1.27	306			

R- REVERSED ELECTRODES

DATE

5-6		5-7	
CH_3OH Vol %	Peak Current ma/cm^2	CH_3OH Vol %	Peak Current ma/cm^2
0.21	79	1.0	200
0.81	161		
1.20	262	ABOVE PERFORMANCE DECAYING - PHYSICAL LOSS OF CATALYST	
1.60	118		
1.01	222		
2.07	371		

PERFORMANCE WITH CONDITION "B" - BRIGHT PLATINUM ELECTRODES

DATE

5-8		5-8		5-9	
CH_3OH Vol %	Peak Current ma/cm^2	CH_3OH Vol %	Peak Current ma/cm^2	CH_3OH Vol %	Peak Current ma/cm^2
.21	1.04	UNKNOWN			
.82	1.76		60	0.2	1.01
1.22	2.41	+0.4	1.36	0.8	1.60

PERFORMANCE WITH CONDITION "B" - 10 GMS/FT^2 CATALYST - NO STIRRING

DATE

5-15		5-16		5-16		5-16		5-17		5-18	
CH_3OH Vol %	Peak Current ma/cm^2	CH_3OH Vol %	Peak Current ma/cm^2	CH_3OH Vol %	Peak Current ma/cm^2	CH_3OH Vol %	Peak Current ma/cm^2	CH_3OH Vol %	Peak Current ma/cm^2	CH_3OH Vol %	Peak Current ma/cm^2
1.1	194	.11	22	.22	51	1.1	210	1.0	115	1.0(b)	282
1.90	134	.20	52	.71	150	2.11	354	PHYSICAL LOSS OF CATALYST FROM ANODE			
		.41	92	1.22	227					5-20	
		.82	160	1.71	286			1.0(B)	287	1.0(B)	292
		1.42	250								
		2.03	333								

R-REVERSED ELECTRODES

PERFORMANCE WITH CONDITION "C" - 10 GMS/FT^2 CATALYST - NO STIRRING

Date	CH_3OH Vol %	Peak Current ma/cm^2
5-24	1.0	171
5-27	1.0	173
5-28	1.0	170
5-29	1.5	174
5-31	1.0	183
6-1	1.0	187
6-4	1.0	194
6-5	1.0	185
6-6	1.0	185
6-7	1.0	175

DATE

5-29		5-31		6-2	
CH_3OH Vol %	Peak Current ma/cm^2	CH_3OH Vol %	Peak Current ma/cm^2	CH_3OH Vol %	Peak Current ma/cm^2
0.2	44	0.21	44	.19	51
0.55	127	0.60	142	.60	109
1.0	179	1.10	184	.94	162
2.0	251			1.64	221
				2.56	296
				3.24	321

APPENDIX C-31

TEST DATA ON SOME POSSIBLE FUEL CELL MOLDING MATERIALS

Material and Identification	"LUSTRAN" Acrylonitrile-Butadiene-Styrene Terpolymer		Viton A Copolymer of Vinylidene Fluoride & Hexafluoropropylene		Epoxy Resin Mineral Filled		Penton Chlorinated Polyether			Escon 125* Hi Thermal Life Polypropylene				
Made By	Monsanto		DuPont		Plastics, Inc.		Hercules			Enjay Company				
Sample No.	A	B	A	B	A	B	A	B		A	B **	C	D	
Treated at 80°C. for 4 hours in	30% H_2SO_4	30% H_2SO_4 + 2% HNO_3 then 30% H_2SO_4	30% H_2SO_4	30% H_2SO_4 + 2% HNO_3 then 30% H_2SO_4	30% H_2SO_4	30% H_2SO_4 + 2% HNO_3 then 30% H_2SO_4	30% H_2SO_4	30% H_2SO_4 + 2% HNO_3 then 30% H_2SO_4	Same Sample Again in 30% H_2SO_4	30% H_2SO_4	30% H_2SO_4 + 2% HNO_3 then 30% H_2SO_4	30% H_2SO_4	30% H_2SO_4 + 2% HNO_3 then 30% H_2SO_4	Same Sample Twice Again in 30% H_2SO_4
Solution Tested for Performance with 1 vol % Methanol at 60°C. Showed Polarization Deviations from Standard in mv at Current Density of:														
1 ma/cm^2	25	25	5	0	0	0	10	-5	0	-10	20	10	-5	0
2 ma/cm^2	10	10	-15	-15	0	-15	15	-5	5	-20	0	10	0	-5
4 ma/cm^2	--	--	--	--	5	--	20	0	5	-10	--	5	0	0
8 ma/cm^2	10	15	-10	-5	5	-5	15	0	0	-5	-5	5	0	0
16 ma/cm^2	10	25	0	0	5	5	25	0	0	-5	10	5	0	0
32 ma/cm^2	20	25	5	0	0	5	20	0	0	-5	25	5	0	-5
64 ma/cm^2	15	20	0	5	-5	10	25	5	5	-5	15	5	5	5
Visual Effects	None	Sl. Yellow	None	None	None	None	None	None	None	None	Sl. Yellow	None	Sl. Yellow	No Change
% Change in Weight	+0.09	+0.10	-0.11	+0.55	+0.065	+0.27	0.00	0.00	-0.08	-0.013	0.00	0.00	0.01	-0.03

* Additives of polypropylene were put into 30% H_2SO_4 and tested for methanol performance. The polarizations increased 75 to 85 millivolts for currents of 16 to 64 ma/cm^2 and 50 to 60 millivolts for currents of 1 to 8 ma/cm^2.

** Higher polarization was noted for this sample compared to sample "D" possibly due to insufficient washing to remove impurities.

APPENDIX C-32

CONSTANT CURRENT DRIVERS

Two models of constant current power line operated power supplies were designed and constructed for use in fuel cell testing.

Model I shown in Figure C-7 provides continuously adjustable current from 0.1 ma to 3.0 amps in 5 ranges. An internal meter providing 2% accuracy has full scale readings of 1 ma, 10 ma, 100 ma, 1 amp , and 3 amps. 1% regulation is obtained with the transistorized circuit for changes of 20% in line voltage and up to 6 volts change in the external cell circuit.

Model 2 shown in Figure C-8 provides preset current values from 10^{-5} to 10 amperes. Present values are available on 6 ranges with 10 steps on each range. Preset accuracy is better than 1.0% as shown in Table C-4 . Line voltage changes of 20% and external cell voltage changes up to 8 volts cause less than 0.2% error in the preset current values.

TABLE C-4

MODEL 2 CONSTANT CURRENT DRIVER CALIBRATION

Dial Settings		Measured Current
Decade	Multiplier	Amperes
10^{-5}	1	1.01×10^{-5}
10^{-5}	10	10.1×10^{-5}
10^{-4}	1	$.996 \times 10^{-4}$
10^{-4}	10	10.01×10^{-4}
10^{-3}	1	$.997 \times 10^{-3}$
10^{-3}	10	10.03×10^{-3}
10^{-2}	1	$.998 \times 10^{-2}$
10^{-2}	10	10.02×10^{-2}
10^{-1}	1	1.00×10^{-1}
10^{-1}	10	10.01×10^{-1}
1	1	.998
1	10	9.91
10^{-1}	1	1.00×10^{-1}
10^{-1}	2	2.00×10^{-1}
10^{-1}	3	2.98×10^{-1}
10^{-1}	4	4.00
10^{-1}	5	5.00×10^{-1}
10^{-1}	6	6.00
10^{-1}	7	7.02×10^{-1}
10^{-1}	8	$8.02 \times$
10^{-1}	9	9.01×10^{-1}
10^{-1}	10	10.01×10^{-1}

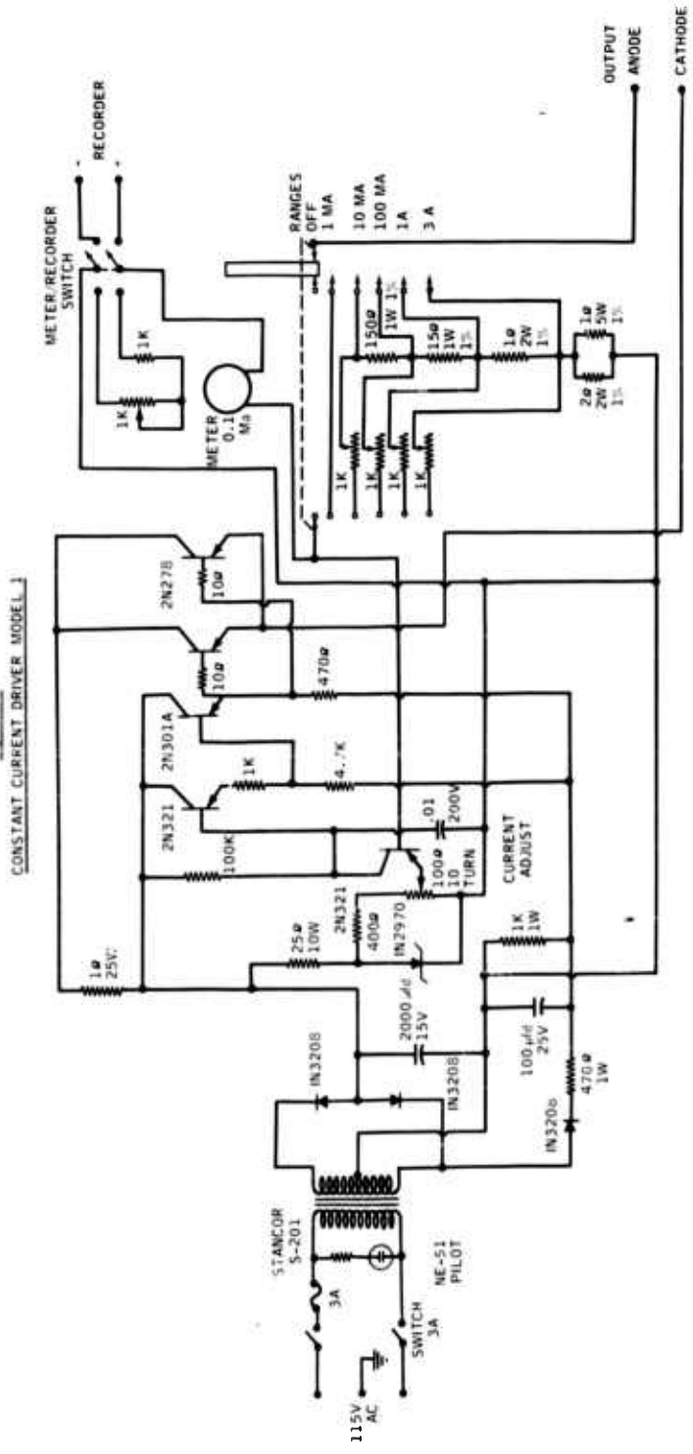

Figure E-7
CONSTANT CURRENT DRIVER MODEL J

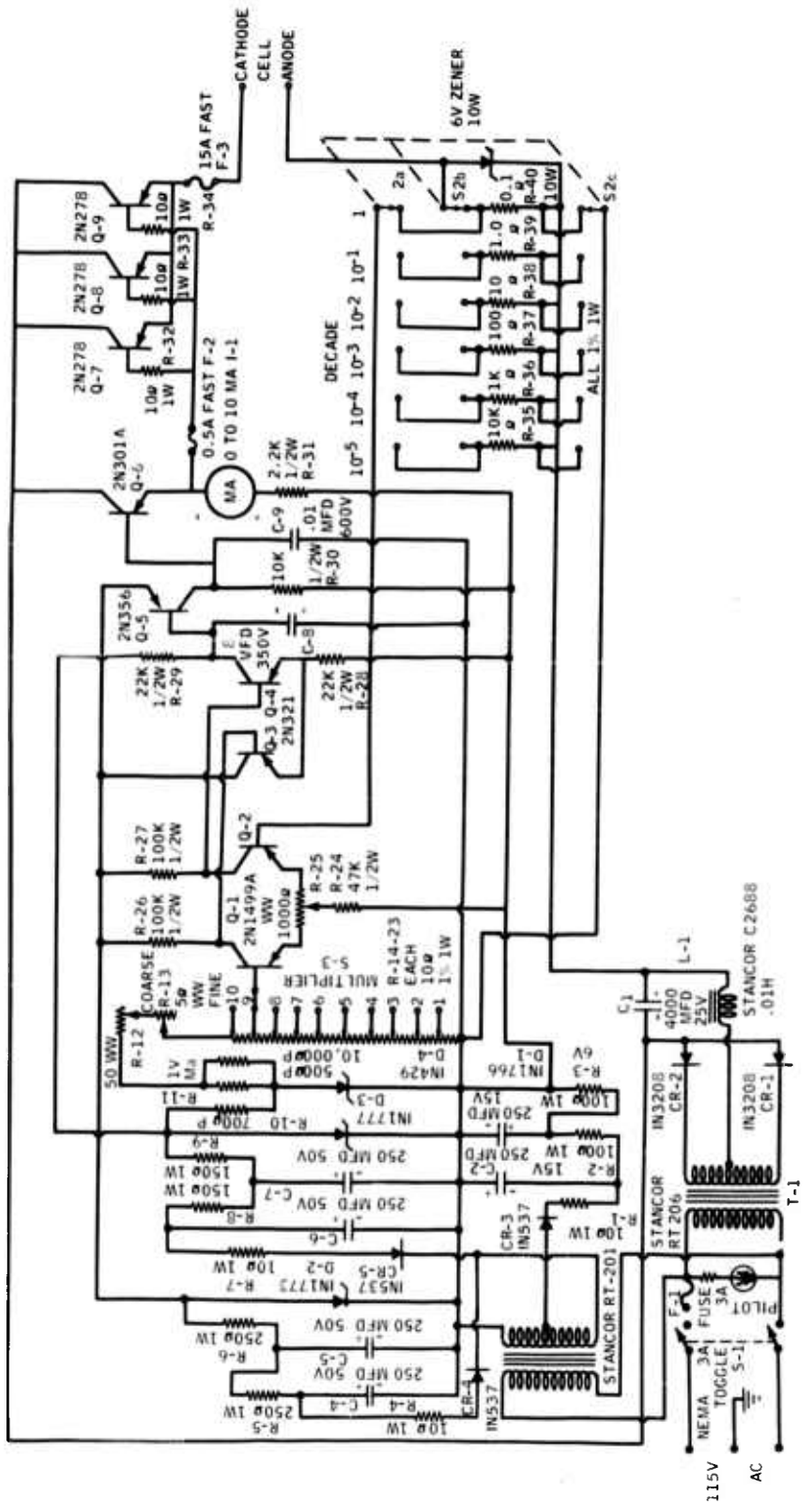

Figure C-6
CONSTANT CURRENT DRIVER MODEL 2

APPENDIX C-33

VOLTAGE MONITOR AND SHUTDOWN DEVICE

As a protection against high electrode polarization conditions during long term runs, a voltage monitor and shutdown has been developed. This consists of a high impedance vacuum tube voltmeter and relay system as shown in Figure C-9. Polarization voltages exceeding the preset level on the relay meter shutdown and lockout the primary electrical power system.

Figure C-9
VOLTAGE MONITOR AND SHUTDOWN DEVICE

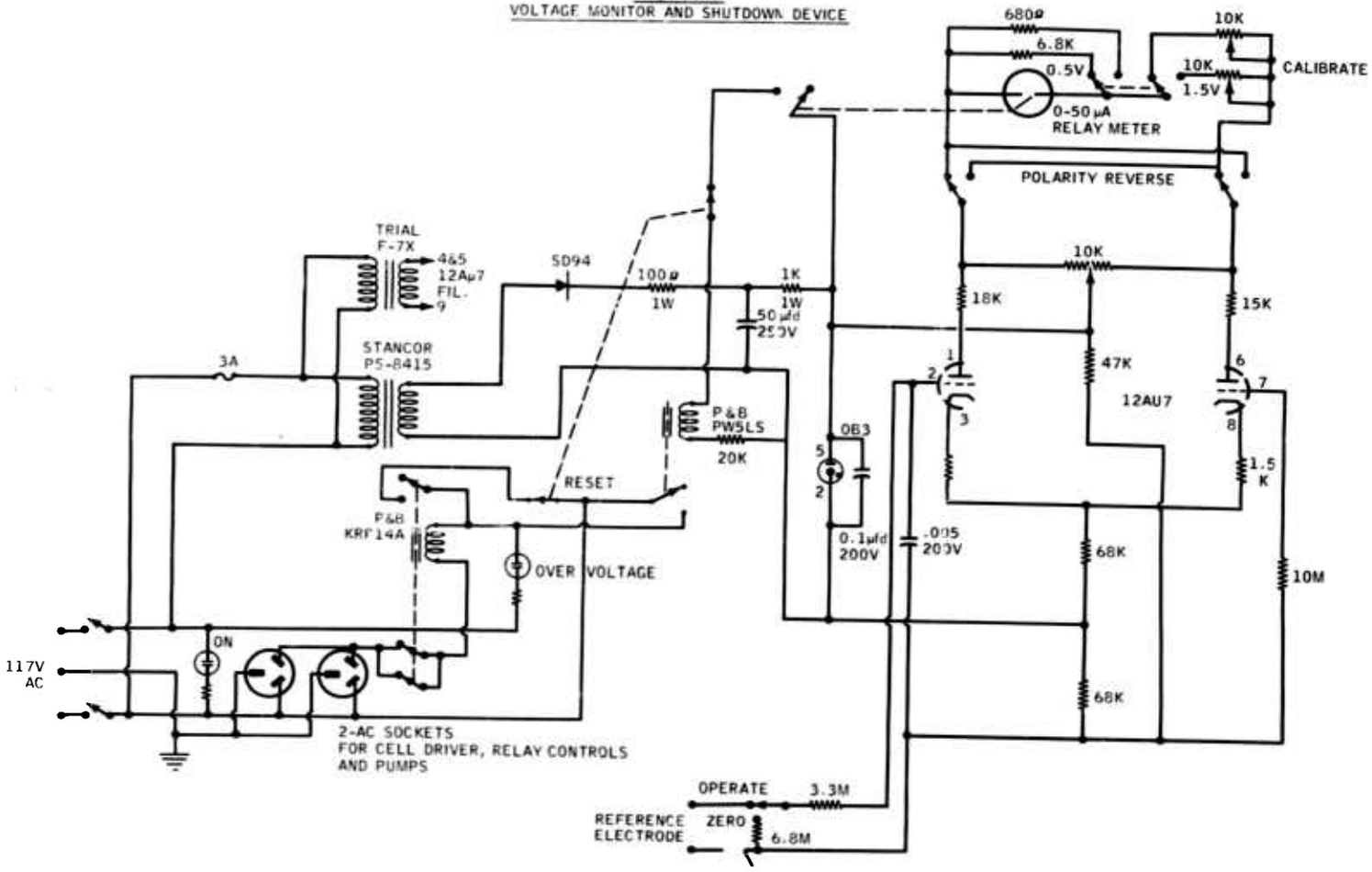

AD- Div.

Esso Research and Engineering Company,
Linden, New Jersey
SOLUBLE CARBONACEOUS FUEL-AIR FUEL CELL, by
Barry L. Tarmy and others. First semi-annual
report, 1 Jan. 1963 - 30 June 1963. 142 pages
incl. illus. tables. (Rept. No. 3; Task No.
OST 761100338)
(Contract DA-36-039 AMC-00134(E)) Unclassified report

Studies were continued aimed toward the ultimate development of a fuel cell using a partially oxidized hydrocarbon as the fuel and air as the oxidant at moderate temperatures and pressures. Included are work carried out on the effects of the fuel, catalyst composition, and other major operating variables on the design and operation of the fuel electrode, experiments performed to improve the over-all efficiency of several types of air electrodes and tests designed to evaluate the

(over)

UNCLASSIFIED

1. Power supplies-Fuel cells
2. Electrolyte-Soluble carbonaceous fuel
3. Acid electrolyte
4. Electrodes

I. Tarmy, B. L.
II. U.S. Army Electronics Research and Development Laboratory
III. Contract DA-36-039 AMC-00134(E)

UNCLASSIFIED

AD- Div.

Esso Research and Engineering Company,
Linden, New Jersey
SOLUBLE CARBONACEOUS FUEL-AIR FUEL CELL, by
Barry L. Tarmy and others. First semi-annual
report, 1 Jan. 1963 - 30 June 1963. 142 pages
incl. illus. tables. (Rept. No. 3; Task No.
OST 761100338)
(Contract DA-36-039 AMC-00134(E)) Unclassified report

Studies were continued aimed toward the ultimate development of a fuel cell using a partially oxidized hydrocarbon as the fuel and air as the oxidant at moderate temperatures and pressures. Included are work carried out on the effects of the fuel, catalyst composition, and other major operating variables on the design and operation of the fuel electrode, experiments performed to improve the over-all efficiency of several types of air electrodes and tests designed to evaluate the

(over)

UNCLASSIFIED

1. Power supplies-Fuel cells
2. Electrolyte-Soluble carbonaceous fuel
3. Acid electrolyte
4. Electrodes

I. Tarmy, B. L.
II. U. S. Army Electronics Research and Development Laboratory
III. Contract DA-36-039 AMC-00134(E)

UNCLASSIFIED

AD- Div.

Esso Research and Engineering Company,
Linden, New Jersey
SOLUBLE CARBONACEOUS FUEL-AIR FUEL CELL, by
Barry L. Tarmy and others. First semi-annual
report, 1 Jan. 1963 - 30 June 1963. 142 pages
incl. illus. tables. (Rept. No. 3; Task No.
OST 761100338)
(Contract DA-36-039 AMC-00134(E)) Unclassified report

Studies were continued aimed toward the ultimate development of a fuel cell using a partially oxidized hydrocarbon as the fuel and air as the oxidant at moderate temperatures and pressures. Included are work carried out on the effects of the fuel, catalyst composition, and other major operating variables on the design and operation of the fuel electrode, experiments performed to improve the over-all efficiency of several types of air electrodes and tests designed to evaluate the

(over)

UNCLASSIFIED

1. Power supplies-Fuel cells
2. Electrolyte-Soluble carbonaceous fuel
3. Acid electrolyte
4. Electrodes

I. Tarmy, B. L.
II. U.S. Army Electronics Research and Development Laboratory
III. Contract DA-36-039 AMC-00134(E)

UNCLASSIFIED

AD- Div.

Esso Research and Engineering Company,
Linden, New Jersey
SOLUBLE CARBONACEOUS FUEL-AIR FUEL CELL, by
Barry L. Tarmy and others. First semi-annual
report, 1 Jan. 1963 - 30 June 1963. 142 pages
incl. illus. tables. (Rept. No. 3; Task No.
OST 761100338)
(Contract DA-36-039 AMC-00134(E)) Unclassified report

Studies were continued aimed toward the ultimate development of a fuel cell using a partially oxidized hydrocarbon as the fuel and air as the oxidant at moderate temperatures and pressures. Included are work carried out on the effects of the fuel, catalyst composition, and other major operating variables on the design and operation of the fuel electrode, experiments performed to improve the over-all efficiency of several types of air electrodes and tests designed to evaluate the

(over)

UNCLASSIFIED

1. Power supplies-Fuel cells
2. Electrolyte-Soluble carbonaceous fuel
3. Acid electrolyte
4. Electrodes

I. Tarmy, B. L.
II. U.S. Army Electronics Research and Development Laboratory
III. Contract DA-36-039 AMC-00134(E)

UNCLASSIFIED

AD- operability of the fuel cell components in complete cells. These tests demonstrated the feasibility of sustaining the performance of these components in compact cells without severe losses in efficiency due to their interaction.	UNCLASSIFIED UNCLASSIFIED	AD- operability of the fuel cell components in complete cells. These tests demonstrated the feasibility of sustaining the performance of these components in compact cells without severe losses in efficiency due to their interaction.	UNCLASSIFIED UNCLASSIFIED
AD- operability of the fuel cell components in complete cells. These tests demonstrated the feasibility of sustaining the performance of these components in compact cells without severe losses in efficiency due to their interaction.	UNCLASSIFIED UNCLASSIFIED	AD- operability of the fuel cell components in complete cells. These tests demonstrated the feasibility of sustaining the performance of these components in compact cells without severe losses in efficiency due to their interaction.	UNCLASSIFIED UNCLASSIFIED

AD- Div.

Esso Research and Engineering Company,
Linden, New Jersey
SOLUBLE CARBONACEOUS FUEL-AIR FUEL CELL, by Barry L. Tarmy and others. First semi-annual report, 1 Jan. 1963 - 30 June 1963. 142 pages incl. illus. tables. (Rept. No. 3; Task No. OST 761100338)
(Contract DA-36-039 AMC-00134(E)) Unclassified report

Studies were continued aimed toward the ultimate development of a fuel cell using a partially oxidized hydrocarbon as the fuel and air as the oxidant at moderate temperatures and pressures. Included are work carried out on the effects of the fuel, catalyst composition, and other major operating variables on the design and operation of the fuel electrode, experiments performed to improve the over-all efficiency of several types of air electrodes and tests designed to evaluate the

(over)

UNCLASSIFIED

1. Power supplies-Fuel cells
2. Electrolyte-Soluble carbonaceous fuel
3. Acid electrolyte
4. Electrodes

I. Tarmy, B. L.
II. U.S. Army Electronics Research and Development Laboratory
III. Contract DA-36-039 AMC-00134(E)

UNCLASSIFIED

AD- Div.

Esso Research and Engineering Company,
Linden, New Jersey
SOLUBLE CARBONACEOUS FUEL-AIR FUEL CELL, by Barry L. Tarmy and others. First semi-annual report, 1 Jan. 1963 - 30 June 1963. 142 pages incl. illus. tables. (Rept. No. 3; Task No. OST 761100338)
(Contract DA-36-039 AMC-00134(E)) Unclassified report

Studies were continued aimed toward the ultimate development of a fuel cell using a partially oxidized hydrocarbon as the fuel and air as the oxidant at moderate temperatures and pressures. Included are work carried out on the effects of the fuel, catalyst composition, and other major operating variables on the design and operation of the fuel electrode, experiments performed to improve the over-all efficiency of several types of air electrodes and tests designed to evaluate the

(over)

UNCLASSIFIED

1. Power supplies-Fuel cells
2. Electrolyte-Soluble carbonaceous fuel
3. Acid electrolyte
4. Electrodes

I. Tarmy, B. L.
II. U. S. Army Electronics Research and Development Laboratory
III. Contract DA-36-039 AMC-00134(E)

UNCLASSIFIED

AD- Div.

Esso Research and Engineering Company,
Linden, New Jersey
SOLUBLE CARBONACEOUS FUEL-AIR FUEL CELL, by Barry L. Tarmy and others. First semi-annual report, 1 Jan. 1963 - 30 June 1963. 142 pages incl. illus. tables. (Rept. No. 3; Task No. OST 761100338)
(Contract DA-36-039 AMC-00134(E)) Unclassified report

Studies were continued aimed toward the ultimate development of a fuel cell using a partially oxidized hydrocarbon as the fuel and air as the oxidant at moderate temperatures and pressures. Included are work carried out on the effects of the fuel, catalyst composition, and other major operating variables on the design and operation of the fuel electrode, experiments performed to improve the over-all efficiency of several types of air electrodes and tests designed to evaluate the

(over)

UNCLASSIFIED

1. Power supplies-Fuel cells
2. Electrolyte-Soluble carbonaceous fuel
3. Acid electrolyte
4. Electrodes

I. Tarmy, B. L.
II. U.S. Army Electronics Research and Development Laboratory
III. Contract DA-36-039 AMC-00134(E)

UNCLASSIFIED

AD- Div.

Esso Research and Engineering Company,
Linden, New Jersey
SOLUBLE CARBONACEOUS FUEL-AIR FUEL CELL, by Barry L. Tarmy and others. First semi-annual report, 1 Jan. 1963 - 30 June 1963. 142 pages incl. illus. tables. (Rept. No. 3; Task No. OST 761100338)
(Contract DA-36-039 AMC-00134(E)) Unclassified report

Studies were continued aimed toward the ultimate development of a fuel cell using a partially oxidized hydrocarbon as the fuel and air as the oxidant at moderate temperatures and pressures. Included are work carried out on the effects of the fuel, catalyst composition, and other major operating variables on the design and operation of the fuel electrode, experiments performed to improve the over-all efficiency of several types of air electrodes and tests designed to evaluate the

(over)

UNCLASSIFIED

1. Power supplies-Fuel cells
2. Electrolyte-Soluble carbonaceous fuel
3. Acid electrolyte
4. Electrodes

I. Tarmy, B. L.
II. U.S. Army Electronics Research and Development Laboratory
III. Contract DA-36-039 AMC-00134(E)

UNCLASSIFIED

AD- operability of the fuel cell components in complete cells. These tests demonstrated the feasibility of sustaining the performance of these components in compact cells without severe losses in efficiency due to their interaction.	UNCLASSIFIED UNCLASSIFIED	AD- operability of the fuel cell components in complete cells. These tests demonstrated the feasibility of sustaining the performance of these components in compact cells without severe losses in efficiency due to their interaction.	UNCLASSIFIED UNCLASSIFIED
AD- operability of the fuel cell components in complete cells. These tests demonstrated the feasibility of sustaining the performance of these components in compact cells without severe losses in efficiency due to their interaction.	UNCLASSIFIED UNCLASSIFIED	AD- operability of the fuel cell components in complete cells. These tests demonstrated the feasibility of sustaining the performance of these components in compact cells without severe losses in efficiency due to their interaction.	UNCLASSIFIED UNCLASSIFIED

DISTRIBUTION LIST
FIRST SEMI-ANNUAL REPORT
CONTRACT NO. DA 36-039 AMC-00134 (E)

Commanding Officer
U.S.A. Electronics Research and
Development Laboratory
Fort Monmouth, N.J.
ATTN: Logistics Division
(MARKED FOR PROJECT
ENGINEER) (6)
ATTN: SELRA/P (1)
ATTN: Dir of Research/Engineering (1)
ATTN: File Unit #1 (1)
ATTN: Technical Document Center (1)

OASD (R&D), Rm 3E1065
ATTN: Technical Library
The Pentagon
Washington 25, D.C. (1)

Chief of Research and Development
OCS, Department of the Army
Washington 25, D.C. (1)

Commanding General
U.S.A. Electronics Command
ATTN: AMSEL-AD
Fort Monmouth, N.J. (3)

Director
U.S. Naval Research Laboratory
ATTN: Code 2027
Washington 25, D.C. (1)

Commanding Officer and Director
U.S. Naval Electronics Laboratory
San Diego 52, California (1)

Air Force Cambridge Research
Laboratories
ATTN: CRZC
L. C. Hanscom Field
Bedford, Massachusetts (1)

Rome Air Development Center
ATTN: RAALD
Griffiss Air Force Base, N.Y. (1)

Commanding General
U.S.A. Electronics Research and
Development Activity
ATTN: Technical Library
Fort Huachuca, Arizona (1)

Commanding Officer
Harry Diamond Laboratories
ATTN: Library, Room 211, Bldg. 92
Connecticut Ave & Van Ness St., N.W.
Washington 25, D.C. (1)

Commanding Officer
U.S.A. Electronics Material Support
Agency
ATTN: SELMS-ADJ
Fort Monmouth, N.J. (1)

Deputy President
U.S.A. Security Agency Board
Arlington Hall Station
Arlington 12, Virginia (1)

Director
Defense Documentation Center
ATTN: TISIA
Cameron Station
Alexandria, Virginia (10)

Chief
U.S.A. Security Agency
Arlington Hall Station
Arlington 12, Virginia (2)

Commander
Aeronautical Systems Division
ATTN: ASAPRL
Wright-Patterson Air Force Base
Ohio (1)

Air Force Cambridge Research Laboratories
ATTN: CRXL-R
L. C. Hanscom Field
Bedford, Massachusetts (1)

Headquarters
U.S.A. Material Command
Research and Development Directorate
ATTN: AMCRD-DE-MO
Washington 25, D.C. (1)

Commanding General
U.S.A. Electronics Command
ATTN: AMSEL-RE-A
Fort Monmouth, N.J. (1)

Commanding General
U.S.A. Combat Developments Command
ATTN: CDCMR-E
Fort Belvior, Virginia (1)

Commanding Officer
U.S.A. Communications and Electronics
Combat Development Agency
Fort Huachuca, Arizona (1)

Director
Fort Monmouth Office
U.S.A. Communications and Electronics
Combat Development Agency
Fort Monmouth, N.J. (1)

Air Force Systems Command
Scientific/Technical Liaison Office
U.S. Naval Air Development Center
Johnsville, Pennsylvania (1)

Director
USAEGIMRADA
ATTN: ENGGM-SS
Fort Belvoir, Virginia (1)

Marine Corps Liaison Office
U.S.A. Electronics Research and
Development Laboratory
Fort Monmouth, N.J. (1)

AFSC Scientific/Technical Liaison Office
U.S.A. Electronics Research and
Development Laboratory
Fort Monmouth, N.J. (1)

USAELRDL Liaison Office
Rome Air Development Center
ATTN: RAOL
Griffiss Air Force Base, N.Y. (1)

Power Information Center
Moore School Building
200 South Thirty-Third Street
Philadelphia 4, Pennsylvania (1)

Dr. Sidney J. Magram
Physical Sciences Division
Army Research Office
3045 Columbia Pike
Arlington, Virginia (1)

Dr. Ralph Roberts
Head, Power Branch
Office of Naval Research (Code 429)
Department of the Navy
Washington 25, D.C. (1)

Mr. Bernard B. Rosenbaum
Bureau of Ships (Code 340)
Department of the Navy
Washington 25, D.C. (1)

Mr. George W. Sherman
Aeronautical Systems Division
ATTN: ASRMFP
Wright-Patterson Air Force Base
Ohio (1)

Dr. John H. Huth
Advanced Research Projects Agency
The Pentagon, Room 3E157
Washington 25, D.C. (1)

Lt. Col. George H. Ogburn, Jr.
Auxiliary Power Branch (SNAP)
Division of Reactor Development
U.S. Atomic Energy Commission
Washington 25, D.C. (1)

Mr. Walter C. Scott
National Aeronautics & Space
Administration
1520 H Street, N.W.
Washington 25, D.C. (1)

Institute for Defense Analysis
1666 Connecticut Avenue, N.W.
Washington 25, D.C. (1)

Director
Advanced Research Projects Agency
Washington 25, D.C. (6)

Commanding Officer
U.S.A. Electronics Research and
Development Laboratory
ATTN: SELRA/DR, ARPA Coordinator
Fort Monmouth, N.J. (1)

Mr. R. A. Osteryoung
Atomics International
Canuga Park, California (1)

Dr. David M. Mason
Stanford University
Stanford, California (1)

Dr. A. E. Levy-Pascal
Astropower, Inc.
2968 Randolph Avenue
Costa Mesa, California (1)

Mr. L. R. Griffith
California Research Corp.
576 Standard Avenue
Richmond, California (1)

Dr. Ralph G. Gentile
Monsanto Research Corp.
Boston Laboratories
Everett 49, Massachusetts (1)

Mr. Ray M. Hurd
Texas Research Associates
1701 Guadalupe Street
Austin 1, Texas (1)

Dr. R. Flannery
American Oil Company
Whiting Laboratories
P.O. Box 431
Whiting, Indiana (1)

Dr. E. A. Oster
General Electric Co., DECO
Lynn, Massachusetts (1)

Dr. Arthur J. Rosenberg
TICO, Incorporated
Materials Research Laboratory
Bear Hill
Waltham 54, Massachusetts (1)

Prof. Herman P. Meissner
Massachusetts Institute of
Technology
Cambridge 39, Massachusetts (1)

Texas Instruments, Inc.
Energy Research Laboratory
P.O. Box 5474
Dallas 22, Texas
ATTN: Dr. C. G. Peattie (1)

Mr. Donald P. Snowden
General Atomics
P.O. Box 608
San Diego 12, California (1)

Dr. C. Tobias
Chemistry Department
University of California
Berkeley, California (1)

Mr. Y. L. Sandler
Westinghouse Research Laboratories
Pittsburgh, Pa. (1)

Engelhard Industries, Inc.
Military Service Department
113 Astor Street
Newark 2, New Jersey
ATTN: Mr. V. A. Forlenza (1)

General Electric Company
Research Laboratory
Schenectady, New York
ATTN: Dr. H. Liebhoafsky (1)

University of Pennsylvania
John Harrison Laboratory of Chemistry
Philadelphia 4, Pennsylvania
ATTN: Dr. J. Bockris (1)

Union Carbide Corporation
Parma Research Center
P.O. Box 6116
Parma 30, Ohio
ATTN: Dr. C. E. Winters (1)

Electrochimica Corporation
1140 O'Brien Drive
Menlo Park, California
ATTN: Dr. M. Eisenberg (1)

Allis-Chalmers Manufacturing Company
Research Division
P.O. Box 512
Milwaukee, Wisconsin
ATTN: Dr. P. Joyner

Allison Division
General Motors Corporation
P.O. Box 894
Indianapolis 6, Indiana
ATTN: Dr. R. E. Henderson (1)

United Aircraft Corporation
Pratt & Whitney Aircraft Divsion
East Hartford 8, Connecticut
ATTN: Mr. J. M. Lee (1)

Melpar, Inc.
3000 Arlinton Boulevard
Falls Church, Virginia
ATTN: Mr. R. T. Foley (1)

Magna Corporation
R&D Laboratories
1001 South East Street
Anaheim, California
ATTN: Dr. Silverman (1)

U.S. Army R&D Liaison Group
(9851 DV)
APO 757
New York, N.Y.
ATTN: Dr. B. R. Stein (1)

UNCLASSIFIED